Inhibition of secretion by asexual reproduction in *Aspergillus niger*

Fengfeng Wang

The research described in this thesis was performed within the Microbiology group of the Science Faculty of Utrecht University and was financed by the Kluyver Centre for Genomics of Industrial Fermentation, which was part of the Netherlands Genomics Initiative / Netherlands Organization for Scientific Research.

ISBN: 978-94-6203-699-4

Cover: Localization of VeA in light (Front) and dark (Back) by localizing fluorescence of VeA-RFP (Red) and the nuclear targeted H2B-GFP fusion protein (Green). Made by Fengfeng Wang and Frits Kindt at Biology Imaging Center of Utrecht University.

Printed and published by CPI-Koninklijke Wöhrmann, Zutphen, The Netherlands

Inhibition of secretion by asexual reproduction in

Aspergillus niger

Remming van secretie door asexuele reproductie in *Aspergillus niger*
(met een samenvatting in het Nederlands)

Proefschrift

ter verkrijging van de graad van doctor aan de Universiteit Utrecht op gezag van de rector magnificus, prof.dr. G.J. van der Zwaan, ingevolge het besluit van het college voor promoties in het openbaar te verdedigen
op woensdag 3 december 2014 des middags te 2.30 uur

door

Fengfeng Wang

geboren op 25 oktober 1979 te Beijing, China

Promotor: Prof.dr. H. A. B. Wösten

This thesis is dedicated to my parents for their love and support.

Contents

Chapter 1

General Introduction

INTRODUCTION

The genus *Aspergillus* comprises a diverse fungal group (Galagan et al., 2005) of up to 837 species (Hawksworth, 2011). Aspergilli are very abundant in nature. For instance, spores (i.e. conidia) of this genus are among the most dominant fungal structures in the air (Bennett, 2010). *Aspergillus niger* and *Aspergillus nidulans* are well studied representatives of the aspergilli. These fungi are not very selective with respect to abiotic growth conditions (Table 1). For instance, *A. niger* can grow at pH values from below 2 to almost 10 and from 6 to 47 °C. Although *A. niger* and *A. nidulans* are most known for their saprobic life style, they can also be pathogenic. *A. niger* has been reported to be a pathogen of *Zingiber officinale* plants (Pawar et al., 2008). Moreover, *A. niger* and *A. nidulans* are opportunistic pathogens of animals and humans. They can cause invasive aspergillosis (involving several organ systems, particularly pulmonary disease), non-invasive pulmonary aspergilloma, allergic bronchopulmonary aspergillosis, and otomycosis (Denning, 1998, Stevens et al., 2000, Bezjak and Arya, 1970, Garcia-Agudo et al., 2011, Rutt and Sataloff, 2008).

Aspergilli release a wide variety of enzymes into their environment to degrade organic polymers into molecules that can be taken up to serve as nutrients. For instance, amylases are secreted to degrade starch, xylanases to degrade xylan and pectinases to degrade pectin within plant material. The amount of enzymes that are released can be very high. For instance, strains of *A. niger* have been selected that produce more than 30 grams per liter of glucoamylase (Finkelstein et al., 1989). The capacity to secrete large amounts of proteins (and other metabolites such as organic acids) in combination with established fermentation technology and molecular biology makes *A. niger* and other aspergilli widely used cell factories. They are used for the production of proteins that find applications in the industry and as pharmaceuticals (Meyer et al., 2011).

Production of proteins has been optimized using mutation and selection, improvement of culture conditions, and molecular approaches such as introduction of multiple copies of genes of interest and the use of strong promoters (Conesa et al.,

2001, Punt et al., 2002). Recently, it was shown that fungal mycelia are heterogeneous with respect to gene expression and secretion (Wösten et al., 2013) and that asexual development represses secretion (Krijgsheld et al., 2013b). These phenomena provide new tools to improve *Aspergillus* cell factories. This chapter describes the current understanding of growth and asexual development of *A. niger* (being a cell factory) and *A. nidulans* (being an important fungal model system) as well as heterogeneity in the *A. niger* mycelium. This chapter ends with the outline of this Thesis.

THE *ASPERGILLUS* MYCELIUM

Formation of the mycelium

Germination of a conidium of *Aspergillus* results in a network of hyphae known as mycelium or colony. The colony extends at its periphery. Its center thus represents the oldest part, while the periphery is newly formed. Depending on the growth conditions, (sub)-millimeter scale micro-colonies or centimeter scale macro-colonies are formed. In the laboratory, aspergilli are routinely grown on agar media or in liquid media. Sub-millimeter scale micro-colonies are formed in liquid shaken cultures or in bioreactors. On agar medium, macro-colonies are formed. The radial symmetrical colonies of *A. nidulan*s (Lee and Adams, 1994b) and *A. niger* (Krijgsheld et al., 2013a) extend their diameter with approximately 0.25 mm per hour in excess of nutrients and at a temperature of 37 °C and 30 °C, respectively. As a result, 7-day-old *A. niger* colonies are approximately 5 cm in diameter. Macro-colonies can be grown directly on the agar medium or between porous polycarbonate membranes (Levin et al., 2007a, Levin et al., 2007b, Wösten et al., 1991). Oxygen, carbon dioxide, water, nutrients and excreted molecules can freely diffuse through the membranes but their pores are too small for hyphae to grow into the underlying medium or to grow into the air. Colonies

Table 1: Conditions for vegetative growth of *A. niger* and *A. nidulans.* Adapted from (Krijgsheld et al., 2013a).

Species	Optimum Temp (°C)	Temp range (°C)	Optimum pH	pH range	Minimal Water activity	Optimum Water activity	Minimum Relative humidity (%)	Optimum Relative humidity (%)	References
A. niger	35-37	6-47	6.0	1.5-9.8	0.77	0.97	88-89	96-98	(Astoreca et al., 2007, Ayerst, 1969, Leong et al., 2006, Mehra and Jaitly, 1995, Panasenko, 1967, Pitt, 1981)
A. nidulans	35-37	6-51	7.0	2-12	0.78		80	95	(Agnihotri, 1964, Al-Doory, 1984 , Panasenko, 1967, Lacey, 1980)

are thus forced to grow nearly 2-dimensionally. The advantage of a sandwiched colony is that it can be easily transferred to a fresh agar plate (e.g. containing radioactive amino acids or a fresh carbon source) (Wösten et al., 1991) or to a ring plate (Levin et al., 2007b). This ring plate consists of 6 concentric wells that can be filled with liquid minimal medium, enabling analysis of spatial protein secretion in the culture medium (Figure 1).

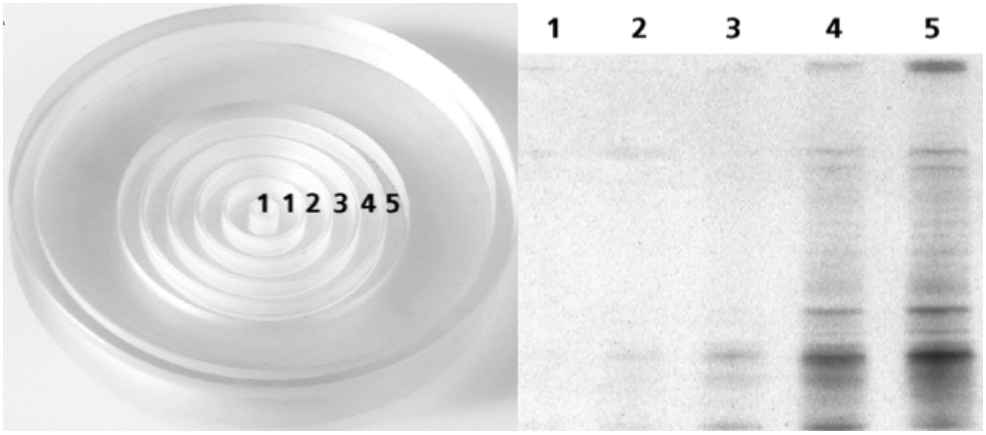

Figure 1. Sandwiched colonies can be transferred from an agar plate to a ring plate (left). This ring plate consists of 6 concentric wells that can be filled with liquid medium. Spatial protein secretion of sandwiched colonies of *A. niger* was analysed by separating radioactively pulse-labelled proteins contained in the wells of the ring plate by SDS PAGE followed by autoradiography. The inner two wells were pooled because of their limited volume. Adapted from (Levin et al., 2007b).

Heterogeneity in the mycelium

The *Aspergillus* mycelium does not consist of a homogeneous collection of hyphae. Zones in micro- and macro-colonies of *A. niger* are heterogeneous with respect to growth (Wösten et al., 1991), secretion (Wösten et al., 1991, Levin et al., 2007b, Krijgsheld et al., 2012) and RNA composition (Vinck et al., 2011, Wösten et al., 2013, Levin et al., 2007a). Protein synthesis occurs throughout macro-colonies of *A. niger.* In contrast, growth and secretion mainly occur at the periphery of the colony (Wösten et al., 1991) (Figure 2A-C). From these data and the fact that proteins are released at tips of growing hyphae (Wösten et al. 1991) it was concluded that growth and secretion are strictly coupled. This strict coupling is predicted by the steady-state growth theory and the bulk flow theory (Wessels, 1988, Wessels, 1993). These the-

ories propose that proteins cannot diffuse through the highly cross-linked cell walls of non-growing hyphae. Protein release would be the result of co-migration with the plastic non-cross-linked cell wall polymers that are extruded at the apex of growing hyphae. These cell wall polymers are pushed to the surface of the hyphae by the action of the internal turgor pressure and the apposition of new cell wall polymers at the inner part of the cell wall. Cross-linking starts at the moment the cell wall polymers are released. The level of cross-linking is still limited at the apical region of the cell wall but has been completed at sub-apical parts. In these subapical parts, the cross-linked cell wall acts as a barrier for protein release. Interestingly, in the last decade it has been shown that protein secretion can occur in non-growing zones of *A. niger* colonies (Levin et al., 2007a, Krijgsheld et al., 2013b). Growth was localized at the periphery of xylose-grown sandwiched colonies when they had been transferred for 24 h to fresh medium (Figure 2D). In contrast, newly synthesized proteins were released throughout the colony with the exception of a sub-peripheral zone (Figure 2F). Absence of protein release in this zone is explained by the phenomenon of sporulation inhibited secretion (see below). Until now it is not known how proteins are released into the culture medium by non-growing hyphae. Possibly, cell wall-degrading enzymes create pores in the highly cross-linked cell walls of non-growing hyphae (Wösten et al., 2013). Alternatively, expansins may modify the cell wall (Fang et al., 2014).

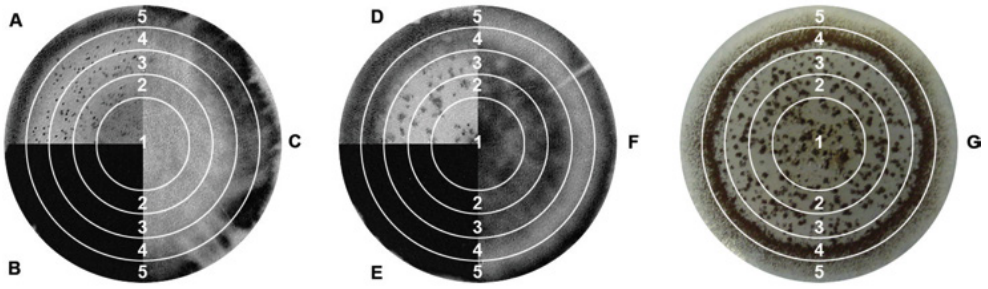

Figure 2. Growth (A,D), protein synthesis (B,E), and secretion (C,F) in 7-day-old xylose-grown wild type colonies of *A. niger*. Colonies were analyzed before (A-C) and after transfer (D-F) to fresh xylose medium. Growth was detected with ^{14}C-labeled N-acetylglucosamine. Protein synthesis and secretion were monitored by incorporation of ^{14}C-labeled amino acids. Secreted proteins were immobilized by a PVDF membrane that had been placed underneath the colony. Conidia forming conidiophores were observed after 24 h of growth in the sub-peripheral zone 4 when the upper membrane of a sandwiched wild-type colony was removed at day 7 (G). Taken from (Krijgsheld et al., 2013b).

The heterogeneity of the macro-colony is also reflected in the RNA composition of different zones of macro-colonies of *A. niger*. For instance, 9 % of the active genes are expressed in only one of five concentric zones of a macro-colony *of A. niger* and more than 25 % of the active genes show at least a two-fold difference in expression between the outer and innermost zone of the colony (Levin et al., 2007a). For instance, accumulation of mRNA of the glucoamylase gene *glaA* was more than 3-fold lower in the center when compared to the periphery of maltose-grown colonies. Similarly, mRNA level of the ferulic acid esterase gene *faeA* was five times lower in the center of xylose grown colonies. Differences in gene expression within macro-colonies of *A. niger* can be explained by nutrient dependent and nutrient independent mechanisms, each contributing about half of the variation (Levin et al., 2007a). These findings imply that differentiation occurs within the vegetative mycelium of *Aspergillus*.

Heterogeneous gene expression is also observed within a zone of a macro-colony of *A. niger.* For instance, only part of the hyphae at the periphery of macro-colonies of *A. niger* secrete glucoamylase (Wösten et al. 1991). This is the result of heterogeneous expression of the glucoamylase gene *glaA* within this zone (Vinck et al. 2005). Two populations of hyphae can be distinguished at the outer zone of the colony; those highly and those lowly expressing *glaA*. The hyphae highly expressing *glaA* also highly express other genes encoding secreted proteins (Vinck et al. 2011). Moreover, they highly express the glyceraldehyde-3-phosphate dehydrogenase gene and are characterized by high 18S rRNA levels. From these results it was concluded that two populations of hyphae are present at the periphery of a colony; one that is lowly and one that is highly metabolically active. The lowly active hyphae were shown to have a growth rate similar to that of the highly active hyphae. From this it was concluded that a “low” activity of hyphae is sufficient to support hyphal growth. However, a “high” metabolism would be needed to support secretion of large amounts of proteins (Vinck et al. 2011). Single hypha transcriptome analysis indicates that heterogeneity between neighboring hyphae goes beyond two types of hyphae. Individual hyphae each have their own RNA composition (de Bekker et al. 2011a).

The phenomenon of heterogeneity in colonies of *A. niger* came to a surprise considering the fact that the ascomycete mycelium is assumed to share a common cytoplasm. This common cytoplasm would result from the large pores in the septa that compartmentalize hyphae of ascomycetes including *A. niger.* These pores allow streaming of cytosol and even organelles enabling mixing of cytoplasm throughout the mycelium. However, it was recently shown that 40% of the septal pores of hyphae at the periphery of colonies of *Aspergillus oryzae* are closed by peroxisome-derived organelles (Bleichrodt et al., 2012). Plugging by these so called Woronin bodies is dynamic. From these results it was extrapolated that only in 5 % and 1% of the cases cytoplasm of two hyphae would be in physical contact when they are separated by 6 and 9 septa, respectively. This physical separation would explain heterogeneity in the mycelium. Indeed, hyphal heterogeneity was abolished in a strain that cannot form Woronin bodies (Bleichrodt et al., 2012). Neighboring hyphae in a wild-type *A. oryzae* colony show heterogeneous expression of the glucoamylase gene *glaA* and the α-glucoronidase gene *aguA.* Two populations of hyphae can be distinguished; one that highly and one that lowly expresses *glaA* or *aguA*. In contrast, *glaA* and *aguA* expression shows a normal distribution in the strain that cannot form Woronin bodies. Together, it was concluded that Woronin bodies maintain hyphal heterogeneity in a fungal mycelium by impeding cytoplasmic continuity. Septal plugging mediated heterogeneity was also shown to occur in *A. niger* (Bleichrodt, 2012). In this *Aspergillus* species it was shown that plugging of septal pores can be induced by environmental conditions.

What would be the function of heterogeneity between and within zones of a colony? Zonal heterogeneity would be functional to adapt to the different nutritional conditions each zone of the colony is exposed to. Moreover, it would enable specific zones to start sexual or asexual development. Heterogeneity within a zone of the colony would increase the chance that (some of the) hyphae survive when this zone of the colony is exposed to stress conditions like the presence of antibiotics, reactive oxygen species or high temperature. In agreement with this, the *A. niger* Δ*hexA* strain

that cannot form Woronin bodies died when exposed for three days to 45 °C, whereas the wild-type strain survived (Bleichrodt et al., 2012).

SPORULATION INHIBITED PROTEIN SECRETION

As mentioned above, all zones except the sub-peripheral zone secreted proteins when xylose-grown sandwiched colonies had been transferred for 24 h to fresh medium (Figure 2F). This non-secreting zone started to sporulate when the upper membrane of the sandwiched colony was removed (Figure 2G) (Krijgsheld et al., 2013b). This indicates that sporulation represses secretion of the vegetative mycelium. This hypothesis was tested by monitoring spatial secretion of proteins in *A. niger* strains that had a deletion of the sporulation genes *flbA* or *brlA* (for their functions see below). Both strains do not form conidia forming conidiophores but they do produce aerial hyphae. It was shown that the Δ*flbA* strain secretes proteins throughout the mycelium. This agreed with the phenomenon of sporulation inhibited secretion. The Δ*brlA* strain shows a secretion pattern similar to the wild-type. This was explained by the fact that this protein functions relatively late in the sporulation pathway (see below). The secretome of the Δ*flbA* strain is also more complex than that of wild type (Krijgsheld et al., 2013b). It consists of 138 proteins with a signal sequence. Of these, 18 had not been reported in any secretome study and 70 had not been identified in the secretome of 7-day-old xylose grown wild type colonies (Krijgsheld et al., 2012, Krijgsheld et al., 2013b).

So far, one gene involved in sporulation inhibited protein secretion has been identified. To understand this phenomenon in more detail, it should be established which other sporulation genes play a role in secretion inhibition. In the next section, I discuss asexual sporulation in *A. nidulans* and *A. niger* in a condensed way. For a more comprehensive review I refer to (Krijgsheld et al., 2013b).

ASEXUAL DEVELOPMENT

Air-exposed colonies of *A. nidulans* and *A. niger* form two types of aerial hyphae after a period of vegetative growth (Figure 3). One type resembles vegetative hyphae and has a diameter of about 2-3 µm. The other type has a diameter of about 4-5 and 6-7 µm in the case of *A. nidulans* and *A. niger,* respectively. These so-called stalks further develop into conidia forming conidiophores (Figure 3). After the stalk has extended about 100 µm into the air, its tip swells and forms a vesicle with a diameter of about 10 µm. Subsequently, a layer of primary sterigmata dubbed metulae is formed as a result of budding that occurs throughout the surface of the vesicle. The metulae in turn bud twice resulting in a second layer of sterigmata called phialides. The phialides give rise to chains of conidia. One conidiophore can produce more than 10.000 of these spores.

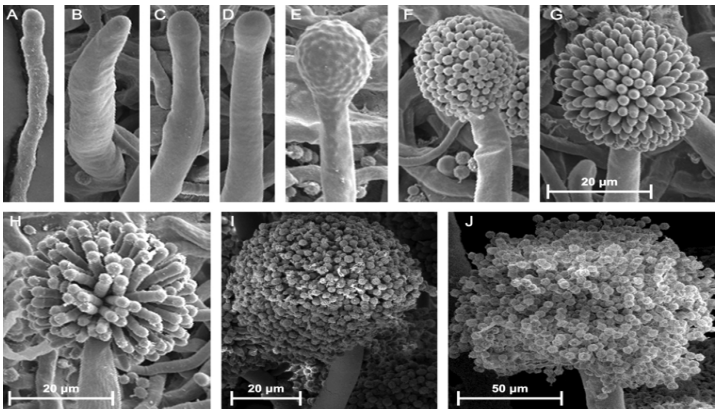

Figure 3. Development of *A. niger* monitored by scanning electron microscopy. The vegetative mycelium forms two types of aerial hyphae. One type is similar to vegetative hyphae (A), while the other type represents stalks (B). The tips of these stalks swell to form a vesicle (C,D). Budding at the vesicle surface (E) results in formation of metulae (F, G). Phialides are formed on top of the metulae (H), which give rise to chains of conidia (I, J). The bar in G also holds for A-F. Taken from (Krijgsheld et al., 2013a).

The process of aerial growth has been proposed to involve signaling of the cell density of the vegetative mycelium (Lee and Adams, 1994b, Wösten et al., 1999, Wösten and Willey, 2000). The 2-3 µm wide aerial hyphae of *A. nidulans* and *A. niger* are formed about 8 h after inoculation of spores on complete medium. The first stalks are formed about 2 h later, while conidiophores have developed 20 h after inoculation (Krijgsheld et al., 2013b). *A. nidulans* can also form conidia in submerged cultures (Adams et al., 1988). In this case, conidiation is induced when the culture gets stressed or when nutrients like the carbon and nitrogen source become limiting.

On the other hand, formation of conidiophores in air-exposed colonies is assumed to be induced by an internal signal that activates a genetic program of sporulation (see below) (Adams et al., 1988). Like *A. nidulans, A. niger* can form conidiophores in submerged conditions. However, these condidiophores do not form spore chains (Krijgsheld et al., 2013b).

The role of fluG, brlA, abaA, wetA, medA, stuA, and vosA in asexual development

Formation of conidiophores has been best studied in *A. nidulans.* It has been shown that mechanisms underlying asexual development in *A. niger* and other *aspergilli* like *A. fumigatus* and *A. oryzae* are similar but not identical to those of *A. nidulans.*

Gene *fluG* is believed to be at the start of the developmental program of asexual reproduction in *A. nidulans*. Overexpression of *fluG* in vegetative hyphae is sufficient to cause sporulation under conditions that normally suppress conidia formation (Lee and Adams, 1996). On the other hand, a Δ*fluG* strain of *A. nidulans* forms aerial hyphae but conidiophores are not being formed in excess of nutrients (Lee and Adams, 1994a). The Δ*fluG* strain does form conidiophores during nutrient deprivation (Lee and Adams, 1996), indicating that FluG is not involved in the stress-related sporulation pathway. Formation of condiophores in the Δ*fluG* strain can be rescued by growing the mutant next to a wild-type strain even when the strains are physically separated by a dialysis membrane with a size exclusion of 6-8 kDa. This indicates that FluG is involved in the production of a low-molecular weight extracellular signaling molecule that initiates asexual development. The homology of *fluG* with bacterial glutamine synthetases suggests that the signaling molecule is related to this amino acid. The role of *fluG* of *A. niger* is discussed in Chapters 2 and 3 of this Thesis.

FluG of *A. nidulans* activates *brlA*. The stalks of a Δ*brlA* strain show “indefinitive” growth. They can be 20-30 times longer than those of the wild-type, resulting in the typical bristle phenotype (Adams et al., 1988). Moreover, conidiophore vesicles are not being formed in the Δ*brlA* strain. BrlA has a similar role in *A. niger* (Krijgsheld et al., 2013b). BrlA activates a central regulatory cascade that controls asexual devel-

opment (Boylan et al., 1987, Mirabito et al., 1989). This complex cascade involves, amongst others, the regulatory genes *abaA, wetA, stuA, medA, and vosA* (Figure 4). Gene *abaA* is activated in *A. nidulans* by BrlA during sterigmata differentiation (Boylan et al., 1987, Breakspear and Momany, 2007). Strain Δ*abaA* forms metulae that bud apically resulting in chains of metula-like cells. Thus, phialides are not produced resulting in the absence of conidia (Boylan et al., 1987, Clutterbuck, 1969, Sewall et al., 1990). AbaA impacts *brlA* expression and regulates expression of *medA, wetA, vosA* and its own gene (Figure 4) (Andrianopoulos and Timberlake, 1994). Gene *wetA* is activated by *abaA* during the late phase of conidiation (Figure 4). The Δ*wetA* strain forms normal conidiophores but its conidia are non-pigmented, are not water repellent, and go in autolysis (Marshall and Timberlake, 1991, Sewall et al., 1990). WetA activates genes in phialides and spores that are involved in making the cell wall of conidia impermeable and mature (Marshall and Timberlake, 1991). In addition, WetA seems to activate its own gene (Adams et al., 1998, Boylan et al., 1987, Marshall and Timberlake, 1991, Ni and Yu, 2007) and represses *abaA* and *brlA* (Tao & Yu 2011) (Figure 4).

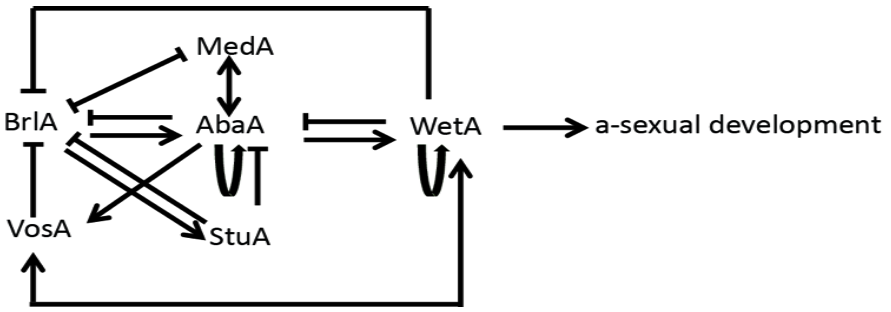

Figure 4. The central regulatory network consisting of BrlA, AbaA and WetA initiates asexual development in *A. nidulans*. StuA, MedA, VosA are regulators of *brlA, abaA,* and *wetA* (Krijgsheld et al., 2013a).

VosA is a predicted transcription factor of the velvet family (Tao and Yu, 2011). This family also includes VeA and VelB of *A. nidulans* (see below). The Δ*vosA* strain shows uncontrolled activation of asexual development, whereas its over-expression blocks sporulation. The latter is probably explained by VosA mediated inhibition of *brlA* (Tao and Yu, 2011) (Figure 4). The proteins encoded by *stuA* and *medA* genes also affect *brlA* expression and also regulate *abaA* (Figure 4). Mutations in *stuA* of

A. nidulans results in shortened aerial hyphae, shortened conidiophores and the absence of metulae and phialides. Moreover, the conidiophores have reduced vesicle size and abnormal numbers of nuclei. Although the morphology of the conidiophores is affected in *stuA* mutants, neither temporal development nor conidiophore density is affected (Wu and Miller, 1997). Expression of *stuA* depends on *brlA* (Breakspear and Momany, 2007, Busby et al., 1996, Miller et al., 1992). In turn, StuA spatially restricts *brlA* and *abaA* expression (Figure 4), thus regulating proper spatial distribution of AbaA and BrlA (Miller et al., 1992, Wu and Miller, 1997). On the other hand, *medA* is involved in proper temporal expression of these genes (Adams et al., 1998, Busby et al., 1996). Gene *medA* acts as a repressor of *brlA* expression, while it activates *abaA* expression (Miller et al., 1992, Busby et al., 1996). The molecular basis of MedA function is not known yet. A Δ*medA* strain forms repeated layers of sterigmata and frequent reinitiated secondary conidiophores (Clutterbuck, 1969, Sewall et al., 1990). Taken together, conidiophore morphogenesis requires a finely tuned balance of at least BrlA, AbaA, MedA, StuA (Busby et al., 1996), VosA and other velvet complex genes (Boylan et al., 1987, Ni and Yu, 2007).

Upstream regulators of BrlA

Signaling cascades in *A. nidulans* are involved in the decision to grow vegetatively or to start asexual development (Figure 5). These cascades involve FluG and independently, two heterotrimeric G-protein complexes, both consisting of SfaD and GpgA (the Gβγ subunits) and the Gα subunits FadA and GanB, respectively. It is beyond the scope of this Thesis to discuss the trimeric G-protein signaling pathways. I will only discuss the role of *flbA*. This gene encodes a RGS domain protein that represses vegetative growth and stimulates sporulation (Figure 5). It stimulates the intrinsic GTPase activity of the Gα subunit FadA of a heterotrimeric G-protein. As a result, the Gα subunit is converted into the inactive GDP bound state (D'Souza et al., 2001, Yu et al., 1996, Yu et al., 1999) (Figure 5). Overexpression of *flbA* represses hyphal growth and stimulates conidiophore development under conditions that normally prevent sporula-

tion (Lee and Adams, 1994b, Lee and Adams, 1996). On the other hand, a Δ*flbA* strain shows reduced *brlA* expression and a fluffy phenotype. The Δ*flbA* strain does not form conidiophores, its mycelium proliferates uncontrolled, and masses of undifferentiated aerial hyphae are formed. Both the submerged and aerial hyphae autolyse when colonies mature (Lee and Adams, 1994b, Wieser et al., 1994). FlbA of *A. niger* has a similar function as its homologue in *A. nidulans* (Krijgsheld et al., 2013b).

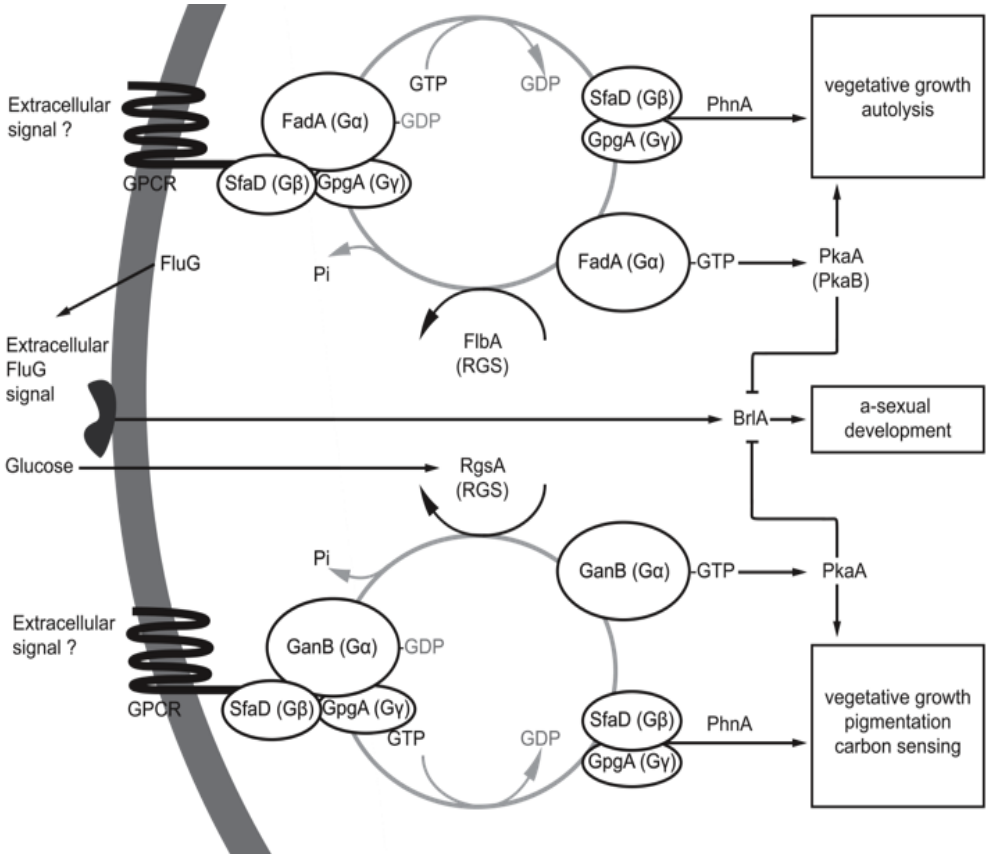

Figure 5. Signaling cascades in *A. nidulans* that result in vegetative growth or asexual reproduction. Signalling involves FluG (see Figure 6) and independently, two heterotrimeric G-protein complexes, both consisting of SfaD and GpgA (the Gβγ subunits) and the Gα subunits FadA and GanB, respectively. GTP-bound FadA and GanB stimulate vegetative growth and repress asexual reproduction via the cAMP PkaA pathway. The RGS proteins FlbA and RgsA hydrolyze the GTP bound to FadA and GanB, respectively, thereby repressing vegetative growth and promoting asexual development. The SfaD-GpgA dimer also stimulates vegetative growth. This is regulated by PhnA. Taken from (Krijgsheld et al., 2013a)

FluG activates sporulation by a derepression pathway that involves the transcription factor SfgA (Figure 6) (Seo et al., 2006). The Δ*sfgA* strain sporulates to a high extent

in liquid submerged cultures. On the other hand, overexpression of *sfgA* results in reduced conidiation, which is accompanied by delayed and reduced levels of brlA mRNA. Together, it was concluded that the primary role of FluG is to remove the repressive effects of SfgA (Seo et al., 2006). The low FluG signaling molecule levels in young colonies would result in *sfgA*-mediated repression of conidiation. Once the FluG factor has accumulated above a certain threshold, it inhibits the repression of conidiation by SfgA (Seo et al., 2006). SfgA has also been proposed to negatively regulate flbA (Figure 6). By this, the repression of SfgA by FluG will result in both activation of conidiation and inhibition of vegetative growth.

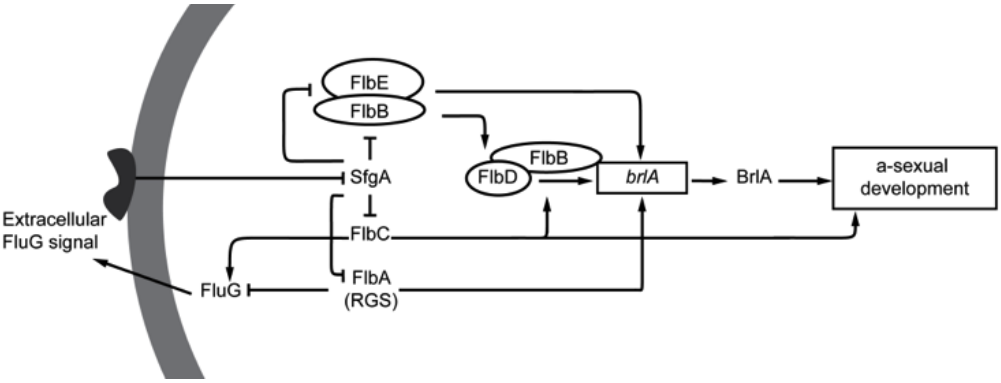

Figure 6. Model of upstream regulation of *brlA*. FluG is involved in the formation of an extracellular signaling molecule that activates an unknown receptor. At a certain concentration of the signaling molecule, the general suppressor SfgA is inhibited removing the repression of the *flb* genes. FlbB and FlbE form a complex that activates *brlA* leading to asexual development. FlbC activates *brlA* together with the FlbB/FlbD transcription complex. FlbC also activates *fluG* and regulatory genes that act downstream of BrlA. FlbA activates *brlA* by inactivating FadA and probably plays a role in repressing *fluG*. Adapted from (Etxebeste et al., 2010).

Apart from *flbA*, four other regulatory genes, *flbB, flbC, flbD, and flbE,* have been identified that act upstream of *brlA* (Wieser et al., 1994). All *flb* mutant strains show low *brlA* expression and a fluffy phenotype (Wieser et al., 1994). The mutants grow indeterminately and produce masses of aerial hyphae. SfgA acts downstream of *fluG* but upstream of *flbA-D*. The position of *flbE* in the developmental pathway is not clear (Seo et al., 2006). FluG would repress *sfgA* thus releasing the repression of the *flb* genes. Notably, *flb* genes are involved in regulation of *fluG* expression (Ruger-Herreros et al., 2011).

THE ROLE OF LIGHT

Regulatory genes involved in light-response

Sexual development of *A. nidulans* occurs in the dark, while asexual development mainly takes place in the light. Highest numbers of conidia are produced in white light or in a combination of red (680 nm) and blue (450 nm) light. Asexual sporulation is reduced when *A. nidulans* is exposed to only red or blue light (Purschwitz et al., 2008). Both blue and red light alone effectively inhibit sexual development to an extent similar to white light. VeA is a main regulator of the light response by acting as a positive regulator of sexual development and as a suppressor of asexual development (Kim et al., 2002). A Δ*veA* strain does not produce sexual fruiting bodies called cleistothecia (Kim et al., 2002). In contrast, *veA* over-expression results in reduced asexual development and increased production of cleistothecia, even under conditions where the wild-type hardly forms these sexual structures (i.e. in liquid medium or on solid medium containing a high concentration of potassium chloride). A sexual cycle has not been reported yet for *A. niger.* The role of VeA in *A. niger* was therefore of interest and was studied in Chapter 4.

Gene *veA* of *A. nidulans* encodes a velvet protein that contains a nuclear localization signal (NLS) (Kim et al., 2002, Stinnett et al., 2007). It is always expressed but its mRNA levels increase during sexual development. VeA migrates from the cytoplasm to the nucleus in the dark or when exposed to red light. Migration of VeA to the nucleus depends on the interaction between its NLS and the α-importin KapA (Stinnett et al., 2007) (Figure 7). Apart from KapA, VeA interacts with the regulator of secondary metabolism LaeA (Bok and Keller, 2004) and the VeA-like protein VelB (Bayram et al., 2008b, Bok and Keller, 2004) (Figure 7). VeA interacts with LaeA in the nucleus, whereas the complex of VeA and VelB can be found both in the cytoplasm and in the nucleus (Bok and Keller, 2004). The interaction with VeA explains why VelB can migrate into the nucleus despite the absence of an apparent NLS (Bayram et al., 2008b). Similar to the Δ*veA* strain, the Δ*velB* strain does not show light-dependent development. The Δ*velB* strain does not form cleistothecia in the light and in the dark.

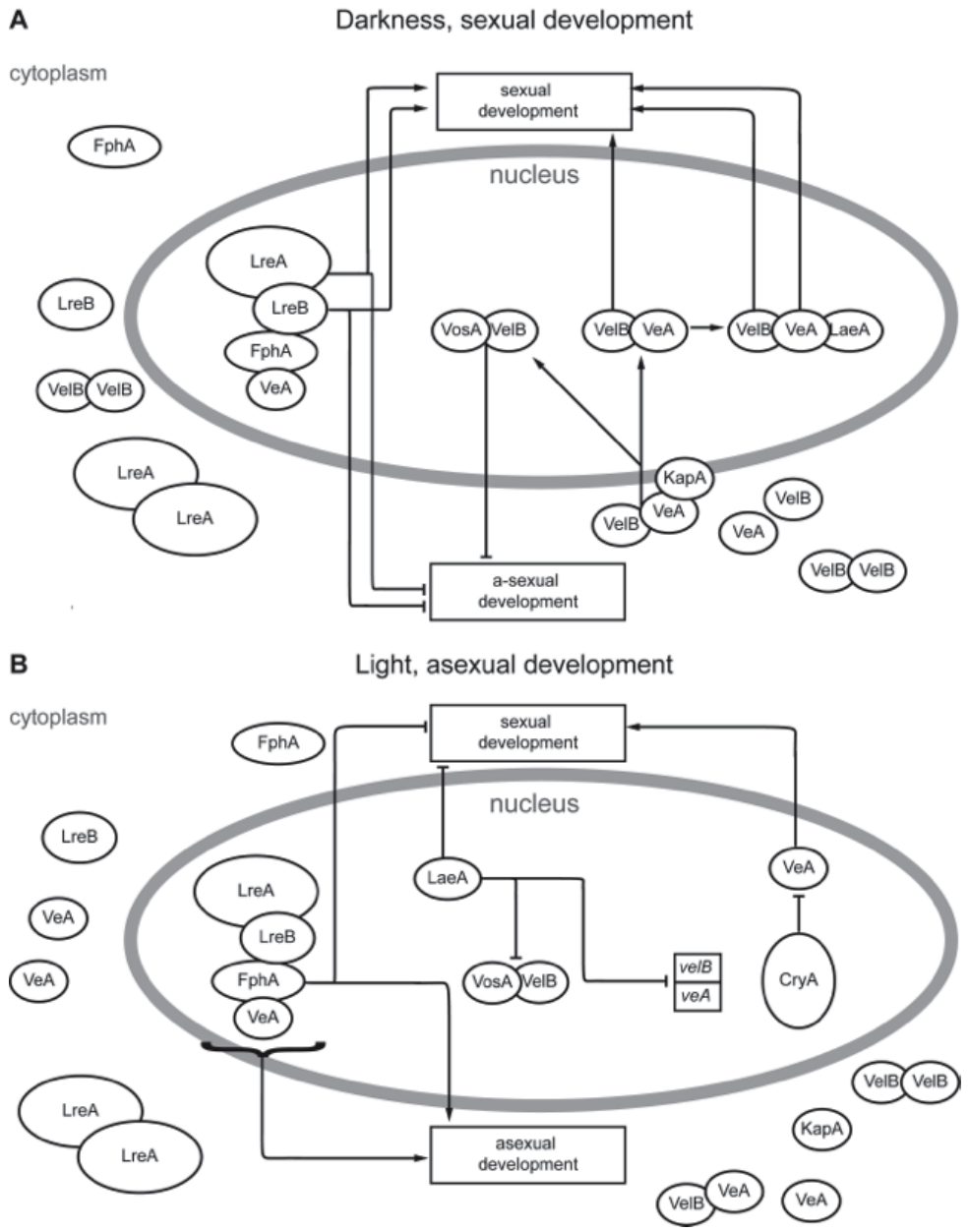

Figure 7. Light-regulated development in *A. nidulans*. (A) VelB enters the nucleus together with VeA and the α-importin KapA in the dark. Nuclear VeA and VelB form a dimeric complex or a trimeric complex together with LaeA to stimulate sexual development. VelB also forms a complex with VosA that represses asexual development. (B) In the light, LeA activity leads to reduced VelB and VosA levels. Consequently, repression of asexual development by the VelB-VosA complex is abolished. Moreover, reduced VelB levels abolishes stimulation of sexual development. Light is detected by the red light receptor FphA and the blue light receptors LreA and LreB. These light receptors form a complex in the nucleus with VeA. The cryptochrome/photolyase CryA also plays a role in light regulated development. Like FphA, it is a repressor of sexual development. Taken from (Krijgsheld et al., 2013a)

The effect of inactivation of *velB* on asexual sporulation, however is not as strong as

in the Δ*veA* strain. Over-expression of *veA* in the Δ*velB* strain and vice versa does not complement the developmental defects. From these it was concluded that a VeA/VelB complex mediates light regulated sexual and asexual development. The binding partner LaeA is also functional in asexual and sexual development (Sarikaya Bayram et al., 2010). The Δ*laeA* strain produces five times less conidia in the light when compared to the wild-type. Consequently, the absolute number of conidia that are produced by the Δ*laeA* strain is similar in the light and in the dark. Cleistothecia formation also occurs in the light in the Δ*laeA* strain. In fact, the number of cleistothecia in the mutant strain is similar in the light and the dark. These results are explained by assuming that the Δ*laeA* strain is unable to perceive light.

LaeA regulates levels of the VeA-like proteins VelB and VosA in a light-depended way. Amounts of VosA and VelB are reduced in the light. Consequently, abundance of the VosA/VelB complex is low, which releases the repression on asexual development (Figure 7). On the other hand, high amounts of VosA and VelB are found in the light in the ΔlaeA strain. Consequently, asexual developmental is inhibited, whereas sexual development is promoted (Sarikaya Bayram et al., 2010).A Δ*laeA* strain shows reduced levels of *abaA* mRNA but not of *brlA.* The effect on *abaA* expression may well explain the reduced ability of Δ*laeA* strains to form conidia. Similar to LaeA, VeA affects expression of downstream genes involved in asexual development. The higher conidiation profile in a Δ*veA* strain is accompanied by a change in expression of *brlA* (Kato et al., 2003).

Photoreceptors involved in light response

Three light sensors have been identified in *A. nidulans*. The phytochrome FphA represents a red-light receptor, while the white-collar complex of LreA and LreB senses blue light. The photolyase/cryptochrome CryA also senses blue light as well as UVA (Bayram et al., 2010). FphA is an activator of asexual development and a repressor of sexual reproduction. Conidiation is slightly reduced in the Δ*fphA* strain, which is irrespective of the presence of light (Purschwitz et al., 2008). Moreover, in contrast

to the wild-type the Δ*fphA* strain reproduces sexually in red light. Yet, the number of cleistothecia is only 10 % of that found in the dark (Blumenstein et al., 2005). Under the latter condition, formation of cleistothecia is similar in the wild-type and the Δ*fphA* strain (Purschwitz et al., 2008). FphA is located in the cytoplasm and in the nucleus (Purschwitz et al., 2008, Blumenstein et al., 2005). FphA that resides in the nucleus interacts with the LreB subunit of the white-collar complex that signals blue light (see below) (Purschwitz et al., 2008) (Figure 7). Nuclear-located FphA also has a physical interaction with VeA (Purschwitz et al., 2008). The light control of VeA might be activated during development via a direct interaction with FphA.

LreA and LreB form the white-collar blue light receptor (Purschwitz et al., 2008). The Δ*lreA* and Δ*lreB* strains form somewhat more conidia when compared to the wild-type, irrespective of the presence of light. This suggests that LreA and LreB repress conidia formation (Purschwitz et al., 2008). Notably, the number of conidiospores in the Δ*lreA*Δ*fphA* strain, the Δ*lreB*Δ*fphA* strain, and the Δ*lreA*Δ*lreB*Δ*fphA* strain is strongly decreased when compared to the wild-type. Yet, both in the dark and in the light a basal level of conidiation is observed in these strains. Cleistothecia production in the dark is reduced by 70 % and 30 %, respectively, in the Δ*lreA* and Δ*lreB* strains when compared to the wild-type. Strains Δ*lreA*Δ*fphA*, Δ*lreB*Δ*fphA*, and Δ*lreA*Δ*lreB*Δ*fphA* behave like the Δ*lreB* strain. When exposed to white light, cleistothecium formation is nearly absent in the Δ*lreA* and Δ*lreB* strains. This effect is suppressed by inactivation of *fphA* in these strains. Taken together, LreA and LreB act as activators of the sexual cycle and their activity is repressed by light through the action of FphA (Purschwitz et al., 2008). LreB is also involved in activation of the asexual cycle by induction of *brlA* (Ruger-Herreros et al., 2011). It may be that LreB directly controls *brlA* via its DNA binding domain (Figure 7).

CryA of *A. nidulans* is a combined cryptochrome/photolyase that has no DNA binding domain. It resides in the nucleus where it repairs UV induced DNA damage and controls fruiting body formation under both UVA and blue light conditions (350-370 and 450 nm) (Bayram et al., 2008a). The Δ*cryA* strain shows no phenotype on

solid medium under standard laboratory conditions but in submerged cultures Hülle cells (nurturing cells of the fruiting bodies), but not cleistothecia (i.e. the fruiting bodies), are formed (Bayram et al., 2008a). These data suggest that CryA is a negative regulator of sexual development but has no role in asexual development.

OUTLINE OF THE THESIS

The aim of this study was to study mechanisms underlying zonal secretion in the mycelium of *A. niger.* I particularly focused on homologues of genes involved in asexual reproduction in *A. nidulans.* These genes were proposed to function in sporulation inhibited secretion in *A. niger.*

Chapter 2 describes the *A. niger* UU-A001.13 strain in which multiple copies of the amylolytic regulatory gene *amyR* had been introduced. Surprisingly, glucoamylase secretion was observed throughout the mycelium of this strain, which contrasts the restricted release of this enzyme at the colony periphery of the wild-type and other *amyR* over-expressing strains. Sequencing the genome of strain UU-A001.13 revealed three loci in which introduced vectors had integrated. Part of the *fluG* gene had been deleted as a consequence of the transformation and its 3' end had been disrupted by integration of the transformation vector. The Δ*fluG* strain of *A. niger* showed breakdown of starch under the whole colony like UU-A001.13. Together with transcriptome analysis these data indicate that *fluG* is involved in zonal expression of amylolytic genes in *A. niger.*

Chapter 3 further explores the role of FluG in *A. niger.* Neither morphology and spatial distribution of conidiophores nor the number of spores produced per surface area and germination efficiency were affected in the Δ*fluG* strain of *A. niger*. Moreover, no changes were observed in spatial patterns of growth and secretion. The Δ*fluG* strain did show increased release of proteins on maltose containing medium. A transcriptome analysis showed that FluG of *A. niger* is affecting spatial expression of genes

including transcription factor genes and genes encoding secreted proteins. The effect on secreted proteins may link FluG to asexual development in *A. niger*

Chapter 4 describes the function of *veA* of *A. niger*. Conidia of the Δ*veA* strain germinated faster when compared to those of the wild-type but radial growth of colonies of the deletion strain was reduced. This was accompanied by a 2-fold reduction in biomass and a wavy phenotype of hyphae. The spatial positioning of the conidiophores of the Δ*veA* strain was also affected. The number of these reproductive structures in the center of the colony was reduced. Moreover, the length and the width of the stalk of the conidiophore was reduced nearly 2-fold in the Δ*veA* strain, while the diameter of the conidiophore vesicle and the conidiophore were 2-fold and 3-fold reduced. The latter explains, at least to a large extent, why the Δ*veA* strain formed about 17 (in the light) to 8 (in the dark) fold less conidia per surface area of the colony.

Chapter 5 describes the role of light on asexual development and secretion in *A. niger.* Cultures grown under white or blue light formed condiophores more equally distributed over the colony surface when compared cultures grown in the dark or under red or green light. Yet, spore numbers per surface area was similar under all light regimes. ^{14}C-labelling showed that light-grown wild-type and Δ*fluG* cultures secrete proteins mainly at the periphery, while protein secretion is more evenly distributed over the colony surface in the case of dark grown cultures. In contrast, the Δ*veA* strain secreted proteins in the colony center both in the light and the dark. This zone produced some conidiophores. Together, these data show that protein release in the culture medium is light and VeA dependent.

Results are summarized and discussed in **Chapter 6.**

REFERENCES

ADAMS, T. H., BOYLAN, M. T. & TIMBERLAKE, W. E. 1988. *brlA* is necessary and sufficient to direct conidiophore development in *Aspergillus nidulans*. *Cell,* 54**,** 353-362.

ADAMS, T. H., WIESER, J. K. & YU, J. H. 1998. Asexual sporulation in Aspergillus nidulans. *Microbiol Mol Biol Rev,* 62**,** 35-54.

AGNIHOTRI, V. P. 1964. Studies on Aspergilli. Xvi. Effect of Ph, Temperature, and Carbon and Nitrogen Interaction. *Mycopathol Mycol Appl,* 24**,** 305-314.

AL-DOORY, Y. (ed.) 1984 *Chapter 3,* Philadelphia: Lea and Febiger.

ANDRIANOPOULOS, A. & TIMBERLAKE, W. E. 1994. The *Aspergillus nidulans abaA* gene encodes a transcriptional activator that acts as a genetic switch to control development. *Mol Cell Biol,* 14**,** 2503-2515.

ASTORECA, A., MAGNOLI, C., RAMIREZ, M. L., COMBINA, M. & DALCERO, A. 2007. Water activity and temperature effects on growth of *Aspergillus niger*, *A. awamori* and *A. carbonarius* isolated from different substrates in Argentina. *Int J Food Microbiol,* 119**,** 314-318.

AYERST, G. 1969. The effects of moisture and temperature on growth and spore germination in some fungi. *J Stored Products Res* 5**,** 127-141.

BAYRAM, O., BIESEMANN, C., KRAPPMANN, S., GALLAND, P. & BRAUS, G. H. 2008a. More than a repair enzyme: *Aspergillus nidulans* photolyase-like CryA is a regulator of sexual development. *Mol Biol Cell,* 19**,** 3254-3262.

BAYRAM, O., BRAUS, G. H., FISCHER, R. & RODRIGUEZ-ROMERO, J. 2010. Spotlight on *Aspergillus nidulans* photosensory systems. *Fungal Genet Biol,* 47**,** 900-908.

BAYRAM, O., KRAPPMANN, S., NI, M., BOK, J. W., HELMSTAEDT, K., VALERIUS, O., BRAUS-STROMEYER, S., KWON, N. J., KELLER, N. P., YU, J. H. & BRAUS, G. H. 2008b. VelB/VeA/LaeA complex coordinates light signal with fungal development and secondary metabolism. *Science,* 320**,** 1504-1506.

BENNETT, J. W. 2010. An overview of the genus *Aspergillus*. *In:* MACHIDA, M. & GOMI, K. (eds.) *Aspergillus: Molecular Biology and Genomics.* Portland: Caister Academic Press.

BEZJAK, V. & ARYA, O. P. 1970. Otomycosis due to Aspergillus niger. *East Afr Med J,* 47**,** 247-253.

BLEICHRODT, R. 2012. Intercompartmental streaming in *Aspergillus*. *PhD Thesis, University of Utrecht.*

BLEICHRODT, R. J., VAN VELUW, G. J., RECTER, B., MARUYAMA, J., KITAMOTO, K. & WÖSTEN, H. A. 2012. Hyphal heterogeneity in *Aspergillus oryzae* is the result of dynamic closure of septa by Woronin bodies. *Mol Microbiol,* 86**,** 1334-1344.

BLUMENSTEIN, A., VIENKEN, K., TASLER, R., PURSCHWITZ, J., VEITH, D., FRANKENBERG-DINKEL, N. & FISCHER, R. 2005. The *Aspergillus nidulans* phytochrome FphA represses sexual development in red light. *Curr Biol,* 15**,** 1833-1838.

BOK, J. W. & KELLER, N. P. 2004. LaeA, a regulator of secondary metabolism in *Aspergillus spp*. *Eukaryot Cell,* 3**,** 527-535.

BOYLAN, M. T., MIRABITO, P. M., WILLETT, C. E., ZIMMERMAN, C. R. & TIMBERLAKE, W. E. 1987. Isolation and physical characterization of three essential conidiation genes from *Aspergillus nidulans*. *Mol Cell Biol,* 7**,** 3113-3118.

BREAKSPEAR, A. & MOMANY, M. 2007. *Aspergillus nidulans* conidiation genes *dewA, fluG*, and *stuA* are differentially regulated in early vegetative growth. *Eukaryot Cell,* 6**,** 1697-1700.

BUSBY, T. M., MILLER, K. Y. & MILLER, B. L. 1996. Suppression and enhancement of the *Aspergillus nidulans* medusa mutation by altered dosage of the bristle and stunted genes. *Genetics,* 143**,** 155-163.

CLUTTERBUCK, A. J. 1969. A mutational analysis of conidial development in *Aspergillus nidulans*. *Genetics,* 63**,** 317-327.

CONESA, A., PUNT, P. J., VAN LUIJK, N. & VAN DEN HONDEL, C. A. 2001. The secretion pathway in filamentous fungi: a biotechnological view. *Fungal Genet and Biol,* 33**,** 155-171.

D'SOUZA, C. A., LEE, B. N. & ADAMS, T. H. 2001. Characterization of the role of the FluG protein in asexual development of *Aspergillus nidulans*. *Genetics,* 158**,** 1027-1036.

DENNING, D. W. 1998. Invasive aspergillosis. *Clin Infect Dis,* 26**,** 781-803.

ETXEBESTE, O., GARZIA, A., ESPESO, E. A. & UGALDE, U. 2010. *Aspergillus nidulans* asexual development: making the most of cellular modules. *Trends Microbiol,* 18**,** 569-576.

FANG, H., ZHANG, W., NIU, X., LIU, Z., LU, C., WEI, H. & YUAN, S. 2014. Stipe wall extension of *Flammulina velutipes* could be induced by an expansin-like protein from *Helix aspersa*. *Fungal Biol,* 118**,** 1-11.

FINKELSTEIN, D. B., RAMBOSEK, J., CRAWFORD, M. S., SOLIDAY, C. L., MCADA, P. C., LEACH, J., HERSHBERGER, C. L., QUEENER, S. W. & HEGEMAN, G. 1989. *Protein secretion in Aspergillus niger,* Washington, DC, American Society for Microbiology.

GALAGAN, J. E., CALVO, S. E., CUOMO, C., MA, L. J., WORTMAN, J. R., BATZOGLOU, S., LEE, S. I., BASTURKMEN, M., SPEVAK, C. C., CLUTTERBUCK, J., KAPITONOV, V., JURKA,

J., SCAZZOCCHIO, C., FARMAN, M., BUTLER, J., PURCELL, S., HARRIS, S., BRAUS, G. H., DRAHT, O., BUSCH, S., D'ENFERT, C., BOUCHIER, C., GOLDMAN, G. H., BELL-PEDERSEN, D., GRIFFITHS-JONES, S., DOONAN, J. H., YU, J., VIENKEN, K., PAIN, A., FREITAG, M., SELKER, E. U., ARCHER, D. B., PENALVA, M. A., OAKLEY, B. R., MOMANY, M., TANAKA, T., KUMAGAI, T., ASAI, K., MACHIDA, M., NIERMAN, W. C., DENNING, D. W., CADDICK, M., HYNES, M., PAOLETTI, M., FISCHER, R., MILLER, B., DYER, P., SACHS, M. S., OSMANI, S. A. & BIRREN, B. W. 2005. Sequencing of *Aspergillus nidulans* and comparative analysis with *A. fumigatus* and *A. oryzae*. *Nature,* 438**,** 1105-1115.

GARCIA-AGUDO, L., AZNAR-MARIN, P., GALAN-SANCHEZ, F., GARCIA-MARTOS, P., MARIN-CASANOVA, P. & RODRIGUEZ-IGLESIAS, M. 2011. Otomycosis due to filamentous fungi. *Mycopathologia,* 172**,** 307-310.

HAWKSWORTH, D. L. 2011. Naming *Aspergillus* species: progress towards one name for each species. *Med Mycol,* 49 Suppl 1**,** S70-76.

KATO, N., BROOKS, W. & CALVO, A. M. 2003. The expression of sterigmatocystin and penicillin genes in *Aspergillus nidulans* is controlled by *veA*, a gene required for sexual development. *Eukaryot Cell,* 2**,** 1178-1186.

KIM, H., HAN, K., KIM, K., HAN, D., JAHNG, K. & CHAE, K. 2002. The *veA* gene activates sexual development in *Aspergillus nidulans*. *Fungal Genet Biol,* 37**,** 72-80.

KRIJGSHELD, P., ALTELAAR, A. F., POST, H., RINGROSE, J. H., MULLER, W. H., HECK, A. J. & WÖSTEN, H. A. 2012. Spatially resolving the secretome within the mycelium of the cell factory *Aspergillus niger*. *J Proteome Res,* 11**,** 2807-2818.

KRIJGSHELD, P., BLEICHRODT, R., VAN VELUW, G. J., WANG, F., MULLER, W. H., DIJKSTERHUIS, J. & WÖSTEN, H. A. 2013a. Development in *Aspergillus*. *Stud Mycol,* 74**,** 1-29.

KRIJGSHELD, P., NITSCHE, B. M., POST, H., LEVIN, A. M., MULLER, W. H., HECK, A. J., RAM, A. F., ALTELAAR, A. F. & WÖSTEN, H. A. 2013b. Deletion of *flbA* Results in Increased Secretome Complexity and Reduced Secretion Heterogeneity in Colonies of *Aspergillus niger*. *J Proteome Res,* 12**,** 1809-1819.

LACEY, J. (ed.) 1980. *The microflora of graindust. In: Occupational pulmonary disease: focus on graindust and health,* New York: Academic Press.

LEE, B. N. & ADAMS, T. H. 1994a. The *Aspergillus nidulans fluG* gene is required for production of an extracellular developmental signal and is related to prokaryotic glutamine synthetase I. *Genes Dev,* 8**,** 641-651.

LEE, B. N. & ADAMS, T. H. 1994b. Overexpression of *flbA*, an early regulator of *Aspergillus* asexual sporulation, leads to activation of *brlA* and premature initiation of development. *Mol Microbiol,* 14**,** 323-334.

LEE, B. N. & ADAMS, T. H. 1996. *fluG* and *flb*A function interdependently to initiate conidiophore development in *Aspergillus nidulans* through *brlA* beta activation. *EMBO J,* 15**,** 299-309.

LEONG, S. L., HOCKING, A. D. & SCOTT, E. S. 2006. Effect of temperature and water activity on growth and ochratoxin A production by Australian *Aspergillus carbonarius* and *A. niger* isolates on a simulated grape juice medium. *Int J Food Microbiol,* 110**,** 209-216.

LEVIN, A. M., DE VRIES, R. P., CONESA, A., DE BEKKER, C., TALON, M., MENKE, H. H., VAN PEIJ, N. N. & WÖSTEN, H. A. 2007a. Spatial differentiation in the vegetative mycelium of *Aspergillus niger*. *Eukaryot Cell,* 6**,** 2311-2322.

LEVIN, A. M., DE VRIES, R. P. & WÖSTEN, H. A. 2007b. Localization of protein secretion in fungal colonies using a novel culturing technique; the ring-plate system. *J Microbiol Methods,* 69**,** 399-401.

MARSHALL, M. A. & TIMBERLAKE, W. E. 1991. *Aspergillus nidulans wetA* activates spore-specific gene expression. *Mol Cell Biol,* 11**,** 55-62.

MEHRA, S. & JAITLY, A. 1995. pH and temperature optima for growth and sporulation in some common fungi from city waste. *Mycoscience* 36**,** 243-246.

MEYER, V., WU, B. & RAM, A. F. 2011. *Aspergillus* as a multi-purpose cell factory: current status and perspectives. *Biotechnol Lett,* 33**,** 469-476.

MILLER, K. Y., WU, J. & MILLER, B. L. 1992. StuA is required for cell pattern formation in *Aspergillus*. *Genes Dev,* 6**,** 1770-1782.

MIRABITO, P. M., ADAMS, T. H. & TIMBERLAKE, W. E. 1989. Interactions of three sequentially expressed genes control temporal and spatial specificity in *Aspergillus* development. *Cell,* 57**,** 859-868.

NI, M. & YU, J. H. 2007. A novel regulator couples sporogenesis and trehalose biogenesis in *Aspergillus nidulans*. *PLoS One,* 2**,** e970.

PANASENKO, V. 1967. Ecology of microfungi. *Bot Rev***,** 189-215.

PAWAR, N. V., PATIL, V. B., KAMBLE, S. S. & DIXIT, G. B. 2008. First report of *Aspergillus niger* as a plant pathogen on *Zingiber officinale* from India. *Plant Disease,* 92**,** 1368-1368.

PITT, J. I. 1981. *Food storage and biodeterioration,* New York, Academic Press.

PUNT, P. J., VAN BIEZEN, N., CONESA, A., ALBERS, A., MANGNUS, J. & VAN DEN HONDEL, C. 2002. Filamentous fungi as cell factories for heterologous protein production. *Trends Biotechnol,* 20**,** 200-206.

PURSCHWITZ, J., MULLER, S., KASTNER, C., SCHOSER, M., HAAS, H., ESPESO, E. A., ATOUI, A., CALVO, A. M. & FISCHER, R. 2008. Functional and physical interaction of blue- and red-light sensors in *Aspergillus nidulans*. *Curr Biol,* 18**,** 255-259.
RUGER-HERREROS, C., RODRIGUEZ-ROMERO, J., FERNANDEZ-BARRANCO, R., OLMEDO, M., FISCHER, R., CORROCHANO, L. M. & CANOVAS, D. 2011. Regulation of conidiation by light in *Aspergillus nidulans*. *Genetics,* 188**,** 809-822.
RUTT, A. L. & SATALOFF, R. T. 2008. *Aspergillus* otomycosis in an immunocompromised patient. *Ear Nose Throat J,* 87**,** 622-623.
SARIKAYA BAYRAM, O., BAYRAM, O., VALERIUS, O., PARK, H. S., IRNIGER, S., GERKE, J., NI, M., HAN, K. H., YU, J. H. & BRAUS, G. H. 2010. LaeA control of velvet family regulatory proteins for light-dependent development and fungal cell-type specificity. *PLoS Genet,* 6**,** e1001226.
SEO, J. A., GUAN, Y. & YU, J. H. 2006. FluG-dependent asexual development in *Aspergillus nidulans* occurs via derepression. *Genetics,* 172**,** 1535-1544.
SEWALL, T. C., MIMS, C. W. & TIMBERLAKE, W. E. 1990. *abaA* controls phialide differentiation in *Aspergillus nidulans*. *Plant Cell,* 2**,** 731-739.
STEVENS, D. A., KAN, V. L., JUDSON, M. A., MORRISON, V. A., DUMMER, S., DENNING, D. W., BENNETT, J. E., WALSH, T. J., PATTERSON, T. F. & PANKEY, G. A. 2000. Practice guidelines for diseases caused by *Aspergillus*. Infectious Diseases Society of America. *Clin Infect Dis,* 30**,** 696-709.
STINNETT, S. M., ESPESO, E. A., COBENO, L., ARAUJO-BAZAN, L. & CALVO, A. M. 2007. *Aspergillus nidulans* VeA subcellular localization is dependent on the importin alpha carrier and on light. *Mol Microbiol,* 63**,** 242-255.
TAO, L. & YU, J. H. 2011. AbaA and WetA govern distinct stages of *Aspergillus fumigatus* development. *Microbiology,* 157**,** 313-326.
VINCK, A., DE BEKKER, C., OSSIN, A., OHM, R. A., DE VRIES, R. P. & WÖSTEN, H. A. 2011. Heterogenic expression of genes encoding secreted proteins at the periphery of *Aspergillus niger* colonies. *Environm Microbiol,* 13**,** 216-225.
WESSELS, J. G. H. 1988. A steady-state model for apical wall growth in fungi. *Acta Bot Neerl***,** 3-16.
WESSELS, J. G. H. 1993. Wall growth, protein excretion and morphogenesis in fungi. *New Phytol* 123**,** 397-413.
WIESER, J., LEE, B. N., FONDON, J., 3RD & ADAMS, T. H. 1994. Genetic requirements for initiating asexual development in *Aspergillus nidulans*. *Curr Genet,* 27**,** 62-69.
WÖSTEN, H. A., MOUKHA, S. M., SIETSMA, J. H. & WESSELS, J. G. 1991. Localization of growth and secretion of proteins in *Aspergillus niger*. *J Gen Microbiol,* 137**,** 2017-2023.
WÖSTEN, H. A., RICHTER, M. & WILLEY, J. M. 1999. Structural proteins involved in emergence of microbial aerial hyphae. *Fungal Genet Biol,* 27**,** 153-160.
WÖSTEN, H. A., VAN VELUW, G. J., DE BEKKER, C. & KRIJGSHELD, P. 2013. Heterogeneity in the mycelium: implications for the use of fungi as cell factories. *Biotechnol Lett,* 35**,** 1155-1164.
WÖSTEN, H. A. & WILLEY, J. M. 2000. Surface-active proteins enable microbial aerial hyphae to grow into the air. *Microbiology,* 146 767-773.
WU, J. & MILLER, B. L. 1997. *Aspergillus* asexual reproduction and sexual reproduction are differentially affected by transcriptional and translational mechanisms regulating stunted gene expression. *Mol Cell Biol,* 17**,** 6191-6201.
YU, J. H., ROSEN, S. & ADAMS, T. H. 1999. Extragenic suppressors of loss-of-function mutations in the aspergillus FlbA regulator of G-protein signaling domain protein. *Genetics,* 151**,** 97-105.
YU, J. H., WIESER, J. & ADAMS, T. H. 1996. The Aspergillus FlbA RGS domain protein antagonizes G protein signaling to block proliferation and allow development. *EMBO J,* 15**,** 5184-90.

Chapter 2

FluG is involved in spatial expression of AmyR regulated genes in *Aspergillus niger*

Fengfeng Wang, Charissa de Bekker, Marc Hulsman, Benjamin M. Nitsche, Arthur F.J. Ram, Marcel Reinders, Ronald P. de Vries and Han A. B. Wösten.

ABSTRACT

Colonies of *Aspergillus niger* are characterized by zonal heterogeneity in gene expression and secretion. For instance, the glucoamylase gene *glaA* is 3-fold higher expressed at the periphery of maltose-grown colonies when compared to the center. As a consequence, its encoded protein is secreted at the outer part of the colony. Here, we introduced multiple copies of *amyR* in *A. niger.* Most transformants over-expressing this regulatory gene of amylolytic genes still displayed heterogeneous *glaA* expression, which correlated with spatial secretion of glucoamylase. However, heterogeneity was abolished in the UU-A001.13 transformant. This transformant showed glucoamylase secretion throughout the mycelium. This was accompanied with starch degradation throughout the medium underlying the colony. Sequencing the genome of strain UU-A001.13 revealed three loci in which introduced vectors had integrated. The endogenous *amyR* copy and part of the *fluG* gene had been deleted as a consequence of the transformation. The 3' end of the latter gene, known to be involved in asexual development in *Aspergillus nidulans,* had also been disrupted by integration of transformation vectors. The Δ*fluG* strain of *A. niger* showed breakdown of starch under the whole colony like UU-A001.13. 6 out of 16 AmyR regulated genes (excluding *glaA*) were upregulated in the outer part of Δ*fluG* colonies and 6 genes were down regulated (including *glaA*) in the center when compared to wild type. This suggests that starch degrading enzymes that are secreted at the colony periphery are slowly released from the cell wall; thus explaining increased starch degrading activity in the center of Δ*fluG* colonies. Together, it is concluded that *fluG* is involved in zonal expression of amylolytic genes in *A. niger* and that absence of this gene partly explains the phenotype of the UU-A001.13 transformant.

INTRODUCTION

The genus *Aspergillus* is well known for its ability to produce large amounts of a variety of enzymes that degrade plant polysaccharides (Coutinho et al., 2009). Zones of colonies of *Aspergillus niger* are heterogeneous with respect to secretion (Levin

et al., 2007b, Krijgsheld et al., 2012, Wösten et al., 1991), and expression of genes encoding secreted proteins (Levin et al., 2007a, de Bekker et al., 2011a, de Bekker et al., 2011b, van Veluw et al., 2013). In fact, secretion (Wösten et al., 1991) and gene expression (Vinck et al., 2005, Vinck et al., 2011, de Bekker et al., 2011b) can even be heterogeneous within a zone of a colony.

Growth mainly occurs at the periphery of *A. niger* colonies (Krijgsheld et al., 2013a). This growth zone secretes proteins such as glucoamylase GlaA (Wösten et al., 1991, Levin et al., 2007a). Secretion of GlaA correlates with expression of its gene. It is three-fold higher expressed at the colony periphery when compared to the colony centre (Levin et al., 2007a). AmyR regulates expression of *glaA* and other genes encoding enzymes that are active on glucose- and galactose-containing oligo- and polysaccharides (Petersen et al., 1999, vanKuyk et al., 2011, Gomi et al., 2000, Tani et al., 2001).

Here, multiple copies of *amyR* were introduced in *A. niger.* Zonal heterogeneity in expression and secretion of GlaA were not affected in transformants except for strain UU-A001.13. In this strain, starch was degraded throughout the medium underlying the colony. As a consequence of the transformation, gene *fluG* had been inactivated in UU-A001.13. Inactivation of this gene in a wild-type background also resulted in starch degradation throughout the medium underlying the mycelium. However, this did not correlate with glaA expression. Thus, inactivation of *fluG* explains partly the phenotype of UU-A001.13.

MATERIAL AND METHODS

Growth condition and strains

Strains of *A. niger* used in this study (Table 1) were grown at 30 °C under constant white light (Osram Lumilux L36w/840, Osram, Munich, Germany) of 700 lux. *A. niger* was grown in minimal medium (MM) with a pH of 6 containing per liter 6 g NaNO3, 1.5 g KH_2PO_4, 0.5 g KCL, 0.5 g $MgSO_4 \cdot 7H_2O$, 200 µl trace element solution according

to (Vishniac and Santer, 1957), 1.5 % agar, and 25 mM maltose as carbon source. Alternatively, *A. niger* was grown at 250 rpm in 250 ml Erlenmeyer flasks in 100 ml complete medium (CM; MM with 2 g l^{-1} trypton, 1 g l^{-1} casamino acids, 1 g l^{-1} yeast extract, 0.5 g l^{-1} yeast ribonucleic acids, and 1 % glucose). If necessary, the medium was supplemented with 0.2 g l^{-1} arginine, 0.2 g l^{-1} leucine, 0.2 g l^{-1} uridine, and / or 1 mg l^{-1} nicotinamide.

Table 1. Strains used in this study.

Strain	Genotype	Reference
N402	*cspA1* derivative of ATCC 9029	(Bos et al., 1988)
NW249	*cspA1*, ΔargB, *pyrA6, nicA1, leuA1*	(Jalving et al., 2000)
UU-049.1	*cspA1*, *pyrA6, nicA1, leuA1*, Δ*argB*::pIM2101[argB+]	(Battaglia et al., 2011)
UU-A001.13	*cspA1*, *pyrA6, nicA1, leuA1*, Δ*argB*::pIM2101[argB+], pJG01	this study
UU-A001.24	*cspA1*, *pyrA6, nicA1, leuA1*, Δ*argB*::pIM2101[argB+], pJG01	this study
N402Δ*fluG*	*cspA1*, Δ*fluG,* hyg^+	this study
N402Δ*fluG fluG*	*cspA1*, *amdS*$^+$*,* hyg^+	this study

Colonies on agar medium were grown as sandwiched cultures in a water saturated box (Wösten et al., 1991). To this end, the fungus was grown in between two perforated polycarbonate (PC) membranes (diameter of 76 mm; pore size 0.1 µm; Osmonics, GE Water Technologies, Trevose, PA) in a 0.2 mm thin layer of 1.25 % agarose. Sandwiched cultures were inoculated in the centre of the PC membrane with 1.5 µl spore suspension (10^5 spores $µl^{-1}$ saline Tween [0.8 % NaCl, 0.005 % Tween-80]). The top membrane was positioned on the agarose layer after 24 h of incubation.

Inactivation of *fluG*

Up- and downstream flanking regions of the coding sequence of *fluG* (An14g03390) were amplified from chromosomal DNA of *A. niger* N402 using Taq polymerase and primer pairs 1 and 2 (Table 2). As a result, a NotI and XbaI / XhoI site had been introduced at the 5' and 3' ends of the upstream flank, respectively, and a XhoI and KpnI site at 5' and 3' ends of the downstream flank, respectively. The amplified products

were blunt end ligated in pJET 1.2 (Fermentas, Thermo scientific, Waltham, USA). The resulting plasmids were digested with NotI and XhoI and XhoI and KpnI, respectively. This was followed by a three point ligation with pBluescriptIISK(+) that had been digested with NotI and KpnI. The XhoI / XbaI fragment of PAN7-1 (Punt et al., 1987) containing the hygromycine resistance cassette was inserted in the pBluescriptIISK(+) vector that contained both flanks of *fluG* and that been digested with the same enzymes. This resulted in the *fluG* deletion construct *BNOfluG*. This construct was digested with NotI and KpnI. The flanking sequences interspersed with the antibiotic resistance cassette were introduced in *A. niger* N402.

Complementation of the Δ*fluG* strain

Upstream and downstream flanking regions and the coding sequence of *fluG* were amplified from chromosomal DNA of *A. niger* N402 using Phusion® High-Fidelity DNA polymerase (Finnzymes; www.finnzymes.com) and primers 3a and 3b (Table 2). As a result, a NotI and HindIII site had been introduced at the 5' and 3' ends of the amplified fragment, respectively. These sites were used to introduce the PCR product into pAN01 that had been cut with the same enzymes. Vector pAN01is a derivative of pAN2-4 vector which contains the *gpd* promoter and *trpC* terminator (Punt et al., 1990, Mullaney et al., 1985). The *gpd* promoter is replaced by the *glaA* promoter of 822 bp in pAN01. By cutting with NotI and HindIII, the *glaA* promoter was replaced by flanking regions and the coding sequence of *fluG.* This resulted in the *fluG* complement construct pAN01*fluG*.

Isolation of genomic DNA

Chromosomal DNA was isolated essentially as described (van Peer et al., 2009). Mycelium from liquid shaken cultures was harvested by filtering over nylon gauze, frozen in liquid nitrogen, and homogenized with a *TissueLyser II* (Qiagen, Venlo, The Netherlands). 200 mg of the homogenate was mixed with 0.9 ml extraction buffer (2 % sodium dodecyl sulfate, 24 mg ml^{-1} 4-aminosalycilic acid, 20 % 5 × RNB [121.1 g

Tris-HCl, 73.04 g NaCl, and 95.1 g EGTA l^{-1}; pH 8.5]) and 0.9 ml *phenol : chloroform : isoamylalcohol* (25 : 24 : 1). After incubation at room temperature for 5 min, the mixture was centrifuged for 10 min at 14000 *g*. The aqueous phase was extracted with 0.5 ml chloroform. The DNA was precipitated with 0.8 volume isopropanol and pelleted at 14000 *g* for 10 min. After washing with 70 % ethanol, the DNA was dissolved in 200 µl TE (10 mM Tris-HCl, 1 mM EDTA; pH8.0) containing 10 µg RNase ml^{-1}.

Transformation

Transformation of *A. niger* was performed as described (Meyer et al., 2010). Protoplasts of *A. niger* were generated using 40 mg lysing enzymes (L-1412, Sigma-Aldrich, Zwijndrecht, Netherlands) per gram wet weight of mycelium. Vector, BNO*fluG* was introduced in protoplasts of N402 to inactivate *fluG*. Transformants were selected on MMS agar (MM containing per liter 325 g sucrose and 12 g agar) supplemented with 200 µg ml^{-1} hygromycine and 50 µg ml^{-1} caffeine. For *amyR* over-expression, plasmids pJG01 and pIM2101 were co-introduced in NW249. Plasmid pJG01 contains the *A. niger amyR* gene (An04g06910) as a 4.3 kb NsiI fragment in pGEM11 (Yuan et al., 2008), while pIM2101 contains the *argB* gene (Lenouvel et al., 2002). Transformants were selected on MMS plates in the absence of arginine. Construct pAN01*fluG* was introduced in Δ*fluG* protoplasts together with construct p35R2 that contains the acetamidase gene *amdS* (Kelly and Hynes, 1985). Transformants of *A. niger* were selected on MMS medium containing 0.3 g l^{-1} acetamide and 0.85 g l^{-1} CsCl. Complementation was confirmed by PCR analysis using primers 4a and 4b (Table 2).

Table 2. Primers used in this study.

Primer	Description	Sequence
1a	5' flank *fluG* fw primer	ATAAGAATGCGGCCGCGTGACTTGGAGGAGAGGAGCTG
1b	5' flank *fluG* rev primer	CCGCTCGAGTTAATCCTAGTCTAGAGCTGATTGGTTGGCCGGTTC
2a	3' flank *fluG* fw primer	CCGCTCGAGACCCTGTGCATACATACATAGC
2b	3' flank *fluG* rev primer	CGGGGTACCCCTCGCACTGATCGCCATATC

Table 2 continued

3a	*fluG* fw NotI	TATAAGCGGCCGCACACGGCTCTAGGAGAACCC
3b	*fluG* bw HindIII	CGCGAAGCTTGGCCGATTACGGAGGACTATG
4a	Chr1-2 GAP Fw	GTACAGCCACGTTTCTGATG
4b	Chr1-2 GAP Bw	GTATCCTGCGGCTAGAATTG

Southern blotting

Southern blotting was performed according to (Schuren et al., 1993)DNA was digested with SalI, separated on a 0.8 % agarose gel, and blotted to nitrocellulose. DNA was hybridized at 65 °C with a ^{32}P-labelled 1.2 kb SalI fragment of the *amyR* gene of *A. niger* or a ^{32}P-labelled 800 bp fragment of*18S* rDNA in 0.2 x SSC (150 mM NaCl, 15 mM Na citrate, pH 7.0). Blots were exposed to X-OMAT film (Kodak, New York, USA).

Sequencing of genomic DNA

Genomic DNA of *A. niger* was processed using the Illumina® Paired-End DNA sequencing Sample Prep Kit (Illumina, San Diego, USA). Fragmentation of the DNA, ligation of sequencing adapters, and PCR amplification of the resulting products was performed according to protocols of the manufacturer. Quality and yield of products was measured with Lab-on-a-Chip analysis. Samples were sequenced on the Illumina Genome Analyzer IIx according to manufacturer's protocols using 8 pmol of DNA. The total number of generated 76 bp paired-end reads (480 +/- 30 bases) was 52475,558. The paired end reads were aligned to the hybrid genome that was created by adding the sequences of PIM2101 and PJG01 to the *A. niger ATCC 1015 sequence (V3;*http://genome.jgi-psf.org/pages/blast.jsf?db=Aspni5*)*. 94.15 % of the pair end reads could be mapped to the hybrid genome. Sequences flanking introduced vectors were extracted using IGV (http://www.broadinstitute.org/igv/).

RNA extraction

Mycelium was frozen in liquid nitrogen and homogenized using the *TissueLyser II* (Qiagen, Venlo, The Netherlands). RNA was extracted using TRIzol reagent (Invitrogen, Carlsbad, CA, USA) according to the instructions of the manufacturer and purified

using N*ucleoSpin*® RNA II (*Macherey-NagelGmBh, Düren, Germany).* Concentration of RNA was measured with a Nanodrop ND-1000 (Thermo scientific, Wilmington, DE, USA) and quality of the RNA was analyzed with an Agilent 2100 bioanalyzer (Agilent Technology, Palo Alto, CA) using an RNA6000 LabChip kit.

RNA sequencing and analysis

RNA sequencing was performed at ServiceXS (Leiden, the Netherlands) using Illumina HiSeq2000 (Illumina, San Diego, USA), and Illumina protocols. The poly-A containing mRNA was isolated from 10 µg total RNA using poly-T oligo-attached magnetic beads. The mRNA was fragmented using divalent cations and copied into first strand cDNA using reverse transcriptase and random primers. This was followed by second strand cDNA synthesis using DNA Polymerase I and RNaseH. Adapters were ligated to the cDNA after end-repair and addition of a single 'A' base at the ends. The cDNA fragments were amplified by PCR to create the final cDNA library. Quality and yield of the fragments were measured with a DNA 1000 Lab-on-a-Chip (Agilent Technology, Waldbronn, Germany). The size of cDNA fragments was approximately 300 bp, as expected. Fragments were sequenced in paired-end mode resulting in two 100 bp reads with an average insert size of 157 bp (± 3.9 bp across samples). For each sample (6 conditions, 3 replicates) an average of 12.1 (± 1.7 standard deviation) million fragments was obtained. The minimum fragment number was 10.1 million.Trimmomatic 0.22 (Lohse et al., 2012) was used to remove adapters and leading / trailing bases below quality 3. Reads were cut when a 4 base stretch had an average quality below 15 and they were removed when they had a length < 36 bases. Fragments of which both reads survived (89 %, ± 2 %) were mapped to the *A. niger* N402 genome using STAR (Dobin et al., 2012). In total, 45331 splice sites (after quality filtering) were found. This information was used to improve alignments across splice sites, by realigning all reads. An average unique alignment rate of 95.5 % was obtained, while on average 1.82 % of the reads mapped at multiple locations. To perform expression analysis, gene annotations were transferred from the CBS 513.88 genome (http://www.asper-

gillusgenome.org/SequenceContents.shtml) to the N402 genome using RATT (Otto et al., 2011) Of 14070 genes, 13070 genes could be transferred completely and 106 genes partially. Cufflinks 2.1.1(Trapnell et al., 2013) was used to process these annotations with the discovery of new genes / transcripts disabled. Cuffdiff 2.1.1 (Trapnell et al., 2013) was also used to quantify differential expression. Conditions were analyzed simultaneously to make use of expression variability information across multiple conditions. on across multiple conditions.

Localization of starch degrading activity

Starch-degrading activity was detected by transferring 7-day-old maltose grown sandwiched colonies to agar MM containing 1 % soluble starch. After 4 h, colonies were removed and the medium was sprayed with 5 % (w / v) iodine / 10 % (w / v) potassium iodide solution (Lugol) (Wösten et al., 1991).

RESULTS

Plasmid pJG01 that contains the *A. niger amyR* gene was co-introduced with vector pIM2101 into *A. niger* strain NW249 selecting for arginine prototrophy. Secretion of glucoamylase was monitored by immuno-localization on PVDF membranes that had been placed under sandwiched colonies (Figure 1). The amount of secreted glucoamylase was higher in most of the transformants. The majority of the strains (e.g. UU-A001.24) showed a spatial secretion pattern like the control strains N402 and UU-A049.1. These strains secreted glucoamylase mainly at the periphery of the colony. In contrast, transformant UU-A001.13 released glucoamylase throughout the colony. Spatial release and the level of secretion of glucoamylase correlated with the zonal expression of the glucoamylase gene *glaA* (Figure 1). The control strain and UU-A001.24 mainly expressed *glaA* in the two outer zones of 7-day-old colonies. The latter strain showed a much higher expression than the wild-type and expression was also observed in the colony centre. Gene *glaA* was active throughout the colony in the case of UU-A001.13. The expression in the outer zones was similar to that of the

control.

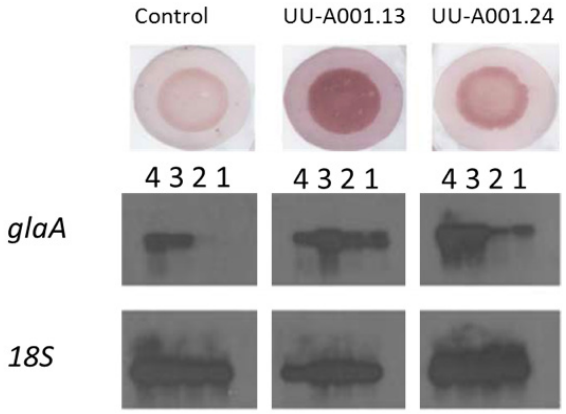

Figure 1. Immuno-localization of glucoamylase (upper panels) and *glaA* mRNA accumulation (middle panels) in the *amyR* multicopy strains UU-A001.13 and UU-A001.24 and the control strain UU-A049.1.*18S* rRNA (lower panels) was used as a RNA loading control. Zone 4 represents the periphery of the colony; zone 1 the inner center.

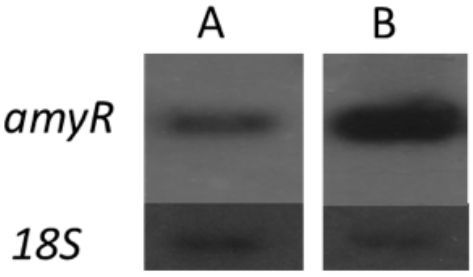

Figure 2. Southern hybridization of the control strain N402 (A) and UU-A001.13 (B) using probes of *amyR* and*18S* rDNA.

UU-A001.13 was selected for further analysis because of the changed spatial expression of *glaA* and secretion of its encoding protein. Southern analysis showed the presence of several extra copies of *amyR* in this strain based on the intensity of the hybridization signal (Figure 2).

The genome of UU-A001.13 was sequenced with 107-time coverage to localize the insertions of the transforming plasmids. Three insertion points of PIM2101 or PJG01 were identified (Figure 3). It was difficult to discriminate which vector caused the break points due to the high similarity between PIM2101 and PJG01.The insertion in chromosome 1 was identified in the 3' end of the coding sequence of *fluG* (An14g03390). This was accompanied by a deletion of 850 bp coding sequence upstream of the insertion (Figure 3A). Another insertion site was found in chromosome 4 (Figure 3B). In this case, the integration had occurred in the untranslated region (180 bp from the start codon) of a phosphate / phosphoenolpyruvate translocator

gene (An02g08670). An integration in chromosome 6 (Figure 3C) disrupted the 5' end of the open reading frame of the α-glucosidase gene *agdA* (An04g06920). This was accompanied by a deletion of the coding sequence of the endogenous copy of *amyR* (An04g06910) with its up- and downstream flanking regions.

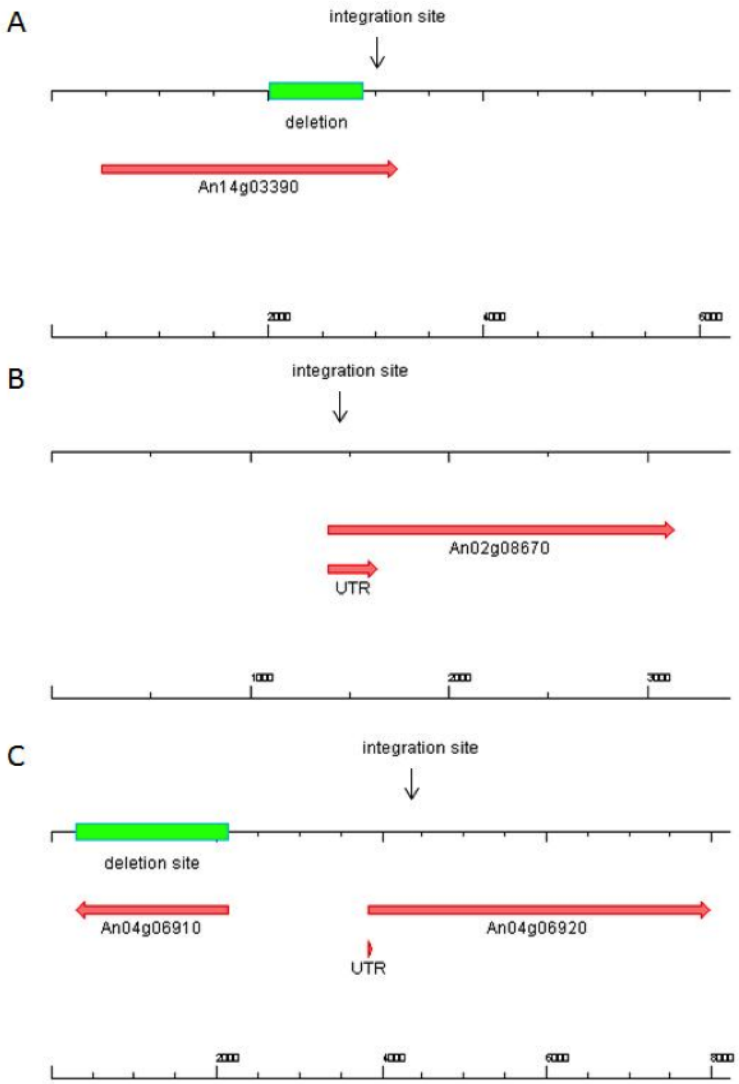

Figure 3. Integration of PIM2101 and PJG01 in the genome of strain UU-A001.13. (A) An integration site was identified at the 3' end of the coding sequence of *fluG* (An14g03390) in chromosome 1. This was accompanied by a 850 bp deletion upstream of the integration site. (B) An insertion site disrupted the 5' end of the untranslated region of a putative phosphate / phosphoenolpyruvate translocator (An02g08670). (C) An insertion disrupted the 5' end of the coding sequence of an α-glucosidase gene (An04g06920). This was accompanied by the deletion of the endogenous copy of *amyR* (An04g06910) with is up- and downstream flanks. The scales indicate the size (bp) of the genes. Arrows represent integration sites and green bars represent deletions.

In the next step, it was assessed whether the phenotype of UU-A001.13 could be attributed to inactivation of *fluG*. To this end, *fluG* was inactivated by introducing vector *BMOfluG* in N402 (data not shown). As a control, the coding sequence was reintroduced in the Δ*fluG* strain, resulting in strain Δ*fluG fluG.* Seven-day-old maltose grown sandwiched colonies of N402 (wild type), UU-A001.13, the Δ*fluG* strain, and the Δ*fluG fluG* strain were transferred for 4 h to a starch containing agar plate. Lugol staining demonstrated that the wild-type and the Δ*fluG fluG* strain degraded starch everywhere except for a subperipheral zone and the central zone (note degradation in the subperipheral zone was more intense in the case of the complemented Δ*fluG* strain). On the other hand, the Δ*fluG* strain and strain UU-A001.13 degraded starch throughout the medium underlying the colony (Figure 4). This shows that FluG has an effect on spatial starch degradation.

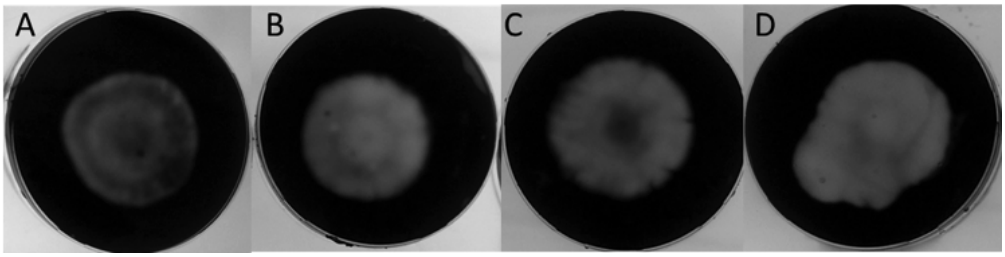

Figure 4. Lugol staining of starch plates after 4 h incubation of 7-day-old maltose growth colonies of N402 (control) (A), Δ*fluG* (B), Δ*fluG fluG* (C), and UU-A001.13 (D).

Expression of *amyR* and its 16 regulated genes was determined at the periphery (zone 5), an intermediate zone (zone 3) and the center (zone 1) of 7-day-old maltose grown sandwiched colonies of N402 and the Δ*fluG* strain (Tables supplement 3-5; Figure 5). None of the genes showed significant changed expression with a fold change ≥ 2 when zones 1 and 3 of the wild-type strain were compared. 5 genes (*agdB, glaB, bgl, bglA, mstF*) were ≥ 2-fold upregulated in zone 1 or 3 when compared to zone 5, while 2 genes (α galactosidase genes *aglB* and *aglC*) were down regulated when compared to zone 5 (Table 3). Spatial expression profiles were different in strain Δ*fluG* (Table 4). 8 out of 16 AmyR regulated genes as well as *amyR* itself were ≥ 2-fold

upregulated in more peripheral zones, while only two genes (*mstF* and *glaB*) were ≥ 2-fold downregulated at the periphery. The changed spatial expression of the *amyR* regulated genes in Δ*fluG* was also reflected in the ratios of the mRNA levels when the 3 zones of Δ*fluG* were compared with the respective zones of N402 (Table 5; Figure 5). Down-regulation (≥ 2-fold) of 6 out of the 16 AmyR regulated genes (including *glaA*) was observed in the central zone of the Δ*fluG* strain when compared to the wild-type. On the other hand, 6 genes (including acid amylase *aamA*) were up-regulated more than 2-fold at the periphery of colonies of the Δ*fluG* strain. Together, FluG plays a role in zonal expression of AmyR-regulated genes and partly explains the phenotype of UU-A001.13.

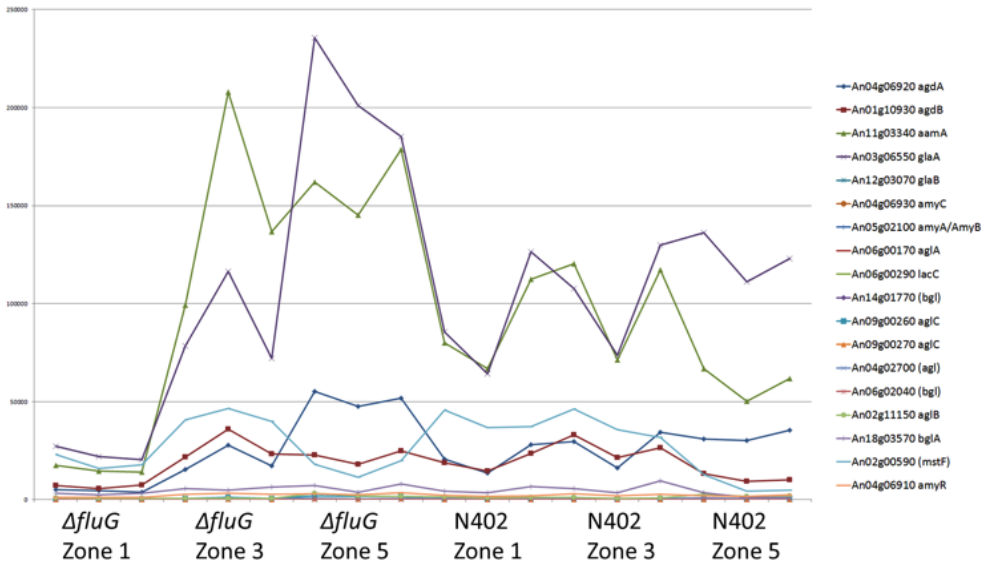

Figure 5. Expression profiles of genes regulated by *amyR* that show differential expression in at least one of the concentric zones 1, 3, and 5 when strains N402 and Δ*fluG* are compared.

Table 3. Expression of *amyR* and its regulated genes in the outer zone 5, the intermediate zone 3, and the central zone 1 of 7-day-old maltose grown colonies of N402. The ^{2}log ratio of differences in gene expression is indicated. A number ≥ 1 shows a ≥ 2 fold decrease in the second zone in the comparison; whereas a number ≤ -1 shows a ≥ 2 fold increase in this zone. The green and red shading indicate significant ≥ 2 fold upregulation and downregulation of genes; light green and red shading indicates ≤ 2-fold but significant up and down regulation of genes. An09g00260 and An09g00270 represent truncated ORFs of α-galactosidase C (*aglC*) and thus represent one gene.

Gene id	gene name	Description	log2_fold_change		
			n402 zone 3 / n402 zone 1	n402 zone 5 / n402 zone 1	n402 zone 5 / n402 zone 3
An04g06920	agdA	extracellular α-glucosidase	0,357362	0,63302	0,275658
An01g10930	agdB	Putative α-glucosidase	0,506088	-0,790265	-1,29635
An11g03340	aamA	acid alpha-amylase aamA	0,240682	-0,549849	-0,79053
An03g06550	glaA	glucoamylase glaA	0,166282	0,413587	0,247305
An12g03070	glaB	Putative glucoamylase	-0,421863	-4,04902	-3,62715
An04g06930	amyC	α-amylase	-0,137068	-0,7216	-0,584532
An05g02100	amyA	extracellular α-amylase amyA	ND	ND	ND
An06g00170	aglA	alpha-galactosidase	ND	ND	ND
An06g00290	lacC	β-galactosidase lacC	ND	ND	ND
An14g01770	bgl	strong similarity to β-glucosidase	0,459257	-0,813096	-1,27235
An09g00260	aglC	α-galactosidase C aglC [truncated ORF]	0,698624	1,413	0,714374
An09g00270	aglC	α-galactosidase C aglC [truncated ORF]	0,253318	0,965988	0,71267
An04g02700	agl	hypothetical protein	0,603066	0,643724	0,0406572
An06g02040	bgl	strong similarity to β-glucosidase	0,144934	0,41446	0,269527
An02g11150	aglB	identical to α-galactosidase	-0,288768	0,905355	1,19412
An18g03570	bglA	β-glucosidase	0,349416	-1,29361	-1,64303
An02g00590	mstF	strong similarity to high-affinity glucose transporter	-0,0816058	-2,41745	-2,33585
An04g06910	amyR	transcription regulator of maltose utilization	0,375819	0,0967851	-0,279034

Table 4. Expression of *amyR* and its regulated genes in the outer zone 5, the intermediate zone 3, and the central zone 1 of 7-day-old maltose grown colonies of Δ*fluG*. The ^{2}log ratio of differences in gene expression is indicated. A number ≥ 1 shows a ≥ 2 fold decrease in the second zone in the comparison; whereas a number ≤ -1 shows a ≥ 2 fold increase in this zone. The green and red shading indicate significant ≥ 2 fold upregulation and downregulation of genes; light green and red shading indicates ≤ 2-fold but significant up and down regulation of genes. An09g00260 and An09g00270 represent truncated ORFs of α-galactosidase C (*aglC*) and thus represent one gene.

Gene id	gene name	Description	log2_fold_change		
			Δ*fluG* zone 3 / Δ*fluG* zone 1	Δ*fluG* zone 5 / Δ*fluG* zone 1	Δ*fluG* zone 5 / Δ*fluG* zone 3
An04g06920	agdA	extracellular α-glucosidase	2,14493	3,49202	1,34709
An01g10930	agdB	Putative α-glucosidase	1,99175	1,69288	-0,298861
An11g03340	aamA	acid alpha-amylase aamA	3,27008	3,3757	0,105613
An03g06550	glaA	glucoamylase glaA	1,93835	3,13647	1,19812
An12g03070	glaB	Putative glucoamylase	0,262712	-2,04267	-2,30538
An04g06930	amyC	α-amylase	0,618824	0,288562	-0,330263
An05g02100	amyA	extracellular α-amylase amyA	ND	ND	ND
An06g00170	aglA	alpha-galactosidase	ND	ND	ND
An06g00290	lacC	β-galactosidase lacC	ND	ND	ND
An14g01770	Bgl	strong similarity to β-glucosidase	0,54222	-0,39406	-0,93628
An09g00260	aglC	α-galactosidase C aglC [truncated ORF]	2,32574	3,47434	1,1486
An09g00270	aglC	α-galactosidase C aglC [truncated ORF]	2,12952	3,57457	1,44504
An04g02700	Agl	hypothetical protein	0,113626	0,101274	-0,0123518
An06g02040	Bgl	strong similarity to β-glucosidase	-1,17933	-0,445808	0,73352
An02g11150	aglB	identical to α-galactosidase	-0,121398	1,7121	1,83349
An18g03570	bglA	β-glucosidase	0,883157	1,05544	0,172287
An02g00590	mstF	strong similarity to high-affinity glucose transporter	1,16005	-0,200083	-1,36014
An04g06910	amyR	transcription regulator of maltose utilization	1,3399	1,40368	0,0637803

Table 5. Expression of *amyR* and its regulated genes in the outer zone 5, the intermediate zone 3, and the central zone 1 of 7-day-old maltose grown colonies of N402 and Δ*fluG*. The ^{2}log ratio of differences in gene expression is indicated. A number ≥ 1 shows a ≥ 2 fold decrease in the second zone in the comparison; whereas a number ≤ -1 shows a ≥ 2 fold increase in this zone. The green and red shading indicate significant ≥ 2 fold upregulation and downregulation of genes; light green and red shading indicates ≤ 2-fold but significant up and down regulation of genes. An09g00260 and An09g00270 represent truncated ORFs of α-galactosidase C (*aglC*) and thus represent one gene.

Gene id	gene name	Description	log2_fold_change		
			n402 zone 1 / Δ*fluG* zone 1	n402 zone 3 / Δ*fluG* zone 3	n402 zone 5 / Δ*fluG* zone 5
An04g06920	agdA	extracellular α-glucosidase	2,17737	0,389808	-0,681626
An01g10930	agdB	Putative α-glucosidase	1,4731	-0,012554	-1,01005
An11g03340	aamA	acid alpha-amylase aamA	2,49646	-0,532945	-1,42909
An03g06550	glaA	glucoamylase glaA	1,98288	0,210809	-0,740003
An12g03070	glaB	Putative glucoamylase	2,43551	1,75094	0,429164
An04g06930	amyC	α-amylase	0,68023	-0,07566	-0,329929
An05g02100	amyA	extracellular α-amylase amyA	ND	ND	ND
An06g00170	aglA	alpha-galactosidase	ND	ND	ND
An06g00290	lacC	β-galactosidase lacC	ND	ND	ND
An14g01770	Bgl	strong similarity to β-glucosidase	-0,0545	-0,137424	-0,473498
An09g00260	aglC	α-galactosidase C aglC [truncated ORF]	0,08726	-1,53986	-1,97408
An09g00270	aglC	α-galactosidase C aglC [truncated ORF]	1,07795	-0,798254	-1,53063
An04g02700	Agl	hypothetical protein	-0,3673	0,122091	0,1751
An06g02040	Bgl	strong similarity to β-glucosidase	-0,7789	0,545328	0,081335
An02g11150	aglB	identical to α-galactosidase	0,71179	0,544418	-0,0949533
An18g03570	bglA	β-glucosidase	0,66005	0,126312	-1,689
An02g00590	mstF	strong similarity to high-affinity glucose transporter	1,06434	-0,177316	-1,15303
An04g06910	amyR	transcription regulator of maltose utilization	0,767391	-0,19669	-0,539505

DISCUSSION

Aspergilli are characterized by a complex program of asexual reproduction (Krijgsheld et al., 2013a). Gene *fluG* was identified in *A. nidulans* as a gene involved in this developmental process (Lee and Adams, 1996). Overexpression of *fluG* in *A. nidulans* induces sporulation in liquid-submerged culture where conidia formation is normally suppressed (D'Souza et al., 2001). On the other hand, inactivation of *fluG* abolishes asexual development under nutrient rich conditions but this process is not affected under carbon starvation (Lee and Adams, 1996). Sporulation under nutrient rich conditions could be rescued in the Δ*fluG* strain by growing this strain next to a wild-type. This was also the case when these strains were separated by a dialysis membrane. From this and other data it was proposed that FluG is involved in sporulation resulting from a developmental program, but not from a stress response resulting from starvation, by producing an extracellular signaling molecule that initiates conidiophore formation (Lee and Adams, 1994a). This molecule would release the inhibition of SfgA on the *flbA-E* genes, which leads to the activation of *brlA* that encodes the central transcription factor of asexual development (Seo et al., 2006). FlbA is an example of a product of the *flb* genes. Absence of this RGS protein results in low *brlA* expression. As a consequence, aerial hyphae are formed but not conidiophores (Wieser et al., 1994, Lee and Adams, 1994b). The underlying mechanism of asexual developmental of *A. nidulans* and *A. niger* has been proposed to be similar (Pel et al., 2007). This is supported by the finding that BrlA and FlbA have a similar role in asexual reproduction in these fungi (Krijgsheld et al., 2013b). FluG of *A. niger* on the other hand, does not have a role in asexual development on maltose containing medium (Chapter 3).

Multiple copies of *amyR* were introduced in *A. niger* to assess whether over-expression of this regulator would impact production levels of glucoamylase and its spatial release in colonies. Most transformants did indeed show higher production of glucoamylase. This shows that introduction of multiple copies of *amyR* is an effective strategy to improve production of glucoamylase as was shown in *Aspergillus awamori* (Vinetskii Iu et al., 2010). Presence of multiple copies of *amyR* did not affect

the ratio of glucoamylase released at the periphery and within the center of most of the transformants. However, over-expression did increase absolute levels of *glaA* mRNA and release of its encoded protein in these zones of the transformants. Expression of *glaA,* however, was identical in all zones of transformant UU-A001.13 being equivalent to that found at the periphery of wild-type colonies. This loss of heterogeneity in *glaA* expression was accompanied by loss of spatial heterogeneity in release of glucoamylase and starch degrading activity. Clearly, this loss of heterogeneity was not the result of over-expression of *amyR* since colonies of other transformants still showed heterogeneous zonal expression of *glaA* and heterogeneous GlaA release. Therefore, it was assessed whether an integration site of the introduced vectors caused the loss of heterogeneity in UU-A001.13. Whole genome sequencing revealed three integration sites affecting four genes. One insertion locus was found in chromosome 4 in the UTR region of a phosphate / phosphoenolpyruvate translocator. Integration in chromosome 6 resulted in disruption of the 5' end of the open reading frame of α-glucosidase *agdA*, while the coding sequence of *amyR* with its up- and downstream flanking regions was deleted. The insertion in chromosome 1 was accompanied by a deletion of 0.9 kb coding sequence of *fluG*. Sequencing the UU-A001.13 genome thus showed that integration of plasmids is accompanied with deletion events near the integration site. This is something to consider when phenotypes of deletion or over-expression strains are being evaluated.

Inactivation of *fluG* in a wild-type background showed a starch degrading activity under the colony similar to that of UU-A001.13. However, expression of AmyR regulated genes was not in line with the starch degrading activity. The starch degrading activity predicted that AmyR regulated genes would be up-regulated in the centre of Δ*fluG* colonies. However, 6 out of 16 AmyR regulated genes (including *glaA*) were ≥ 2-fold down-regulated in the center of Δ*fluG* colonies when compared to N402. In contrast 6 AmyR regulated genes were ≥ 2-fold up-regulated in the peripheral zone of Δ*fluG* colonies. How can we explain the discrepancy in spatial *glaA* expression and the starch degrading activity? A discrepancy between gene expression and se-

cretome activity was also observed in the case of the Δ*flbA* strain of *A. niger*. It was shown that 70 proteins are secreted by the Δ*flbA* strain that are not found in the medium of the wild-type (Krijgsheld et al., 2013b). Only in the case of 22 proteins this could be explained by upregulation of the encoding genes (Krijgsheld and Wösten, 2013). This discrepancy was suggested to be due to (post)-translational regulation or by induction of genes after transfer to fresh medium. Gene expression profiling was done with colonies that had not been transferred, while secretome analysis was done after transfer to fresh medium. We used a similar approach in this study. RNA profiling was done without transfer, while starch degrading activity included a transfer to fresh medium. The discrepancy between starch degrading activity and gene expression could also be explained by an increased retention time of secreted proteins in the cell wall. Proteins secreted at the periphery would thus be mainly released in the medium when this part of the colony has become a more central zone. Together our data show that FluG affects spatial expression of amylolytic genes and that absence of this protein partly explains the phenotype of the UU-A001.13 transformant.

REFERENCES

BATTAGLIA, E., VISSER, L., NIJSSEN, A., VAN VELUW, G. J., WÖSTEN, H. A. & DE VRIES, R. P. 2011. Analysis of regulation of pentose utilisation in *Aspergillus niger* reveals evolutionary adaptations in Eurotiales. *Stud Mycol,* 69**,** 31-38.

BOS, C. J., DEBETS, A. J., SWART, K., HUYBERS, A., KOBUS, G. & SLAKHORST, S. M. 1988. Genetic analysis and the construction of master strains for assignment of genes to six linkage groups in *Aspergillus niger*. *Curr Genet,* 14**,** 437-443.

COUTINHO, P. M., ANDERSEN, M. R., KOLENOVA, K., VANKUYK, P. A., BENOIT, I., GRUBEN, B. S., TREJO-AGUILAR, B., VISSER, H., VAN SOLINGEN, P., PAKULA, T., SEIBOTH, B., BATTAGLIA, E., AGUILAR-OSORIO, G., DE JONG, J. F., OHM, R. A., AGUILAR, M., HENRISSAT, B., NIELSEN, J., STALBRAND, H. & DE VRIES, R. P. 2009. Post-genomic insights into the plant polysaccharide degradation potential of *Aspergillus nidulans* and comparison to *Aspergillus niger* and *Aspergillus oryzae*. *Fungal Genet Biol,* 46 Suppl 1**,** S161-S169.

D'SOUZA, C. A., LEE, B. N. & ADAMS, T. H. 2001. Characterization of the role of the FluG protein in asexual development of *Aspergillus nidulans*. *Genetics,* 158**,** 1027-1036.

DE BEKKER, C., BRUNING, O., JONKER, M. J., BREIT, T. M. & WÖSTEN, H. A. 2011a. Single cell transcriptomics of neighboring hyphae of *Aspergillus niger*. *Genome Biol,* 12**,** R71.

DE BEKKER, C., VAN VELUW, G. J., VINCK, A., WIEBENGA, L. A. & WÖSTEN, H. A. 2011b. Heterogeneity of *Aspergillus niger* microcolonies in liquid shaken cultures. *Appl Environm Microbiol,* 77**,** 1263-1267.

DOBIN, A., DAVIS, C. A., SCHLESINGER, F., DRENKOW, J., ZALESKI, C., JHA, S., BATUT, P., CHAISSON, M. & GINGERAS, T. R. 2012. STAR: ultrafast universal RNA-seq aligner. *Bioinformatics,* 29**,** 15-21.

GOMI, K., AKENO, T., MINETOKI, T., OZEKI, K., KUMAGAI, C., OKAZAKI, N. & IIMURA, Y. 2000. Molecular cloning and characterization of a transcriptional activator gene, *amyR*, involved in the amylolytic gene expression in *Aspergillus oryzae*. *Biosci Biotechnol Biochem,* 64**,** 816-827.

JALVING, R., VAN DE VONDERVOORT, P. J., VISSER, J. & SCHAAP, P. J. 2000. Characterization of the kexin-like maturase of *Aspergillus niger*. *Appl Environ Microbiol,* 66**,** 363-368.

KELLY, J. M. & HYNES, M. J. 1985. Transformation of *Aspergillus niger* by the amdS gene of *Aspergillus nidulans*. *EMBO J,* 4**,** 475-479.

KRIJGSHELD, P., ALTELAAR, A. F., POST, H., RINGROSE, J. H., MULLER, W. H., HECK, A. J. & WÖSTEN, H. A. 2012. Spatially resolving the secretome within the mycelium of the cell factory *Aspergillus niger*. *J Proteome Res,* 11**,** 2807-2818.

KRIJGSHELD, P., BLEICHRODT, R., VAN VELUW, G. J., WANG, F., MULLER, W. H., DIJKSTERHUIS, J. & WÖSTEN, H. A. 2013a. Development in *Aspergillus*. *Stud Mycol,* 74**,** 1-29.

KRIJGSHELD, P., NITSCHE, B. M., POST, H., LEVIN, A. M., MULLER, W. H., HECK, A. J., RAM, A. F., ALTELAAR, A. F. & WÖSTEN, H. A. 2013b. Deletion of *flbA* Results in Increased Secretome Complexity and Reduced Secretion Heterogeneity in Colonies of *Aspergillus niger*. *J Proteome Res,* 12**,** 1809-1819.

KRIJGSHELD, P. & WÖSTEN, H. A. 2013. Transcriptome analysis of zones of colonies of the ΔflbA strain of *Aspergillus niger Fungal Genom Bio,* 3**,** 109.

LEE, B. N. & ADAMS, T. H. 1994a. The *Aspergillus nidulans fluG* gene is required for production of an extracellular developmental signal and is related to prokaryotic glutamine synthetase I. *Genes Dev,* 8**,** 641-651.

LEE, B. N. & ADAMS, T. H. 1994b. Overexpression of *flbA*, an early regulator of *Aspergillus* asexual sporulation, leads to activation of *brlA* and premature initiation of development. *Mol Microbiol,* 14**,** 323-334.

LEE, B. N. & ADAMS, T. H. 1996. *fluG* and *flb*A function interdependently to initiate conidiophore development in *Aspergillus nidulans* through *brlA* beta activation. *EMBO J,* 15**,** 299-309.

LENOUVEL, F., VAN DE VONDERVOORT, P. J. & VISSER, J. 2002. Disruption of the *Aspergillus niger argB* gene: a tool for transformation. *Curr Genet,* 41**,** 425-432.

LEVIN, A. M., DE VRIES, R. P., CONESA, A., DE BEKKER, C., TALON, M., MENKE, H. H., VAN PEIJ, N. N. & WÖSTEN, H. A. 2007a. Spatial differentiation in the vegetative mycelium of *Aspergillus niger*. *Eukaryot Cell,* 6**,** 2311-2322.

LEVIN, A. M., DE VRIES, R. P. & WÖSTEN, H. A. 2007b. Localization of protein secretion in fungal colonies using a novel culturing technique; the ring-plate system. *J Microbiol Methods,* 69**,** 399-401.

LOHSE, M., BOLGER, A. M., NAGEL, A., FERNIE, A. R., LUNN, J. E., STITT, M. & USADEL, B. 2012. RobiNA: a user-friendly, integrated software solution for RNA-Seq-based transcriptomics. *Nucleic Acids Res,* 40**,** W622-627.

MEYER, V., RAM, A. F. J. & PUNT, P. J. 2010. Genetics, Genetic Manipulation, and Approaches to Strain Improvement of Filamentous Fungi. *Genetics, Genetic Manipulation, and Approaches to Strain Improvement of Filamentous Fungi.* Washington DC: ASM

press.
MULLANEY, E. J., HAMER, J. E., ROBERTI, K. A., YELTON, M. M. & TIMBERLAKE, W. E. 1985. Primary structure of the *trpC* gene from *Aspergillus nidulans*. *Mol Gen Genet,* 199**,** 37-45.
OTTO, T. D., DILLON, G. P., DEGRAVE, W. S. & BERRIMAN, M. 2011. RATT: Rapid Annotation Transfer Tool. *Nucleic Acids Res,* 39**,** e57.
PEL, H. J., DE WINDE, J. H., ARCHER, D. B., DYER, P. S., HOFMANN, G., SCHAAP, P. J., TURNER, G., DE VRIES, R. P., ALBANG, R., ALBERMANN, K., ANDERSEN, M. R., BENDTSEN, J. D., BENEN, J. A., VAN DEN BERG, M., BREESTRAAT, S., CADDICK, M. X., CONTRERAS, R., CORNELL, M., COUTINHO, P. M., DANCHIN, E. G., DEBETS, A. J., DEKKER, P., VAN DIJCK, P. W., VAN DIJK, A., DIJKHUIZEN, L., DRIESSEN, A. J., D'ENFERT, C., GEYSENS, S., GOOSEN, C., GROOT, G. S., DE GROOT, P. W., GUILLEMETTE, T., HENRISSAT, B., HERWEIJER, M., VAN DEN HOMBERGH, J. P., VAN DEN HONDEL, C. A., VAN DER HEIJDEN, R. T., VAN DER KAAIJ, R. M., KLIS, F. M., KOOLS, H. J., KUBICEK, C. P., VAN KUYK, P. A., LAUBER, J., LU, X., VAN DER MAAREL, M. J., MEULENBERG, R., MENKE, H., MORTIMER, M. A., NIELSEN, J., OLIVER, S. G., OLSTHOORN, M., PAL, K., VAN PEIJ, N. N., RAM, A. F., RINAS, U., ROUBOS, J. A., SAGT, C. M., SCHMOLL, M., SUN, J., USSERY, D., VARGA, J., VERVECKEN, W., VAN DE VONDERVOORT, P. J., WEDLER, H., WÖSTEN, H. A., ZENG, A. P., VAN OOYEN, A. J., VISSER, J. & STAM, H. 2007. Genome sequencing and analysis of the versatile cell factory *Aspergillus niger* CBS 513.88. *Nature Biotechnol,* 25**,** 221-231.
PETERSEN, K. L., LEHMBECK, J. & CHRISTENSEN, T. 1999. A new transcriptional activator for amylase genes in *Aspergillus*. *Mol Gen Genet,* 262**,** 668-676.
PUNT, P. J., DINGEMANSE, M. A., KUYVENHOVEN, A., SOEDE, R. D., POUWELS, P. H. & VAN DEN HONDEL, C. A. 1990. Functional elements in the promoter region of the *Aspergillus nidulans gpdA* gene encoding glyceraldehyde-3-phosphate dehydrogenase. *Gene,* 93**,** 101-109.
PUNT, P. J., OLIVER, R. P., DINGEMANSE, M. A., POUWELS, P. H. & VAN DEN HONDEL, C. A. 1987. Transformation of *Aspergillus* based on the hygromycin B resistance marker from *Escherichia coli*. *Gene,* 56**,** 117-124.
SCHUREN, F. H., HARMSEN, M. C. & WESSELS, J. G. 1993. A homologous gene-reporter system for the basidiomycete *Schizophyllum commune* based on internally deleted homologous genes. *Mol Gen Genet,* 238**,** 91-96.
SEO, J. A., GUAN, Y. & YU, J. H. 2006. FluG-dependent asexual development in *Aspergillus nidulans* occurs via derepression. *Genetics,* 172**,** 1535-1544.
TANI, S., KATSUYAMA, Y., HAYASHI, T., SUZUKI, H., KATO, M., GOMI, K., KOBAYASHI, T. & TSUKAGOSHI, N. 2001. Characterization of the *amyR* gene encoding a transcriptional activator for the amylase genes in *Aspergillus nidulans*. *Curr Genet,* 39**,** 10-15.
TRAPNELL, C., HENDRICKSON, D. G., SAUVAGEAU, M., GOFF, L., RINN, J. L. & PACHTER, L. 2013. Differential analysis of gene regulation at transcript resolution with RNA-seq. *Nat Biotechnol,* 31**,** 46-53.
VAN PEER, A. F., DE BEKKER, C., VINCK, A., WÖSTEN, H. A. & LUGONES, L. G. 2009. Phleomycin increases transformation efficiency and promotes single integrations in *Schizophyllum commune*. *Appl Environ Microbiol,* 75**,** 1243-1247.
VAN VELUW, G. J., TEERTSTRA, W. R., DE BEKKER, C., VINCK, A., VAN BEEK, N., MULLER, W. H., ARENTSHORST, M., VAN DER MEI, H. C., RAM, A. F., DIJKSTERHUIS, J. & WÖSTEN, H. A. 2013. Heterogeneity in liquid shaken cultures of *Aspergillus niger* inoculated with melanised conidia or conidia of pigmentation mutants. *Stud Mycol,* 74**,** 47-57.
VANKUYK, P. A., BENEN, J. A., WÖSTEN, H. A., VISSER, J. & DE VRIES, R. P. 2011. A broader role for AmyR in *Aspergillus niger*: regulation of the utilisation of D-glucose or D-galactose containing oligo- and polysaccharides. *Appl Microbiol Biotechnol,* 93**,** 285-293.
VINCK, A., DE BEKKER, C., OSSIN, A., OHM, R. A., DE VRIES, R. P. & WÖSTEN, H. A. 2011. Heterogenic expression of genes encoding secreted proteins at the periphery of *Aspergillus niger* colonies. *Environm Microbiol,* 13**,** 216-225.
VINCK, A., TERLOU, M., PESTMAN, W. R., MARTENS, E. P., RAM, A. F., VAN DEN HONDEL, C. A. & WÖSTEN, H. A. 2005. Hyphal differentiation in the exploring mycelium of *Aspergillus niger*. *Mol Microbiol,* 58**,** 693-699.
VINETSKII IU, P., ROZHKOVA, A. M., SEREDA, A. S., TSURIKOVA, N. V., NURTAEVA, A. K., SEMENOVA, M. V., ZOROV, I. N. & SINITSYN, A. P. 2010. Increase in glucoamylase productivity of *Aspergillus awamori* strain by combination of radiating mutagenesis and plasmid transformation methods. *Prikl Biokhim Mikrobiol,* 46**,** 685-692.
VISHNIAC, W. & SANTER, M. 1957. The thiobacilli. *Bacteriol Rev,* 21**,** 195-213.
WIESER, J., LEE, B. N., FONDON, J., 3RD & ADAMS, T. H. 1994. Genetic requirements for initiating asexual development in *Aspergillus nidulans*. *Curr Genet,* 27**,** 62-69.
WÖSTEN, H. A., MOUKHA, S. M., SIETSMA, J. H. & WESSELS, J. G. 1991. Localization of growth and secretion of proteins in *Aspergillus niger*. *J Gen Microbiol,* 137**,** 2017-2023.
YUAN, X. L., VAN DER KAAIJ, R. M., VAN DEN HONDEL, C. A., PUNT, P. J., VAN DER MAAREL,

M. J., DIJKHUIZEN, L. & RAM, A. F. 2008. *Aspergillus niger* genome-wide analysis reveals a large number of novel alpha-glucan acting enzymes with unexpected expression profiles. *Mol Genet Genomics,* 279**,** 545-561.

Chapter 3

FluG of *Aspergillus niger* affects zonal expression of genes

Fengfeng Wang, Marc Hulsman, Pauline Krijgsheld, Wally H. Müller, and Han A. B. Wösten.

Submited for publication

ABSTRACT

FluG of *Aspergillus nidulans* and *Aspergillus oryzae* is involved in a developmental program of initiation of conidiophore formation. In contrast, a Δ*fluG* strain of *A. fumigatus* still forms conidiophores. Here, the role of FluG of *Aspergillus niger* was assessed. Inactivation of *fluG* did neither affect morphology and spatial distribution of conidiophores nor the number of spores produced per surface area and germination efficiency. Moreover, spatial patterns of growth and secretion were not affected. The Δ*fluG* strain also did not show changed biomass formation on xylose and maltose containing medium but did show increased release of proteins on the latter carbon source. Genes encoding proteins with a signal sequence were more often downregulated in the central zone of maltose-grown Δ*fluG* colonies and upregulated in the intermediate part and periphery when compared to the wild-type. This was also the case for XlnR regulated genes. 4 out of 16 of these genes were downregulated at least 2-fold in the central zone of maltose-grown Δ*fluG* colonies when compared to wild-type, while 5 and 7 of these genes were upregulated in the intermediate and peripheral zones. Moreover, 56 out of 623 transcription factor genes were differentially expressed with a fold change ≥ 2 in at least one zone of the Δ*fluG* colonies when compared to wild-type. Together, these and other data indicate that FluG of *A. niger* is a repressor of secretion. This function may link it to asexual development.

INTRODUCTION

Aspergillus niger is a common saprotrophic fungus that grows on a wide variety of carbon sources and in a wide range of temperature, pH, and water activity (Krijgsheld et al., 2013a). It is used for the commercial production of organic acids (e.g. citric acid) and enzymes (e.g. glucoamylase) (Andersen et al., 2011). Its role as a cell factory is based on its long history of safe use (van Dijck et al., 2003, Schuster et al., 2002) and enormous secretion capacity (Conesa et al., 2001, Punt et al., 2002). The latter is exemplified by the fact that some strains secrete up to 30 gram of protein per liter (Finkelstein et al., 1989).

A. niger forms a mycelium, also known as colony, that consists of a network of interconnected hyphae. Zones in colonies of *A. niger* are heterogeneous with respect to growth (Wösten et al., 1991), RNA composition (de Bekker et al., 2011, Levin et al., 2007a), secretion (Levin et al., 2007b, Wösten et al., 1991, Krijgsheld et al., 2012) and sporulation (Krijgsheld et al., 2013b). For instance, formation of asexual reproductive structures known as conidiophores mainly takes place in the sub-peripheral part of the colony. This zone does not secrete proteins (Krijgsheld et al., 2013b), suggesting that sporulation inhibits secretion. Indeed, inactivation of the sporulation gene *flbA* results in a strain that secretes proteins throughout the colony (Krijgsheld et al., 2013b). In addition, the non-sporulating strain grows in all zones of the mycelium. Notably, zonal heterogeneity in gene expression is not reduced in Δ*flbA* colonies (Krijgsheld and Wösten, 2013).

Three signaling cascades have been identified in *A. nidulans* that are involved in asexual reproduction (Figure 5, Chapter 1). Signalling involves FluG and, independently, two heterotrimeric G-protein complexes both consisting of SfaD and GpgA (the Gβγ subunits) and the Gα subunits FadA and GanB, respectively. The *fluG* gene is believed to be at the start of the asexual sporulation program in aspergilli. Overexpression of *fluG* in vegetative hyphae is sufficient to cause sporulation under conditions that normally suppress conidia formation (Lee and Adams, 1996). A Δ*fluG* strain of *A. nidulans* does form aerial hyphae but conidiophores are not being formed in excess of nutrients (Lee and Adams, 1994). During nutrient starvation, however, conidiophore development is not affected (Lee and Adams, 1996). From these data it was concluded that FluG is involved in a developmental program of sporulation but not in a stress-related sporulation pathway. Formation of conidiophores in a Δ*fluG* colony is rescued by growing a wild-type colony next to it, even when the colonies are physically separated by a dialysis membrane with a size exclusion of 6-8 kDa (Lee and Adams, 1994). This led to the hypothesis that FluG is involved in the production of a low-molecular weight extracellular signaling molecule that is involved in the formation of conidiophores. This signaling molecule would activate an unknown receptor. As

a result, the suppressor protein SfgA would be inhibited (Seo et al., 2006), enabling expression of the *flb* genes such as *flbA* (Figure 6, Chapter 1). FlbA activates the central regulatory gene of asexual development *brlA* by inactivating the Gα subunit FadA (Figure 5, Chapter 1). FlbA has been proposed to also repress *fluG*. The FlbB / FlbE complex as well as a complex consisting of FlbB and FlbD together with FlbC also activate *brlA* (Figure 6, Chapter 1).

Experimental evidence indicates that FluG of *Aspergillus oryzae* has a similar role as that of *A. nidulans* (Ogawa et al., 2010). In contrast, a Δ*fluG* strain of *A. fumigatus* still sporulates in air-exposed cultures (Mah and Yu, 2006). Here, it is shown that FluG of *A. niger* also does not have a role in conidiophore development. In stead, it seems to repress secretion under certain environmental conditions. This would link FluG to asexual development.

MATERIAL AND METHODS

Strain and growth conditions

A. niger strain N402 (*cspAI* derivative of ATCC 9029) (Bos et al., 1988), the derived Δ*fluG* strain (Chapter 2) and the complemented Δ*fluG* strain (Chapter 2) were grown at 30 °C under constant 700 lux white light (Osram Lumilux L36w/840, Osram, Munich, Germany) on minimal medium (MM, pH 6, containing per liter 6 g NaNO3, 1.5 g KH_2PO_4, 0.5 g KCL, 0.5 g $MgSO_4 \cdot 7H_2O$, and 200 µl trace element solution according to (Vishniac and Santer, 1957) in the presence or absence of 1.5 % agar. 25 mM maltose was used as a carbon source. Sporulation assays were peformed in the dark and at 1200 lux light. Colonies were grown as sandwiched cultures (Wösten et al., 1991). To this end, the fungus was grown in between two perforated polycarbonate (PC) membranes (diameter of 76 mm; pore size, 0.1 µm; Osmonics, GE Water Technologies, Trevose, PA) in a 0.2 mm thin layer of 1.25 % agarose that had been placed on top of solidified (1.5 % agar) minimal medium with 25 mM maltose as a carbon source. Sandwiched cultures were inoculated with 1.5 µl of spore suspension

(10^8 spores ml^{-1} saline Tween [0.8 % NaCl, 0.005 % Tween-80]). Germination assays were performed directly on agar medium and accessed using a MULTIZOOM AZ100 microscope *(*Nikon Corporation Instruments Company*,* Japan*).*

RNA extraction

Mycelium was frozen in liquid nitrogen and homogenized using the *TissueLyser II* (Qiagen, Venlo, The Netherlands). RNA was extracted using TRIzol reagent (Invitrogen, Carlsbad, CA, USA) according to the instructions of the manufacturer and purified using NucleoSpin® RNA II (Macherey-NagelGmBh, Düren*,* Germany)*.* Concentration and quality of RNA were measured with a Nanodrop ND-1000 (Thermo scientific, Wilmington, DE, USA) and an Agilent 2100 bioanalyzer (Agilent Technology, Palo Alto, CA), respectively.

RNA sequencing and analysis

RNA sequencing was done at ServiceXS (Leiden, the Netherlands) using Illumina HiSeq2000 (Illumina, San Diego, USA) and Illumina protocols. mRNA was isolated from 10 µg total RNA using oligo dT-linked to magnetic beads. The mRNA was fragmented using divalent cations and copied into cDNA using reverse transcriptase and random primers. Double strand cDNA was synthesized using DNA Polymerase I and RNaseH. Adapters were ligated to the cDNA after end-repair and addition of a single 'A' nucleotide at the ends. The cDNA fragments were amplified by PCR to create the final cDNA library. Quality and yield of fragments were measured with a DNA 1000 Lab-on-a-Chip (Agilent Technology, Waldbronn, Germany). The size of cDNA fragments was approximately 300 bp. Fragments were sequenced in paired-end mode resulting in two 100 bp reads with an average insert size of 157 bp (± 3.9 bp across samples). For each sample (6 conditions, 3 replicates) an average of 12.1 (± 1.7 standard deviation) million fragments was obtained. The minimum fragment number was 10.1 million.Trimmomatic 0.22 (Lohse et al., 2012) was used to remove adapters and leading / trailing bases below quality 3. Reads were cut when a 4 base stretch had an

average quality below 15 and they were removed when they had a length < 36 bases. Fragments of which both reads survived (89 ± 2 %) were mapped to the *A. niger* N402 genome (AFR Ram, unpublished) using STAR (Dobin et al., 2012). In total, 45331 splice sites (after quality filtering) were found. This information was used to improve alignments across splice sites, by realigning all reads. An average unique alignment rate of 95 % was obtained, while on average 1.8 % of the reads mapped at multiple locations. To perform expression analysis, gene annotations were transferred from the CBS 513.88 genome (http://www.aspergillusgenome.org/SequenceContents.shtml) to the N402 genome using RATT (Otto et al., 2011). Of 14070 genes, 13070 genes could be transferred completely and 106 genes partially. Cufflinks 2.1.1(Trapnell et al., 2013) was used to process these annotations with the discovery of new genes / transcripts disabled. Cuffdiff 2.1.1 was also used to quantify differential expression. Conditions were analyzed simultaneously to make use of expression variability information across multiple conditions.

Go analysis

Significant differentially expressed genes in zones 1, 3, and 5 between the wild type and the Δ*fluG* strain were analyzed by Fetgoat (Nitsche et al., 2011). Fetgoat applies a Fisher's exact test to identify Gene Ontology terms that are overrepresented / underrepresented in a list of differential expressed genes. Benjamini & Hochberg correction method was used to correct for multiple testing.

Localization of protein synthesis and protein section

Protein synthesis, secretion, and growth were monitored as described (Wösten et al., 1991, Krijgsheld et al., 2012). Sandwiched colonies were labeled for 4 h with 185 kBq^{14}C- amino acids (NEC 455E amino acid mixture, L-[^{14}C (U)] – specific activity 1.94G Bq milliatom^{-1}; Perkin Elmer, Waltham MA, USA) to monitor protein synthesis and secretion. A polyvinylidenediluoride (PVDF) membrane (Immobilon-p, Milipore, Bedford, USA) was placed in between the sandwich colony and the agar medium to

immobilize the secreted proteins. Growth was visualized by labeling for 10 min with 185 kBq ^{14}C-N-acetyylglucosamine (CFA485 N-acetyl-D-[1-14C] glucosamine, specific activity 1.85-2.29GBq mmol^{-1}; GE Healthcare, Westborough, MA, USA). Labelled N-acetylglucosamine or amino acids were placed on top of the colony after absorbing it to a piece of rice paper (Sleicher & Schuell, Dassel, Germany) with the size of the colony. Colonies were fixed with 4 % formaldehyde in phosphate buffered saline (PBS) for 1 h at room temperature. Sandwiched colonies and PVDF membranes were washed 3 times 60 min with 1 % casamino acids (Becton, Dickinson and company, Le-Pont-De-Claix, France) or 0.44 mM N-actyl-glucosamine depending on the label used. After drying over night at room temperature, colonies and PVDF membranes were exposed to Kodak Biomax XAR film (Sigma-Aldrich, Saint Louis, USA).

Scanning electron microscopy

Sandwiched colonies were grown in the absence of an agarose layer between PC membranes. Samples (8 x 5mm) were cut from the periphery and the center of the colony and prepared as described (Krijgsheld et al., 2013b). A Field Emission Scanning Election Microscope (FEI, Eindhoven, The Netherlands) was used to view the samples using an acceleration voltage of 5 kV and a working distance of about 5 mm.

Light response sporulation profile

The upper PC membrane was removed from light or dark grown 6 day-old sandwiched colonies and exposure to light or dark was prolonged for 24 h. Spore concentration was measured by dividing the spore number by the surface area of the colony. Statistical analysis was performed with IBM Statistics 20 (SPSS statistics; IBM New York, USA).

SDS-PAGE

SDS-PAGE and Coomassie Brilliant Blue staining were performed as described (Levin et al., 2007b)

RESULTS

Phenotypic characterization of Δ*fluG*

Sporulation was assessed in 6-day-old sandwiched colonies of the wild-type strain, the Δ*fluG* strain, and the complemented Δ*fluG* strain by removing the upper PC membrane for 24 h. Spatial patterns of sporulation (Figure 1) and spore numbers (Table 1) did not significantly differ between the strains when colonies were grown in the light or in the dark using maltose or xylose as carbon source. All three strains formed less spores on xylose when compared to maltose (Table 1). Scanning electron microscopy revealed that Δ*fluG* colonies form fully developed conidiophores similar to those of wild type (Figure 2). Spores of the Δ*fluG* strain germinated like the wild-type when incubated in MM with maltose (Figure 3), xylose, or in the absence of a carbon source (data not shown). Moreover, biomass was not siginificantly different between Δ*fluG* colonies and wild type on either maltose or xylose containing medium (Figure 4).

Table 1. Density (spore number cm^{-2}) of spores produced by wild type N402, the Δ*fluG* strain, and the Δ*fluG* complemented (FC) strain under light (1200 lux) and dark conditions using maltose or xylose as a carbon source. The upper PC membrane of 6-day-old sandwiched colonies was removed and spores were harvested after 24 h. Standard deviation is indicated.

		light			dark	
Maltose	**N402**	**Δ*fluG***	**FC**	**N402**	**Δ*fluG***	**FC**
Average	$67\ 10^6 \pm 0$	$57\ 10^6 \pm 0{,}3\ 10^6$	$60\ 10^6 \pm 3\ 10^6$	$59\ 10^6 \pm 7\ 10^6$	$62\ 10^6 \pm 1\ 10^6$	$53\ 10^6 \pm 2\ 10^6$
Xylose	**N402**	**Δ*fluG***	**FC**	**N402**	**Δ*fluG***	**FC**
Average	$15\ 10^6 \pm 0.02\ 10^6$	$15\ 10^6 \pm 4\ 10^6$	$22\ 10^6 \pm 1\ 10^6$	$18\ 10^6 \pm 7\ 10^6$	$11\ 10^6 \pm 2\ 10^6$	$30\ 10^6 \pm 5\ 10^6$

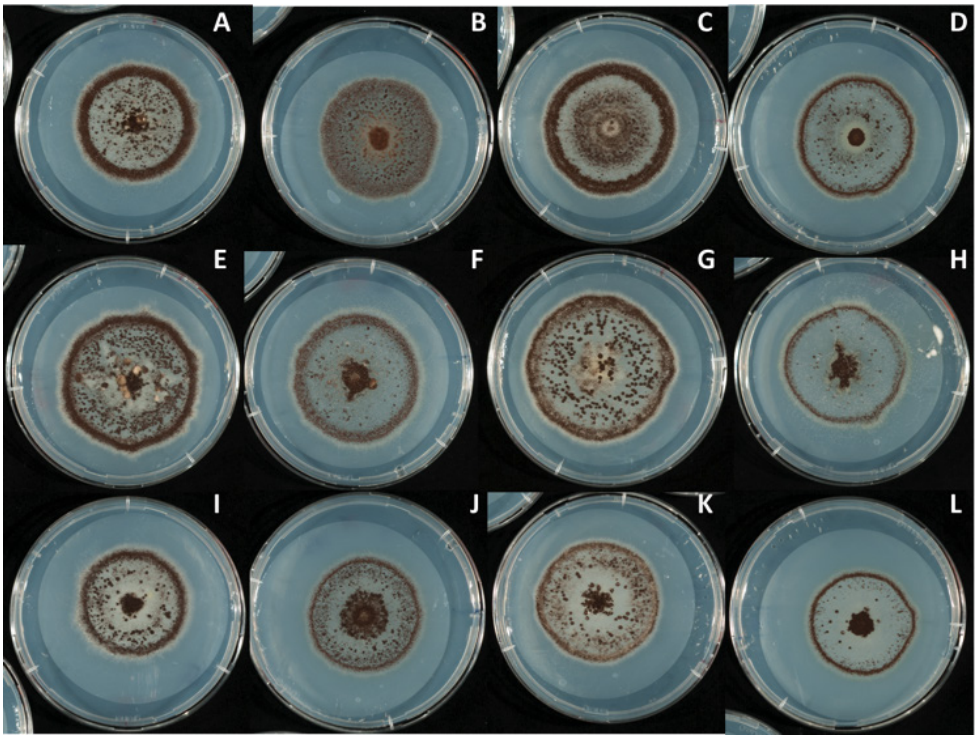

Figure 1. Sporulation profiles of wild type N402 (A-D), the Δ*fluG* strain (E-H), and the Δ*fluG* complemented strain (I-L) under the light (1200 lux) (A, B, E, F, I, and J.) and in the dark (C, D, G, H, K, and L) using maltose (A, C, E, G, I, and K) or xylose (B, D, F, H, J, and L) as a carbon source. The upper PC membrane of 6-day-old sandwiched colonies was removed and spores were allowed to form for 24 h.

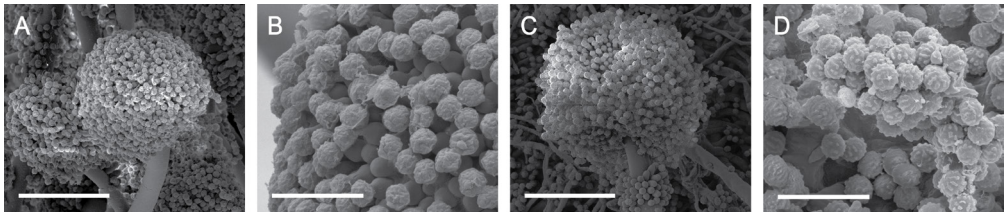

Figure 2. Scanning electron microscopy of conidiophores formed during a 24 h period after removing the upper PC membrane from 6-day old sandwiched colonies of *A. niger* wild-type N402 (A, B) and the Δ*fluG* strain (C, D). Bars represent 40 µm (A,C) and 10 µm (B, D).

Growth was localized at the periphery of 7-day-old colonies of the wild-type and the Δ*fluG* strain by labelling with ^{14}C N-acetylglucosamine (Figure 5). Protein synthesis and secretion, as monitored by labelling with ^{14}C amino acids, was localized throughout the mycelium and at the periphery of the colonies, respectively (Figure 5). Thus, spatial growth and secretion patterns have not been changed in Δ*fluG* colonies when compared to the wild-type. Protein profiles in the medium were monitored by

transferring 6-day-old colonies to ring plates for 24h (Levin et al., 2007b). These ring plates consist of a plate with 5 concentric wells that are filled with medium. It was found that Δ*fluG* colonies release more proteins on maltose and similar levels on xylose (Figure 6).

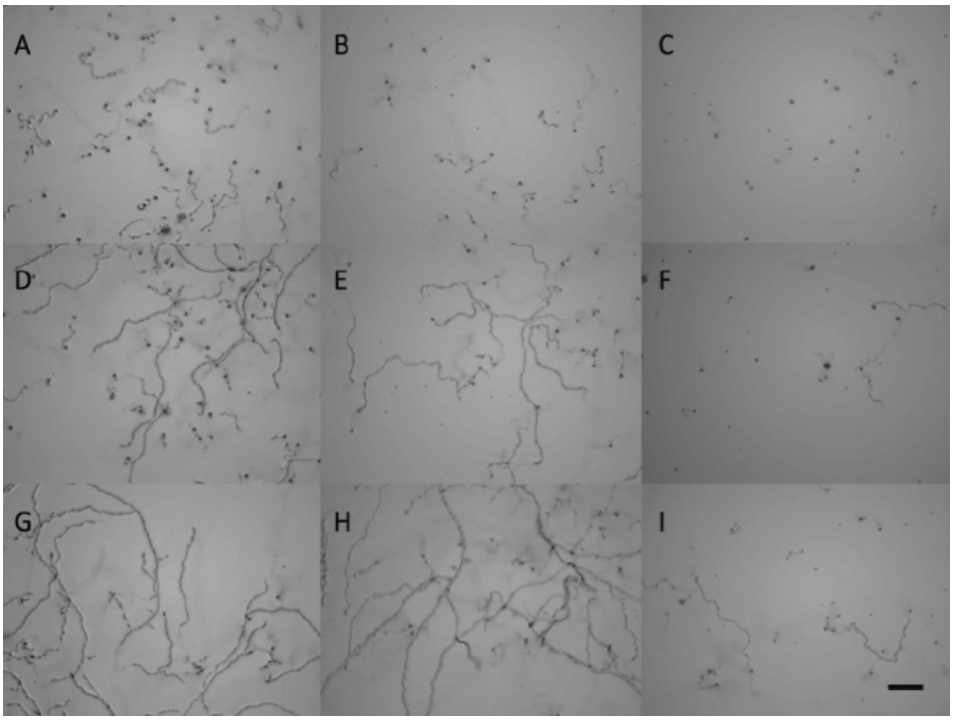

Figure 3. Germination of N402 (control) (A, D, G), **Δ***fluG* (B, E, H), and complemented **Δ***fluG* (C, F, I) after 8 (A-C), 16 (D-F), and 24 h in MM containing maltose. Bar represents 100 µm.

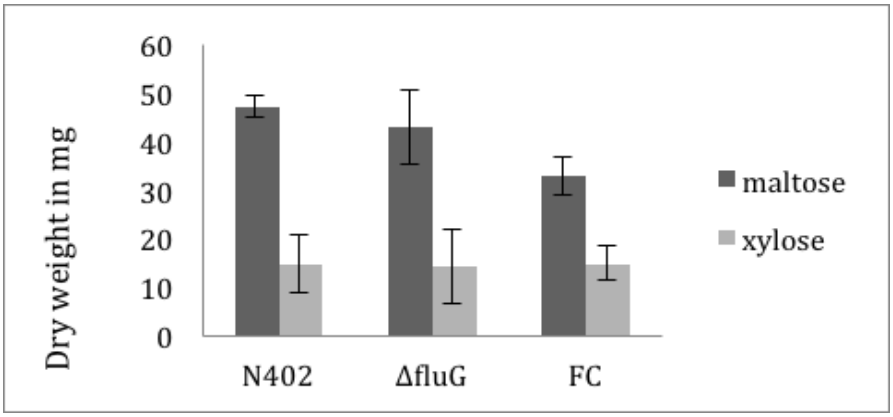

Figure 4. Dry weight of a 7-day-old maltose- and xylose-grown colony of wild-type (N402), Δ*fluG*, and the complemented Δ*fluG* (FC) strain.

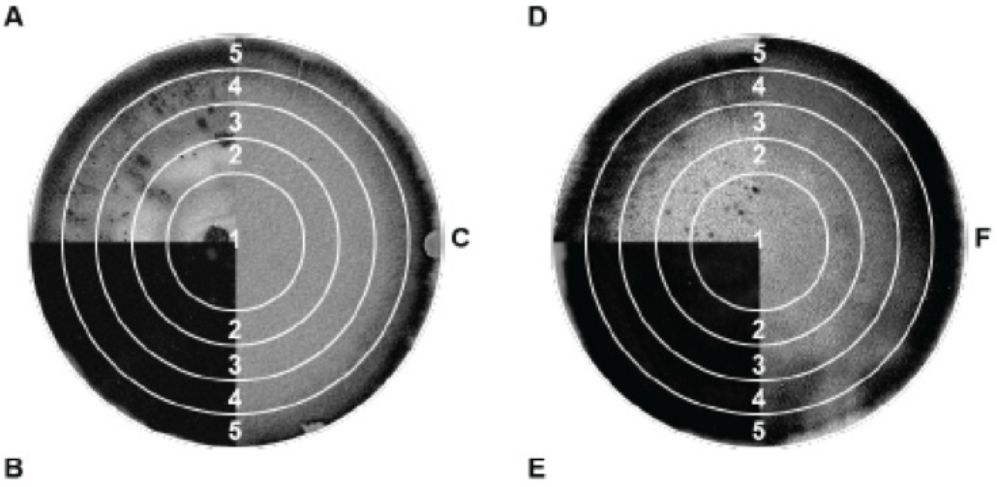

Figure 5. Growth (A,D), protein synthesis (B,E), and secretion (C,F) in 7-day-old maltose-grown wild-type (A-C) and Δ*fluG* (D-F) colonies. Growth was monitored by labelling with ^{14}C N-acetylglucosamine, while protein synthesis and secretion were monitored by incorporation of ^{14}C-labeled amino acids. Secreted proteins were immobilized by a PVDF membrane that had been placed underneath the colony.

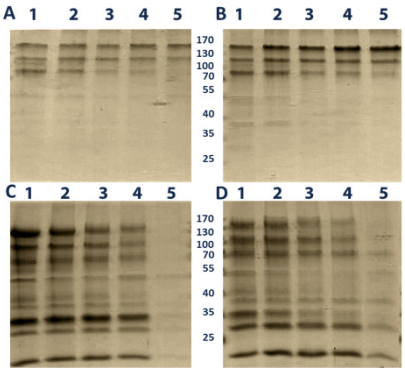

Figure 6. SDS PAGE of proteins contained in the culture medium of ring plate cultures of a 7-day-old maltose-grown wild-type (A) and Δ*fluG* (B) colony and of a 7-day-old xylose-grown wild-type (C) and Δ*fluG* (D) colony. Lanes 1 and 5 represent the most central and peripheral zones, respectively.

RNA profiles in zones of Δ*fluG* colonies

The mycelium of 7-day-old maltose-grown sandwiched colonies of N402 and the Δ*fluG* strain were divided in 5 concentric zones (Levin et al., 2007a, Levin et al., 2007b). Gene expression was assessed in the central zone 1, the intermediate zone 3, and the outer zone 5 using RNAseq. Principal component analysis (PCA) showed that the transcriptomes from zone 1 and 3 of N402 and Δ*fluG* separated from zone 5 of these strains. This component accounted for 51 % of the variation in the datasets (Figure 7). The second component of the PCA accounted for 14 % of the variation and separated the zones of the wild-type from that of the Δ*fluG* strain. Expression in the central zone 1 and the intermediate zone 3 of the wild-type

(N402) correlated to a high extent (Pearson's $r^2 \geq 0.98$, Figure 7), while correlation of these profiles with zone 5 was less ($r^2 = 0.92$ in both cases). A similar result was found in the case of the Δ*fluG* strain with a r^2 of 0.98 and 0.94, respectively. Expression profiles of zones 1 of the wild-type and the Δ*fluG* strain showed a r^2 of 0.97. A similar high correlation was found when zones 3 or zones 5 were compared (r^2 of 0.98 in both cases).

A

	f1	f3	f5	n1	n3	n5
f1	1.	0.98	0.94	0.97	0.96	0.93
f3		1.	0.94	0.97	0.98	0.91
f5			1.	0.93	0.93	0.98
n1				1.	0.98	0.92
n3					1.	0.92
n5						1.

B

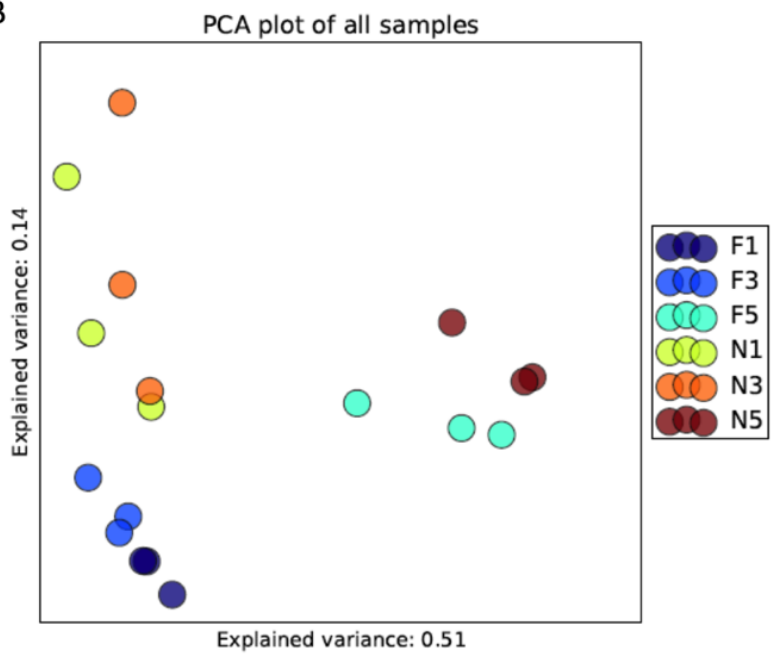

Figure 7. Pearson correlation (r2) (A) and principal component analysis (B) of the transcriptomes of zones 1, 3, and 5 of wild-type (N) and Δ*fluG* (F) colonies.

Gene expression comparison and GO analysis

A total of 1451 genes were differentially expressed in zone 1 of Δ*fluG* colonies (472 up- and 979 down-regulated) when compared to zone 1 of N402 colonies. Similarly

993 (506 up- and 487 down-regulated) and 1047 (375 up- and 672 down-regulated) were differentially expressed in zones 3 and 5, respectively. A total of 210 and 620 genes were up- and down-regulated, respectively, in zone 1 when a fold-change ≥2 was used as cut-off. These numbers were 340 and 257 and 472 and 187 for zones 3 and 5.

GO analysis (biological process, cellular component, and molecular function) was performed on the differentially expressed genes with a fold change ≥ 2. A single cellular process GO term (plasma membrane enriched fraction) was overrepresented in the upregulated gene group in zone 1 of the wild-type strain when compared to the respective zone in the Δ*fluG* colony (Table S 1). In this gene group 10 biological process (Table S 2) and 6 molecular process (Table S 3) terms were overrepresented. Of the biological process terms, 8 were related to carbohydrate metabolic and catabolic processes, while 3 out of 6 molecular process terms were related to hydrolase activity. No GO terms were overrepresented in the intermediate zone 3 and the peripheral zone of wild type colonies. Only 4 biological process GO terms (carboxylic acid biosynthetic process, secondary metabolic process, fatty acid biosynthetic process, and organic acid biosynthetic process) were overrepresented in the upregulated gene group of zone 1 of Δ*fluG* colonies (Table S 4 & 5). In contrast, 18 and 16 biological process and molecular process terms, respectively, were overrepresented in the upregulated gene group of zone 3 of Δ*fluG* colonies (Table S 4 & 5). Of these terms, 12 and 4, respectively, were related to carbohydrate catabolic and metabolic processes. Similarly, 27 and 15 biological process and molecular process terms, respectively, were overrepresented in the upregulated gene group of zone 5 of Δ*fluG* colonies (Table S 4 & 5). Of these, 16 and 4 were related to carbohydrate metabolic and catabolic processes.

Expression analysis of selected functional gene classes

Genes involved in sexual and sexual development

68 genes have been implicated in asexual and sexual development in *A. niger* (Pel et al., 2007). Four extra genes (homologs of *flbB, flbD, flbE,* and *sfgA*) were added to this list (Krijgsheld and Wösten, 2013). Of these 72 genes, only 5 genes had a ≥ 2-fold change in expression in at least one of the zones of Δ*fluG* colonies when compared to the respective zones of the wild-type (Table S 6). The *brlA* gene of *A. niger* was down-regulated in all three zones of Δ*fluG* colonies, while *flbC* was downregulated in zone 1.

Cell wall biosynthesis genes

102 genes are considered to be involved in cell wall synthesis (Pel et al., 2007). Of these, only 11 had a ≥ 2-fold change in expression in at least one of the zones of Δ*fluG* colonies when compared to the respective zones of the wild-type (Table S 7). These genes do not include chitin synthase or β-glucan synthase genes. The glucanosyl-transferase genes *bgt1* (An08g03580) and *gel1* (An01g03090) were downregulated (fold change ≥ 2) in the central zone 1 and upregulated in zones 3 and 5, respectively, of Δ*fluG* colonies. Moreover, chitinase genes *cfcA* and *chiD* were up- and downregulated in zone 3 of Δ*fluG* colonies, respectively, whereas chitinase gene *cfcI* was upregulated in zone 5 of Δ*fluG* colonies.

Genes encoding proteins with a signal sequence for secretion

The *A. niger* genome contains 2554 genes that encode proteins with a predicted signal sequence for secretion (Pel et al., 2007). Within this gene group, 433 genes were found to have a significant ≥ 2-fold change in expression in at least one zone of the Δ*fluG* colony when compared to wild type (Table S 8). A total of 60 and 157 genes were ≥ 2-fold up- and down-regulated, respectively, in the center of the Δ*fluG* colony when compared to the wild-type. Similarly, 135 and 50 genes and 165 and 57 genes were up- and down-regulated in the intermediate zone 3 and the peripheral zone 5 of the Δ*fluG* colony. Thus, genes encoding proteins with a signal sequence were more often downregulated in zone 1 and upregulated in zone 3 and 5 of the Δ*fluG* colony.

XlnR regulated genes

As mentioned above, wild-type and Δ*fluG* colonies had been grown on MM with maltose. This carbon source activates AmyR, a transcriptional regulator that controls 16 genes. Expression of these genes has been described in Chapter 2. XlnR is the regulator of 16 genes encoding xylanolytic enzymes (van Peij et al., 1998b, van Peij et al., 1998a, Gielkens et al., 1999, de Vries and Visser, 2001, Hasper et al., 2000, Hasper et al., 2004). Genes *axeA, lacA, faeA,* and *eglC* were downregulated at least 2-fold in the central zone of Δ*fluG* strain colonies (Table S 9). In contrast, 5 out of 16 genes (*cbhA, cbhB, eglA, faeA,* and *xynB*) were upregulated ≥ 2-fold in the intermediate zone 3 of Δ*fluG* colonies (Table S 9). Seven xylanolytic genes (*xlnD, axeA, abfB, aguA, lacA, eglC, anId cbhB*) were upregulated at least 2-fold at the periphery of Δ*fluG* colonies.

Genes involved in carbohydrate degradation

In *A. niger,* 172 genes show carbohydrase activity (Pel et al., 2007). Within this gene group, 131 genes are secreted and 40 genes encode intercellular enzymes (Pel et al., 2007). When compared to wild type, 5 and 22 genes encoding extracellular carbohydrases are significant up- and down-regulated in zone 1 of Δ*fluG* colonies with a fold change ≥ 2, respectively (Table S 10). 26 and 1 gene and 32 and 3 genes were significant up- and down-regulated in the intermediate zone 3 and the peripheral zone 5 of the Δ*fluG* colony, respectively.

Transcription factor genes

The genome of *A. niger* contains 623 genes encoding transcription factors (Pel et al., 2007) Of these genes, 56 were differentially expressed with a fold change ≥ 2 in at least one zone of Δ*fluG* colonies (Table S 11). 6 and 14 genes showed significant ≥ 2-fold up- and down- regulation respectively in the center of the Δ*fluG* colony when compared to the wild-type. 13 and 17 genes and 15 and 8 genes were ≥ 2-fold up- and down- regulated in the intermediate zone 3 and the peripheral zone 5, respectively.

DISCUSSION

The sporulation pathway in *A. niger* has been proposed to be similar, if not identical, to that of *A. nidulans* (Pel et al., 2007). Indeed, BrlA and FlbA have a similar role in asexual reproduction in these fungi (Krijgsheld et al., 2013b). However, here it was shown that FluG of *A. niger* has a different role. FluG of *A. nidulans* and *A. oryzae* is involved in initiation of conidiophore formation. In contrast, Δ*fluG* strains of *A. fumigatus* and *A. niger* still form conidiophores. Notably, *A. oryzae* and *A. niger* are most related of these four aspergilli, while *A. nidulans* is most unrelated (Houbraken et al., 2014). This implies that loss / gain of function of FluG in asexual development has occurred at least two independent times in the evolution of aspergilli. We also showed that asexual development does not depend on light in the case of *A. niger,* while it preferentially takes place in the light in the case of *A. nidulans* (Purschwitz et al., 2008). In contrast to *A. nidulans*, conidiation is repressed by white and red light in *A. oryzae* (Hatakeyama et al., 2007)In *A. fumigatus,* light affects conidial germination, and increases hyphal pigmentation, resistance to ultraviolet light and oxidative stress, and susceptibility to cell wall perturbation (Fuller et al., 2013). The effect of light on reproduction of *A. fumigatus* has not yet been assessed.

Zonal formation of conidiophores was similar in wild-type and Δ*fluG* colonies of *A. niger*. In addition, morphology of the conidiophores, and the number of spores formed per surface area were similar. This was observed in light- and dark-grown colonies and in colonies grown on maltose or xylose. The impact of *fluG* inactivation on expression of genes involved in asexual development of *Aspergillus* was minimal. Only 5 out of 72 genes were differentially expressed in the Δ*fluG* strain when compared to the wild-type strain. Of these 5 genes, *brlA* and *flbC* are known to play a central role in asexual development of *A. nidulans* (Figure 6, Chapter 1). Gene *brlA* of *A. niger* was downregulated in all three zones of Δ*fluG* colonies, while *flbC* was downregulated in zone 1. The downregulation of *brlA* in the Δ*fluG* strain was expected from expression data of *A. nidulans* (Lee and Adams, 1996). However, in *A. niger* this did not result in a phenotypic change in asexual development. Apparently, the

reduced *brlA* expression is sufficient to induce sporulation. The impact of FluG on *flbC* expression was not expected a priori. Expression of this gene in the Δ*fluG* strain of *A. nidulans* was not assessed in the past.

The *fluG* transcripts are present in relatively constant levels during late vegetative growth and conidiation. Notably, a 4-fold higher *fluG* expression level is found in germinating spores of *A. nidulans* during their isotropic growth (3 hours after inoculation) when compared to polar growing germlings (5 hours after inoculation) (Breakspear and Momany, 2007). This suggests that *fluG* is not only involved in conidiophore formation but also in germination. We could not confirm this in *A. niger.* Deletion of *fluG* gene did not cause an obvious change in germination incidence or rate. Biomass and zonal growth patterns were also similar in wild-type and the Δ*fluG* strain. In agreement, only few genes predicted to be involved in cell wall synthesis showed differential expression in these two strains. For instance, chitin and glucan synthases showed similar expression in the two strains. Notably, FluG did impact expression of genes encoding proteins with a signal sequence for secretion. Out of 2554 of these genes, 433 were differentially expressed. A total of 60 and 157 genes were ≥ 2-fold up- and down-regulated, respectively, in the center of the Δ*fluG* colony when compared to the wild-type. This ratio was reversed in the intermediate and peripheral zones. 135 and 50 genes and 165 and 57 genes were up- and down-regulated in these zones, respectively. Among these genes were xylanolytic genes. XlnR is the regulator of 16 genes encoding xylanolytic enzymes (van Peij et al., 1998b, van Peij et al., 1998a, Gielkens et al., 1999, de Vries and Visser, 2001, Hasper et al., 2000, Hasper et al., 2004). Four of these genes (*axeA, lacA, faeA,* and *eglC*) were downregulated at least 2-fold in the central zone of Δ*fluG* strain colonies, while 5 (*cbhA, cbhB, eglA, faeA,* and *xynB*) and 7 (*xlnD, axeA, abfB, aguA, lacA, eglC, anId cbhB*) of these genes were upregulated ≥ 2-fold in the intermediate zone 3 and the peripheral zone 5 of Δ*fluG* colonies, respectively when compared to the wild-type. It should be noted that expression of genes encoding secreted proteins has not yet been assessed using xylose; the carbon source that activates XlnR. This should be done in future studies

keeping in mind that we do not have indications for increased protein release when colonies are grown on this carbon source. In contrast, amylolytic proteins are released throughout the mycelium in the Δ*fluG* strain (Chapter 2). It was proposed that this was due to increased leakage of proteins that are normally retained in the cell wall. Data presented in this chapter agree with this hypothesis. SDS PAGE combined with CBB staining showed increased protein release in all zones of the Δ*fluG* strain when compared to the wild-type, while pulse labelling with radioactively labelled amino acids showed protein secretion mainly at the outer part of the colony (Chapter 5). Together, FluG is not involved in growth and sporulation but does affect zonal expression of genes including transcription factors genes, and genes encoding secreted proteins. A role as a suppressor of secretion under particular environmental conditions would link FluG to asexual development.

Table S 1. Cellular component GO terms that are overrepresented in the upregulated genes in zones 1 (center), 3 (intermediate), and 5 (periphery) of wild-type colonies (n1, n3, and n5, respectively) when compared to the respective zones in Δ*fluG* colonies.

GO term	Description
n1	
GO:0001950	plasma membrane enriched fraction
n3	
n5	

Table S 2. Biological process GO terms that are overrepresented in the upregulated genes in zones 1 (center), 3 (intermediate), and 5 (periphery) of wild-type colonies (n1, n3, and n5, respectively) when compared to the respective zones in Δ*fluG* colonies.

GO term	Description
n1	
GO:0044262	cellular carbohydrate metabolic process
GO:0044275	cellular carbohydrate catabolic process
GO:0005996	monosaccharide metabolic process
GO:0006066	alcohol metabolic process
GO:0044264	cellular polysaccharide metabolic process
GO:0005976	polysaccharide metabolic process
GO:0034614	cellular response to reactive oxygen species
GO:0005975	carbohydrate metabolic process
GO:0016052	carbohydrate catabolic process
GO:0006800	oxygen and reactive oxygen species metabolic process
n3	
n5	

Table S 3. Molecular function GO terms that are overrepresented in the upregulated genes in zones 1 (center), 3 (intermediate), and 5 (periphery) of wild-type colonies (n1, n3, and n5, respectively) when compared to the respective zones in Δ*fluG* colonies.

GO term	Description
n1	
GO:0016798	hydrolase activity, acting on glycosyl bonds
GO:0052689	carboxylic ester hydrolase activity
GO:0016491	oxidoreductase activity
GO:0004091	carboxylesterase activity
GO:0015926	glucosidase activity

Table S 3 continued

GO:0004553	hydrolase activity, hydrolyzing O-glycosyl compounds
n3	
n5	

Table S 4. Biological process GO terms that are overrepresented in the upregulated genes in zones 1 (center), 3 (intermediate), and 5 (periphery) of Δ*fluG* colonies (f1, f3, and f5, respectively) when compared to the respective zones of the wild-type.

GO term	Description
f 1	
GO:0046394	carboxylic acid biosynthetic process
GO:0019748	secondary metabolic process
GO:0006633	fatty acid biosynthetic process
GO:0016053	organic acid biosynthetic process
f3	
GO:0030243	cellulose metabolic process
GO:0044042	glucan metabolic process
GO:0044262	cellular carbohydrate metabolic process
GO:0045490	pectin catabolic process
GO:0009056	catabolic process
GO:0044275	cellular carbohydrate catabolic process
GO:0046942	carboxylic acid transport
GO:0044264	cellular polysaccharide metabolic process
GO:0015849	organic acid transport
GO:0005976	polysaccharide metabolic process
GO:0009251	glucan catabolic process
GO:0000272	polysaccharide catabolic process
GO:0045488	pectin metabolic process
GO:0044247	cellular polysaccharide catabolic process
GO:0005975	carbohydrate metabolic process
GO:0015804	neutral amino acid transport
GO:0016052	carbohydrate catabolic process
GO:0006544	glycine metabolic process
f5	
GO:0030243	cellulose metabolic process
GO:0044262	cellular carbohydrate metabolic process

Table S 4 continued

GO:0045493	xylan catabolic process
GO:0045490	pectin catabolic process
GO:0009056	catabolic process
GO:0015837	amine transport
GO:0044275	cellular carbohydrate catabolic process
GO:0006865	amino acid transport
GO:0010410	hemicellulose metabolic process
GO:0044282	small molecule catabolic process
GO:0044036	cell wall macromolecule metabolic process
GO:0005996	monosaccharide metabolic process
GO:0010383	cell wall polysaccharide metabolic process
GO:0046942	carboxylic acid transport
GO:0071705	nitrogen compound transport
GO:0044264	cellular polysaccharide metabolic process
GO:0015849	organic acid transport
GO:0045491	xylan metabolic process
GO:0005976	polysaccharide metabolic process
GO:0000272	polysaccharide catabolic process
GO:0045488	pectin metabolic process
GO:0044247	cellular polysaccharide catabolic process
GO:0005975	carbohydrate metabolic process
GO:0015804	neutral amino acid transport
GO:0016052	carbohydrate catabolic process
GO:0071702	organic substance transport
GO:0009057	macromolecule catabolic process

Table S 5. Molecular function GO terms that are overrepresented in the upregulated genes in zones 1 (center), 3 (intermediate), and 5 (periphery) of Δ*fluG* colonies (f1, f3, and f5, respectively) when compared to the respective zones in the wild-type.

GO term	**Description**
f1	
f3	
GO:0003824	catalytic activity
GO:0016798	hydrolase activity, acting on glycosyl bonds
GO:0052689	carboxylic ester hydrolase activity
GO:0046943	carboxylic acid transmembrane transporter activity

Table S 5 continued

GO:0016162	cellulose 1,4-beta-cellobiosidase activity
GO:0016837	carbon-oxygen lyase activity, acting on polysaccharides
GO:0004375	glycine dehydrogenase (decarboxylating) activity
GO:0004091	carboxylesterase activity,
GO:0016642	oxidoreductase activity, acting on the CH-NH2 group of donors, disulfide as acceptor
GO:0008810	cellulase activity
GO:0004553	hydrolase activity, hydrolyzing O-glycosyl compounds
GO:0005342	organic acid transmembrane transporter activity
GO:0016298	lipase activity
GO:0008028	monocarboxylic acid transmembrane transporter activity
GO:0016638	oxidoreductase activity, acting on the CH-NH2 group of donors
GO:0004806	triglyceride lipase activity
f5	
GO:0005275	amine transmembrane transporter activity
GO:0003824	catalytic activity
GO:0016798	hydrolase activity, acting on glycosyl bonds
GO:0052689	carboxylic ester hydrolase activity
GO:0046943	carboxylic acid transmembrane transporter activity
GO:0016787	hydrolase activity
GO:0004091	carboxylesterase activity
GO:0015171	amino acid transmembrane transporter activity
GO:0008810	cellulase activity
GO:0004553	hydrolase activity, hydrolyzing O-glycosyl compounds
GO:0005342	organic acid transmembrane transporter activity
GO:0003674	molecular_function
GO:0046556	alpha-N-arabinofuranosidase activity
GO:0004806	triglyceride lipase activity
GO:0015925	galactosidase activity

Table S 6. Differentially expressed genes related to asexual and sexual development (Pel et al., 2007) in the central zone 1, the intermediate zone 3, and the outer zone 5 of 7-day-old maltose-grown colonies of N402 and Δ*fluG*. The ^{2}log ratio of expression values of N402 vs Δ*fluG* is indicated. A number ≥1 (red) and ≤-1 (green) represent a ≥2 fold decrease and increase in Δ*fluG* colonies, respectively.

Gene id	Name	Description	log 2 fold change		
			N402 zone 1 / ΔfluG zone 1	N402 zone 3 / ΔfluG zone 3	N402 zone 5 / ΔfluG zone 5
An02g05420	flbC	strong similarity to hypothetical zinc-finger protein flbC - Aspergillus nidulans	1,01728	0,515692	0,407467
An01g10540	brlA	strong similarity to developmental regulatory protein brlA - Aspergillus nidulans	1,11456	1,35146	1,1185
An01g13660	mcoB	strong similarity to laccase I precursor yA -Aspergillus nidulans	2,75277	0,203482	0,677644
An14g01820	phiA	strong similarity to hypothetical cell wall protein binB - Aspergillus nidulans	-0,255317	-1,6162	-0,16124
An14g01130		strong similarity to rhamnogalacturonase B precursor rhgB - Aspergillus aculeatus	0,534344	-1,54858	-0,895222

Table S 7. Differentially expressed genes related to cell wall synthesis (Pel et al., 2007) in the central zone 1, the intermediate zone 3, and the outer zone 5 of 7-day-old maltose-grown colonies of N402 and Δ*fluG*. The ^{2}log ratio of expression values of N402 vs Δ*fluG* is indicated. A number ≥1 (red) and ≤-1 (green) represent a ≥2 fold decrease and increase in Δ*fluG* colonies, respectively. Pink red and olive green shading indicate a >1 fold and significant down- and up-regulation in Δ*fluG*.

Gene id	Name	Description	log 2 fold change		
			N402 zone 1 / ΔfluG zone 1	N402 zone 3 / ΔfluG zone 3	N402 zone 5 / ΔfluG zone 5
An01g10940		strong similarity to 1,3-beta-glucanosyltransferase bgt1 - Aspergillus fumigatus	1,59209	-0,08171	-1,41847
An08g03580	bgt1	strong similarity to chitinase 1 precursor cts1 - Coccidioides immitis	2,53455	-0,90029	0,833007
An02g07020	cfcA	strong similarity to 1,3-beta-glucanosyltransferase gel1 - Aspergillus fumigatus	-0,43115	-2,08391	-1,16178
An01g03090	chiD	strong similarity to chitinase 1 cts1 -Coccidioides immitis	-0,49315	-1,56084	-1,4105
An08g09030		strong similarity to mitogen-activated protein kinase sty1p - Schizosaccharomyces pombe	-0,41268	1,4908	-0,09548
An18g05270	cfcI	strong similarity to endochitinase - Aphanocladium album	0,148693	-0,0665	-1,4175
An02g13580		similarity to filamentous growth protein Dfg5 - Saccharomyces cerevisiae	0,696502	-0,63083	-1,33354
An11g01240	exgA	strong similarity to 43 kDa secreted glycoprotein precursor gp43 - Paracoccidioides brasiliensis	-0,69545	-0,87819	-1,0655
An18g04100		similarity to cell wall synthesis protein KRE9 - Candida albicans	0,310338	-0,25535	1,19065
An05g00130		strong similarity to beta-glucan synthesis	0,200453	0,140337	1,37222
An02g03980		associated protein Kre6 - Saccharomyces cerevisiae	0,541569	0,951166	2,08263

Table S 8. Differentially expressed genes encoding proteins with a signal sequence (Pel et al., 2007) in the central zone 1, the intermediate zone 3, and the outer zone 5 of 7-day-old maltose-grown colonies of N402 and Δ*fluG*. The ^{2}log ratio of expression values of N402 vs Δ*fluG* is indicated. A number ≥1 (red) and ≤-1 (green) represent a ≥2 fold decrease and increase in Δ*fluG* colonies, respectively. Pink red and olive green shading indicate a >1 fold and significant down- and up-regulation in Δ*fluG* colonies.

Gene id	Name	Description	log 2 fold change		
			N402 zone 1 / ΔfluG zone 1	N402 zone 3 / ΔfluG zone 3	N402 zone 5 / ΔfluG zone 5
An02g12350		similarity to neuronal long splice form of ankyrin ANK2 - Homo sapiens	-0,23082	0,175829	1,01862
An09g00480		similarity to BCU0021 protein SEQ ID 8 from patent WO2003029421-A2 - Homo sapiens.	-0,81841	-0,66073	1,0517
An11g10270		strong similarity to aspartic protease polypeptide #4 from patent WO200268623-A2. - Aspergillus niger	-0,70567	0,513917	1,05183
An09g02510		strong similarity to hypothetical membrane protein YLR251w - Saccharomyces cerevisiae	0,025896	0,91063	1,05291
An07g04020		strong similarity to protein kinase Sky1 -Saccharomyces cerevisiae	0,55295	0,420682	1,08289
An11g07080		strong similarity to hypothetical protein AAO78637.1 - Bacteroides thetaiotaomicron	-0,42156	0,330859	1,08451
An12g04210		strong similarity to phenylacetate 2-hydroxylase phacA - Aspergillus nidulans	0,468791	0,584909	1,09457
An09g06200		strong similarity to transmembrane protein PTH11 - Magnaporthe grisea	-0,12314	0,588957	1,11053
An07g00850			-0,16155	0,546877	1,11104
An18g04100	exgA	strong similarity to 43 kDa secreted glycoprotein precursor gp43 - Paracoccidioides brasiliensis	0,310338	-0,25535	1,19065
An03g05560		strong similarity to developmentally regulated spherulin 4 - Physarum polycephalum	0,139962	0,053761	1,24225

Table S 8 continued

An14g03870		strong similarity to cytochrome P450 monooxygenase avnA - Aspergillus parasiticus	-0,19284	0,162161	1,27865
An14g05110		weak similarity to hypothetical protein AT4g01140 - Arabidopsis thaliana	-3,95456	#NAME?	1,29908
An05g00130		similarity to cell wall synthesis protein KRE9 - Candida albicans	0,200453	0,140337	1,37222
An18g00260		strong similarity to cytochrome P450 monooxygenase avnA - Aspergillus parasiticus	0,140907	0,569442	1,421
An12g09620			-0,79869	#NAME?	1,4281
An07g06210			-0,49975	-0,06708	1,42946
An07g06210			-0,49975	-0,06708	1,42946
An11g00040		weak similarity to cDNA for 59-kDa readthrough protein RT - Sorghum chlorotic spot virus	0,162739	0,574886	1,47012
An09g03010		strong similarity to EST an_2241 -Aspergillus niger	-0,65132	-0,17809	1,47701
An15g01930		similarity to integral membrane protein PTH11 - Magnaporthe grisea	-0,37631	0,111473	1,60298
An16g01780		similarity to protein CAP22 - Colletotrichum gloeosporioides	0,709228	0,603232	1,6099
An01g08960	mcoH	strong similarity to iron transport multicopper oxidase Fet3 - Candida albicans	1,86005	-1,01562	1,6665
An10g00110		strong similarity to O-methylsterigmatocystin oxidoreductase ordA - Aspergillus parasiticus	0,616156	0,849183	1,67747
An14g02170		strong similarity to cutinase precursor cutA - Fusarium solani	0,634394	-0,55815	1,73275
An02g01180	dppA	similarity to diacylglycerol pyrophosphate phosphatase Dpp1 - Saccharomyces cerevisiae	-0,18552	0,795433	1,79493
An01g06310		strong similarity to glutaminase A gtaA -Aspergillus oryzae	0,368935	0,332292	1,84679
An01g10970		strong similarity to quinate transporter qa-y - Neurospora crassa	0,29162	0,393674	1,89881
An12g05440		strong similarity to urea transport protein Dur3 - Saccharomyces cerevisiae	1,04421	-0,16831	2,40979
An14g03130			-0,54472	-0,07913	3,13953
An07g00170			1,94343	-1,26033	5,04996

Table S 8 continued

An08g04550		strong similarity to hypothetical protein B1D1.190 - Neurospora crassa [putative frameshift]	0,965549	0,509037	5,29225
An03g00420		similarity to hypothetical integral membrane protein pth11 like hypothetical protein CAC28570.2 -Neurospora crassa	0,965394	-1,74049	-3,35228
An14g02710		weak similarity to inward rectifier potassium channel protein cIRK1 - Gallus gallus	1,26413	0,080941	-3,07971
An11g08850		weak similarity to collagen fiber-associated protein RGD-CAP - Sus scrofa	0,213735	-0,6224	-2,99008
An18g00440		strong similarity to monosaccharide transporter AmMst-1 - Amanita muscaria	0,757752	-0,32112	-2,72684
An17g00230		similarity to hypothetical protein slr0789 -Synechocystis sp.	0,023713	-0,38077	-2,65416
An01g09970		weak similarity to Lactobacillus crispatus silent surface layer protein cbsB - Lactobacillus crispatus	0,789767	0,086195	-2,63096
An14g04540			-0,07365	-0,03535	-2,61397
An11g03540		strong similarity to cytochrome P450 monooxygenase TRI11 - Fusarium sporotrichioides	0,201882	-0,48181	-2,49194
An08g01900		strong similarity to xylan 1,4-beta-xylosidase - Butyrivibrio fibrisolvens	0,702329	0,098215	-2,47725
An03g02080	rgxB	strong similarity to exopolygalacturonase pgaX - Aspergillus tubingensis	1,65282	0,109435	-2,41187
An03g06740	pgxB	strong similarity to exo-alpha 1,4-polygalacturonase PGX1 - Cochliobolus carbonum	0,694498	0,14473	-2,29061
An01g14740	goxC		-1,87315	#NAME?	-2,26162
An01g14740	goxC		-1,87315	#NAME?	-2,26162
An02g00330			0,744321	-0,19973	-2,25765
An11g03430		strong similarity to hypothetical O-methylsterigmatocystin oxidoreductase ord1 - Aspergillus flavus	0,028066	-1,32522	-2,11306
An05g02450		similarity to halogenase bhaA from patent DE19926770-A1 - Amycolatopsis mediterranei	0,352281	-0,23461	-2,03736
An16g00540		similarity to large secreted protein -Streptomyces coelicolor [truncated ORF]	2,30179	1,17815	-2,03002

Table S 8 continued

An09g04920			-0,13005	-0,21309	-1,99716
An18g05500		strong similarity to mitochondrial ceramidase AAF86240.1 - Homo sapiens	0,335837	-0,57946	-1,89925
An09g04390		strong similarity to salicylate hydroxylase sal - Pseudomonas putida	0,43414	-0,07849	-1,8658
An11g01220		strong similarity to precursor of tannase -Aspergillus oryzae	0,292909	-0,00864	-1,8534
An14g05820		strong similarity to beta-galactosidase lacA - Aspergillus niger	0,106617	-0,57545	-1,84419
An04g08030		strong similarity to hexose transporter Hxt2 - Saccharomyces cerevisiae	0,948492	0,013847	-1,82019
An07g04430		strong similarity to hexose transporter ght2p - Schizosaccharomyces pombe	0,066317	0,090372	-1,81424
An12g05100		strong similarity to 3-oxoacyl-(acyl-carrier-protein) reductase fabG - Bacillus subtilis	-0,24531	-0,27468	-1,75652
An01g09960	xlnD		0,27645	0,185712	-1,75537
An12g02660			0,907748	0,544745	-1,65035
An01g08030		similarity to frenolicin gene cluster protein 18 from patent JP10094395-A - Streptomyces roseofulvus	0,981178	-0,21121	-1,64111
An17g00300	xarB	strong similarity to bifunctiona xylosidase-arabinosidase xarB - Thermoanaerobacter ethanolicus [putative frameshift]	-0,11165	-0,49825	-1,6257
An05g00730		strong similarity to hexose transporter Hxt3 - Saccharomyces cerevisiae	-0,07925	-0,12938	-1,60508
An01g01370		strong similarity to hypothetical protein encoded by An06g01030 - Aspergillus niger	0,403398	-0,34823	-1,59285
An16g06580		strong similarity to quinate transport protein qutD - Aspergillus nidulans	0,076117	0,22377	-1,57872
An06g02540			-1,3569	-0,95284	-1,55172
An12g03860		strong similarity to precursor of cephalosporin esterase - Rhodosporidium toruloides [putative frameshift]	0,578201	-0,15746	-1,53386
An01g01630		strong similarity to hypothetical protein encoded by An09g00510 - Aspergillus niger	-1,80498	-1,9495	-1,52773

Table S 8 continued

An05g01000		similarity to hypothetical protein CG12065 -Drosophila melanogaster	0,272509	-0,11381	-1,49466
An12g04250		strong similarity to cytochrome P450 pisatin demethylase PDAT9 - Nectria haematococca [putative frameshift]	0,231211	-0,45838	-1,42705
An07g04470		strong similarity to butyrylcholinesterase BChE - Oryctolagus cuniculus	0,105745	-0,01928	-1,42606
An04g08440		strong similarity to cytochrome P450 monooxygenase TRI11 - Fusarium sporotrichioides	0,588263	-0,5052	-1,41795
An16g05730		similarity to integral membrane protein PTH11 - Magnaporthe grisea	0,062087	-2,39071	-1,35744
An02g13580	cfcI	strong similarity to endochitinase from patent EP531218-A - Aphanocladium album	0,696502	-0,63083	-1,33354
An09g00510		strong similarity to hypothetical protein encoded by An01g01630 - Aspergillus niger	-0,75604	-0,88526	-1,31722
An04g09990		strong similarity to 2,5-dichloro-2,5-cyclohexadiene-1,4-diol dehydrogenase linC - Sphingomonas paucimobilis	0,142985	0,225704	-1,27472
An04g09990		strong similarity to 2,5-dichloro-2,5-cyclohexadiene-1,4-diol dehydrogenase linC - Sphingomonas paucimobilis	0,142985	0,225704	-1,27472
An03g06720		strong similarity to cytochrome P-450 CYP4D2 - Drosophila melanogaster	-0,18501	0,571255	-1,26759
An01g15200		strong similarity to mature penicillin V amidohydrolase PVA from patent US5516679-A - Fusarium oxysporum [truncated ORF]	0,234214	-0,28475	-1,25158
An04g09360		strong similarity to hypothetical protein CC0812 - Caulobacter crescentus	0,760069	-0,0596	-1,24115
An12g03580		strong similarity to microsomal glutathione S-transferase 3 MGST3 - Homo sapiens	0,011806	-0,07555	-1,24099
An15g07000		strong similarity to phytase phyA -Aspergillus fumigatus	0,484045	0,044847	-1,2351
An11g03770		strong similarity to hypothetical blastomyces yeast phase-specific protein 1 related protein CAD70756.1 - Neurospora crassa	-0,19223	-0,92666	-1,22322
An01g01330		similarity to acetate regulatory DNA binding protein facB - Aspergillus nidulans	0,258394	-0,10163	-1,223

Table S 8 continued

An15g04780	strong similarity to protein fragment SEQ ID NO:37791 from patent EP1033405-A2 - Arabidopsis thaliana	-0,36511	0,235135	-1,21634
An12g00870	strong similarity to sulfite resistant protein Ssu1 - Saccharomyces cerevisiae	-0,66929	-0,31545	-1,20199
An08g04330	similarity to hypothetical endo alpha-1,4 polygalactosaminidase - Pseudomonas sp.	0,043632	0,087889	-1,17558
An12g04260	similarity to UDP-glucose 4-epimerase GALE -Streptomyces lividans	0,127968	0,002279	-1,17024
An18g06310	strong similarity to L-fucose permease fucP -Escherichia coli	0,637908	-0,47642	-1,16623
An14g01620	weak similarity to heparanase - Homo sapiens	-0,23153	0,157608	-1,14446
An01g02680		0,548341	0,002772	-1,13532
An14g04330	similarity to hypothetical short chain alcohol dehydrogenase cta - Cucumis sativus	0,390693	-0,10527	-1,12851
An01g14730	similarity to cis,cis-muconate lactonizing enzyme I TcMLE - Trichosporon cutaneum	-0,60359	-0,60263	-1,10347
An14g02960	similarity to hypothetical protein encoded by An01g14870 - Aspergillus niger	0,478908	-0,34769	-1,05892
An07g09050	similarity to hypothetical transcription regulator SC5F2A.29 - Streptomyces coelicolor	0,59963	0,092905	-1,01174
An15g03940	strong similarity to monosaccharide transporter AmMst-1 - Amanita muscaria	0,626276	-0,67458	-1,00782
An13g03140	weak similarity to endo-beta-1,4-glucanase celA1 - Streptomyces halstedii	1,0022	-0,45212	-0,23695
An07g06010	strong similarity to hypothetical protein YKR070w - Saccharomyces cerevisiae	1,00464	0,950265	0,381268
An01g11880	strong similarity to O-methylsterigmatocystin oxidoreductase ordA - Aspergillus parasiticus [putative frameshift]	1,00882	-0,10501	-1,18518
An15g02250		1,00916	-1,2641	7,04485
An16g02250	strong similarity to lysosomal pepstatin insensitive protease CLN2 - Homo sapiens	1,01168	0,422363	0,737053

Table S 8 continued

An12g08630		strong similarity to cytochrome P450 monooxygenase TRI11 - Fusarium sporotrichioides	1,01401	-0,6468	-0,767
An18g06360		similarity to mycelial surface antigen Csa1 -Candida albicans	1,01665	2,10025	0,811472
An06g02270		similarity to arabinose transport protein araE - Escherichia coli	1,02804	0,209778	-0,28063
An14g02100	cwpA	strong similarity to cell wall antigen MP1 -Penicillium marneffei	1,02961	0,222003	0,296098
An11g09710		strong similarity to 4-coumarate-CoA ligase -Populus tremuloi-des	1,03502	0,198553	-0,57987
An15g00620			1,03711	0,939202	-0,00373
An15g04280		strong similarity to 1-acyldihydroxyacetone-phosphate reductase Ayr1 -Saccharomyces cerevisiae	1,03826	0,879308	0,930259
An04g03170		strong similarity to beta-glucosidase bglB -Candida wickerhamii	1,03831	0,227806	-0,5319
An11g06350		strong similarity to carboxypeptidase C cpy1p - Schizosaccharo-myces pombe	1,03966	0,360407	-1,19943
An12g06180		weak similarity to isoenzyme B of UDP-N-acetylglucosamine:al-pha-1,3-D-mannoside beta-1,4-N-acetylglucosaminyltransferase IV MGAT4B - Homo sapiens	1,04168	1,13977	1,81075
An12g07750		similarity to hypothetical serine repeat antigen BAA78500.1 - Plasmodium falciparum	1,052	1,45132	-0,35725
An16g07370		similarity to hypothetical protein SPBC146.10 - Schizosaccharo-myces pombe	1,05266	0,539493	-0,10292
An02g00610		similarity to beta-galactosidase bgaM -Bacillus megaterium	1,05545	0,17568	-0,58172
An02g00590		strong similarity to high-affinity glucose transporter HGT1 - Kluyveromyces lactis	1,06434	-0,17732	-1,15303
An03g01910		strong similarity to N-acetylglutamate kinase AGK - Neurospora crassa	1,06619	1,13767	0,320118
An07g03950		strong similarity to beta-ketoacyl-ACP reductase Clkr27 - Cuphea lanceolata	1,06831	0,397618	-0,09256
An01g14670	pgaE		1,06873	0,143097	-1,40498
An02g00580		similarity to pyruvate dehydrogenase phosphatase PDPc - Bos taurus	1,0703	-0,42873	-0,57876

Table S 8 continued

An13g01880	strong similarity to cephalosporin esterase -Rhodosporidium toruloides	1,07609	0,526592	0,113897
An02g04690	strong similarity to serine-type carboxypeptidase I cdpS - Aspergillus saitoi	1,07618	-0,46725	0,221127
An05g01490	strong similarity to hypothetical protein PA3762 - Pseudomonas aeruginosa	1,08698	0,566175	-0,18707
An03g06560	strong similarity to triacylglycerol lipase Lip2 - Candida rugosa	1,09155	-0,38556	-1,11494
An09g03760	strong similarity to triacylglycerol lipase lipI - Geotrichum candidum	1,09491	1,34726	0,192063
An14g06730	strong similarity to adenine-repressible gene rds1p - Schizosaccharomyces pombe	1,09567	0,717732	-0,22681
An09g06720	weak similarity to hypothetical protein B13I18.100 - Neurospora crassa	1,10133	0,792099	0,430918
An16g08060	strong similarity to isobutene-forming enzyme and benzoate 4-hydroxylase P450rm - Rhodotorula minuta	1,1016	-1,94626	-0,46206
An12g04510	strong similarity to benzoate 4-monooxygenase cytochrome P450 53 bphA - Aspergillus niger	1,10606	0,50533	0,409925
An01g08950	strong similarity to high-affinity iron permease CaFTR2 - Candida albicans	1,12091	0,614153	1,24007
An08g08940	strong similarity to nitrilase NIT3 -Arabidopsis thaliana	1,13387	0,077056	-1,21582
An15g07520	similarity to hypothetical protein mlr2143 -Mesorhizobium loti	1,13797	1,50533	0,183883
An08g06390	similarity to 3-hydroxyisobutyrate dehydrogenase mmsB - Pseudomonas aeruginosa	1,13978	0,865021	0,185402
An01g00490	strong similarity to isoamyl alcohol oxidase mreA - Aspergillus oryzae	1,14801	0,58658	0,4132
An03g06270	strong similarity to isoamyl alcohol oxidase mreA - Aspergillus oryzae	1,15314	-0,82706	-3,17102
An03g04500	similarity to hypothetical protein F16J13.50 - Arabidopsis thaliana	1,16141	0,938233	-0,34719
An03g04500	similarity to hypothetical protein F16J13.50 - Arabidopsis thaliana	1,16141	0,938233	-0,34719

Table S 8 continued

An03g01050		similarity to endo-beta-1,4-glucanase -Bacillus polymyxa	1,16957	-0,18037	-1,18703
An03g01770		strong similarity to EST an_3645 -Aspergillus niger	1,18292	-1,89241	0,312556
An09g00840		similarity to plastic-degradation enzyme within SEQ ID NO:6 from patent WO2004038016-A1 -Aspergillus oryzae	1,19685	-1,06153	-5,63828
An04g04200			1,1994	1,00589	-0,45749
An12g09540		strong similarity to hypothetical yellow-related protein DR1790 - Deinococcus radiodurans	1,2063	-0,44138	-0,21597
An01g05530			1,20923	0,300386	-0,20012
An14g05430		similarity to meso-2,3-butanediol dehydrogenase (D-acetoin forming) budC - Klebsiella pneumoniae	1,21379	0,458457	-0,14684
An11g00890			1,22304	1,17186	0,335467
An11g07700		similarity to esterase es4 from patent WO9730160-A1 - Cetacea sp.	1,23249	1,08417	-0,05644
An07g08030	pepF		1,23553	-0,79605	0,332322
An13g02120		similarity to hypothetical protein CAD37048.1 - Neurospora crassa [truncated ORF]	1,23858	-0,74632	-1,86762
An04g02600		strong similarity to 3-phytase B phyB -Aspergillus niger	1,2487	0,741458	-0,92436
An16g01270		similarity to integral membrane protein PTH11 - Magnaporthe grisea	1,25202	-0,37863	-0,19391
An01g04140		similarity to EST an_2919 - Aspergillus niger	1,25504	0,33286	0,191749
An01g04140		similarity to EST an_2919 - Aspergillus niger	1,25504	0,33286	0,191749
An12g00830		strong similarity to nitrogen assimilation regulatory protein nit-4 - Neurospora crassa	1,26397	0,901738	-0,90182
An07g00440		strong similarity to secretory lipase LIP2 -Candida albicans	1,2649	1,13172	-0,64111
An05g01880		strong similarity to hypothetical chloroperoxidase cpo - Agaricus bisporus	1,26953	0,310989	0,280699
An09g02240		strong similarity to beta-N-acetylhexosaminidase from patent WO9839459-A1 -Penicillium chrysogenum	1,2784	0,178653	-0,89525

Table S 8 continued

An18g01090		strong similarity to lysophospholipase from patent WO0127251-A - Aspergillus oryzae	1,27898	0,333778	1,48881
An10g00790		similarity to hypothetical protein SCE6.29 -Streptomyces coelicolor	1,29822	-0,78461	-3,33981
An16g07420		strong similarity to hypothetical protein AAF27107.1 - Arabidopsis thaliana [putative sequencing error]	1,29935	0,748395	0,15829
An11g02580		strong similarity to Na+/H+ antiporter Cnh1 -Candida albicans	1,30445	-0,08216	1,17583
An16g01900		similarity to hypothetical protein encoded by An04g06980 - Aspergillus niger	1,31414	0,658443	0,395655
An07g08950	eglC		1,31633	-0,33999	-2,04195
An11g02100		strong similarity to furostanol glycoside 26-O-beta-glucosidase CSF26G1 - Costus speciosus	1,32785	0,224845	-2,12927
An05g02400		weak similarity to nuclear migration protein Num1 - Saccharomyces cerevisiae	1,32859	-0,83161	-0,91192
An18g04810	rgxC	strong similarity to exo-polygalacturonase PGX from patent WO9414966-A - Aspergillus tubingensis	1,35287	0,519242	-1,60756
An12g05010	axeA		1,35626	-0,61555	-2,23092
An19g00280		similarity to hypothetical protein CG12065 -Drosophila melanogaster	1,35928	0,178687	0,074491
An01g01360		similarity to hypothetical transmembrane protein CAD18032.1 - Ralstonia solanacearum	1,37291	-0,00477	-1,49164
An08g00180		strong similarity to cytochrome P450 monooxygenase lovA - Aspergillus terreus	1,38306	0,519467	-0,51155
An04g09710		similarity to acetylcholinesterase AChE -Rattus norvegicus	1,39244	-1,84552	-4,63724
An01g12810		similarity to BAX-associated protein fragment SEQ ID NO:242 from patent WO200264766-A2 - Saccharomyces cerevisiae	1,40399	1,19631	0,370156
An05g02420		similarity to integral membrane protein PTH11 - Magnaporthe grisea	1,40885	0,225484	-0,86691
An18g00630			1,41946	-1,49291	-1,35476
An02g11890		strong similarity to hypothetical protein encoded by An14g01330 - Aspergillus niger	1,42697	0,16979	-1,15428

Table S 8 continued

An02g09890		strong similarity to EST an_2336 -Aspergillus niger	1,43061	-0,89388	2,24061
An18g06410		strong similarity to hypothetical conserved protein encoded by B2F7.030 - Neurospora crassa	1,44187	1,65162	-0,21204
An16g06570			1,45773	1,86306	2,59681
An01g10930	agdB	strong similarity to enzyme with sugar transferase activity from patent JP11009276-A - Acremonium sp.	1,4731	-0,01255	-1,01005
An01g01750		similarity to lysosomal protease CLN2 -Rattus norvegicus	1,50378	-1,00505	0,629599
An12g03300	protG	strong similarity to aspartic protease pr1 -Phaffia rhodozyma	1,50735	-0,537	-1,31396
An12g06000			1,52828	0,946453	0,614716
An12g06380		similarity to fibroin heavy chain Fib-H -Bombyx mori	1,55583	0,647458	0,963035
An01g01240		similarity to HC-toxin efflux pump TOXA -Cochliobolus carbonum [truncated ORF]	1,55947	1,9725	-0,78639
An04g07120		similarity to protein FRM2 involved in fatty acid regulation - Saccharomyces cerevisiae	1,56789	0,358303	0,017004
An01g10940			1,59209	-0,08171	-1,41847
An16g01880	lipaI	strong similarity to lysophospholipase -Aspergillus foetidus	1,59974	-1,55472	-2,73781
An09g02160			1,60586	-0,09362	-1,63007
An02g02540		strong similarity to acetyl-esterase I from patent WO9502689-A - Aspergillus aculeatus	1,62181	1,08755	0,660999
An16g00220			1,62566	0,655097	-0,43577
An03g01550		similarity to gluconate:NADP 5-oxidoreductase GNO - Gluconobacter oxydans [truncated ORF]	1,62652	0,371488	-2,10612
An11g00670		strong similarity to acidic sphingomyelin phosphodiesterase ASM - Mus musculus	1,64223	-0,58928	-1,84906
An07g00530		strong similarity to pisatin demethylase PDA6-1 - Nectria haematococca	1,64777	-0,06396	0,709974
An03g01140		strong similarity to oxalate decarboxylase (APOXD) from patent WO9842827-A2 - Aspergillus phoenicis	1,65091	1,56555	-0,03135

Table S 8 continued

An18g00380		strong similarity to aminotriazole resistance protein Atr1 - Saccharomyces cerevisiae	1,66102	0,538082	-0,22608
An14g01330		strong similarity to hypothetical protein encoded by An02g11890 - Aspergillus niger	1,66521	0,526503	-2,88099
An09g02180		strong similarity to phospholipase A1 from patent JP10155493-A - Aspergillus oryzae	1,66657	-1,09374	0,81508
An15g05370	pgaII		1,67319	-1,48041	-0,74592
An15g05370	pgaII		1,67319	-1,48041	-0,74592
An03g04310		similarity to hypothetical protein Fun14 -Saccharomyces cerevisiae	1,67861	1,80656	-0,01893
An07g04900		strong similarity to EST an_2589 -Aspergillus niger	1,67943	0,823498	0,487944
An09g00120	faeA		1,68131	-2,58169	-0,31692
An02g06010		weak similarity to protein CARD-6 from patent WO200100826-A2 - Homo sapiens	1,68738	0,166074	-0,56075
An09g06260		similarity to mutanase mutA - Aspergillus oryzae	1,70795	1,32255	-0,5624
An15g05270		strong similarity to carboxylesterase precursor protein ES-4 - Rattus norvegicus	1,70893	-0,25774	-1,70893
An15g04550		strong similarity to xylanase A xynA from patent WO200068396-A2 - Aspergillus niger	1,73039	0,977136	2,31095
An11g09170		similarity to secreted aspartic proteinase SAP8 - Candida albicans	1,73383	0,479755	-0,13044
An08g01800		strong similarity to hypothetical mitochondrial carrier protein AgPET8 - Ashbya gossypii	1,73513	1,29541	0,039533
An03g05930		strong similarity to acid phosphatase pho -Pichia pastoris	1,75693	1,99391	-0,01087
An01g01780		strong similarity to transmembrane protein PTH11 - Magnaporthe grisea	1,78629	1,08588	0,540155
An11g08810		strong similarity to cytochrome P450 monooxygenase P450l - Gibberella fujikuroi	1,80237	0,53916	-0,76958
An01g12150	lacA		1,83027	-0,24463	-2,35327

Table S 8 continued

An15g03100		strong similarity to versicolorin B synthase vbs - Aspergillus parasiticus	1,8346	0,538001	-1,13465
An01g00530	pepB		1,83861	-1,79355	-1,38685
An18g01780		strong similarity to flavohemoglobin hmp -Escherichia coli [putative frameshift]	1,84365	1,46864	0,114325
An03g02110		strong similarity to ketoreductase YDR541c from patent EP918090-A2 - Saccharomyces cerevisiae	1,85157	1,23859	2,01368
An01g10580		strong similarity to ribonuclease T2 precursor rntB - Aspergillus oryzae	1,86789	0,526333	0,418851
An05g02440	pgaC		1,87869	-0,14043	-1,73371
An09g01190	abnA		1,89196	-1,61343	-4,34834
An05g01850		similarity to monocarboxylate transporter MCT2 - Homo sapiens	1,91342	0,710443	-0,14817
An04g09690		strong similarity to pectin methylesterase pme1 - Aspergillus aculeatus	1,94315	-1,42846	-1,63738
An11g06480		weak similarity to antigenic protein f86.aa from patent WO9859071 - Borrelia burgdorferi	1,96462	1,46605	0,2629
An12g08280	inuE		1,97412	-0,43106	-2,44168
An03g06550	glaA		1,98288	0,210809	-0,74
An03g06550	glaA		1,98288	0,210809	-0,74
An07g08940		similarity to acetyl-esterase I from patent WO9502689-A - Aspergillus aculeatus	1,98997	0,119796	-1,59252
An03g01620		strong similarity to high affinity glucose transporter HGT1 - Kluyveromyces lactis	1,99437	1,56686	-0,5071
An08g09420		strong similarity to protein 4MeS -Metarhizium anisopliae	2,01988	0,366036	-0,89143
An04g06920	agdA		2,17737	0,389808	-0,68163
An02g13630		strong similarity to hypothetical protein CC0505 - Caulobacter crescentus	2,18763	0,39711	-1,6268
An02g03260	agsD	strong similarity to hypothetical cell wall alpha-glucan synthase ags1p - Schizosaccharomyces pombe	2,2054	-0,99223	-0,09781

Table S 8 continued

An01g00600		similarity to hypothetical protein YLR011w -Saccharomyces cerevisiae	2,20813	2,58301	0,378143
An14g04710	pepA		2,23985	-1,33803	1,99365
An12g02590		similarity to hypothetical protein SPAC10F6.16 - Schizosaccharomyces pombe	2,2586	1,51536	-0,94652
An09g04360		weak similarity to hypothetical protein SPy1903 - Streptococcus pyogenes	2,30955	0,665418	-1,27507
An15g05280		strong similarity to penicillin V amidohydrolase PVA from patent US5516679-A - Fusarium oxysporum	2,33521	0,126312	-1,74466
An02g01870		strong similarity to peripheral-type benzodiazepine receptor 1 isoquinoline-binding protein MBR - Mus musculus	2,33661	1,51671	-0,30342
An12g04090		similarity to hypothetical protein encoded by An04g09490 - Aspergillus niger	2,37446	2,94949	0,505778
An03g04860		strong similarity to protein involved in non-classical protein export pathway Nce102 - Saccharomyces cerevisiae	2,41396	1,68353	-0,11342
An04g09700		strong similarity to endo-xylogalacturonan hydrolase xghA - Aspergillus tubingensis	2,41411	-1,50939	-0,52034
An11g03340	aamA		2,49646	-0,53295	-1,42909
An11g05970		weak similarity to muramidase-2 -Enterococcus hirae	2,53049	-2,28883	-0,68495
An08g03580	bgt1	strong similarity to 1,3-beta-glucanosyltransferase bgt1 - Aspergillus fumigatus	2,53455	-0,90029	0,833007
An16g04420		strong similarity to meiotic sister-chromatid recombination protein Msc1 - Saccharomyces cerevisiae	2,57514	2,43798	0,120154
An14g07140		strong similarity to alpha-1,6-mannosyltransferase Hoc1 - Saccharomyces cerevisiae	2,58501	1,29587	-0,96369
An04g08320		strong similarity to protease Mch5 -Saccharomyces cerevisiae	2,61849	0,359555	1,25334
An11g02730		similarity to hypothetical serine-rich protein SPCC1322.10 - Schizosaccharomyces pombe	2,63789	-0,21624	1,37898
An13g01470		weak similarity to laminin gamma 3 chain precursor LAMC3 - Homo sapiens	2,6865	-0,06978	4,00702

Table S 8 continued

An09g01050		similarity to platelet-activating factor-acetylhydrolase - Cavia porcellus	2,70823	1,23087	-1,46358
An01g13660	mcoB	strong similarity to laccase I precursor yA -Aspergillus nidulans	2,75277	0,203482	0,677644
An03g02830		strong similarity to phosphatidylserine decarboxylase Psd2 - Saccharomyces cerevisiae	2,76239	2,55944	-0,21327
An01g07060			2,78277	2,68104	0,021546
An02g00070		strong similarity to bialaphos acetylhydrolase bah - Streptomyces hygroscopicus	2,80421	2,38711	-0,68938
An07g06530		strong similarity to multicopy suppressor Sur7 - Saccharomyces cerevisiae	3,1024	2,58257	0,28889
An16g03500		weak similarity to slow myosin heavy chain myoHC-A4 - Notothenia coriiceps	3,24288	2,51654	-0,35215
An04g00100		strong similarity to hypothetical protein SPAC15E1.02c - Schizosaccharomyces pombe	3,37626	2,6155	-0,04244
An15g05360		similarity to actVA-ORF4-like protein from patent WO9911793-A1 - Homo sapiens	4,07478	0,363759	2,9696
An03g02510		weak similarity to hypothetical protein CAD70818.1 - Neurospora crassa	4,4326	3,16317	-1,87372
An08g09880	hfbD	weak similarity to hydrophobin CoH1 -Coprinus cinereus	4,61801	-2,05722	3,32409
An04g08150		strong similarity to EST an_2637 -Aspergillus niger	6,95386	-2,3818	1,53053
An14g01210		strong similarity to fructosyl amine oxygen oxidoreductase - Aspergillus fumigatus	-1,68566	-1,09059	-0,03091
An14g05960		strong similarity to agmatinase speB -Escherichia coli	-1,66973	-0,46652	0,68032
An02g14500		similarity to hypothetical protein encoded by An11g03520 - Aspergillus niger	-1,6317	-1,3974	-0,06174
An01g11520	pgaI		-1,60026	-1,79939	-0,09272
An01g11520	pgaI		-1,60026	-1,79939	-0,09272
An03g05360		strong similarity to neutral amino acid permease mtr - Neurospora crassa	-1,59982	-2,86778	-2,30318

Table S 8 continued

An16g02240	similarity to phenylcoumaran benzylic ether reductase PT1 - Pinus taeda	-1,5819	-1,84737	-0,65331
An15g02590	strong similarity to dimethylglycine dehydrogenase precursor DMGDH - Homo sapiens	-1,5759	-0,64252	-0,51873
An03g05260	similarity to chitosanase csnA - Aspergillus oryzae	-1,57517	-0,04294	0,954388
An09g05550	weak similarity to hypothetical protein EAA53565.1 - Magnaporthe grisea	-1,56172	-1,7359	-1,01774
An09g01850	strong similarity to benzoate 4-monooxygenase cytochrome P450 53 bphA - Aspergillus niger	-1,54902	-3,65399	-1,88289
An09g03120	similarity to hypothetical serine-rich protein - Schizosaccharomyces pombe	-1,54819	-0,81256	0,150569
An06g02350	strong similarity to hypothetical membrane protein YDL144c - Saccharomyces cerevisiae	-1,54524	-1,19844	-1,80241
An09g03210	strong similarity to isobutene-forming enzyme and benzoate 4-hydroxylase P450rm - Rhodotorula minuta	-1,47211	-1,9584	-0,98891
An08g09840	strong similarity to cysteine proteinase polypeptide from patent WO200268623-A2 - Aspergillus niger	-1,46089	-1,65963	0,391585
An15g04900	strong similarity to endoglucanase IV egl4 -Trichoderma reesei	-1,44313	-1,81293	-0,11189
An07g05660	similarity to hypothetical protein EAA64430.1 - Aspergillus nidulans	-1,43732	0,810877	1,9728
An15g05990	strong similarity to D-arabinitol 2-dehydrogenase ARDH - Pichia stipitis	-1,39996	-1,32683	-0,15589
An11g03450	strong similarity to hypothetical protein dag11 - Agaricus bisporus	-1,39897	-3,39895	2,41357
An01g07680	similarity to hypothetical protein encoded by An11g02490 - Aspergillus niger	-1,33634	-4,29431	-0,68374
An04g02930	similarity to integral membrane protein PTH11 - Magnaporthe grisea	-1,29058	-0,77853	-0,6761
An13g02670	0	-1,27312	-0,77704	-0,25171
An04g10010	similarity to integral membrane protein PTH11 - Magnaporthe grisea	-1,24917	-2,27541	-0,7731

Table S 8 continued

An15g01590		similarity to 2-aminobenzenesulfonate dioxygenase large subunit absA - Alcaligenes sp.	-1,24115	-1,75987	-2,01742
An16g05690		similarity to ferulic acid esterase A faeA -Aspergillus tubingensis	-1,18802	-2,85934	0,012712
An16g01850		similarity to blastomyces yeast phase-specific protein 1 bys1 - Ajellomyces dermatitidis	-1,16646	-1,49438	-1,1451
An02g00950		similarity to hypothetical protein B2A19.90 -Neurospora crassa	-1,16249	-1,72711	1,45165
An18g00460		similarity to protein fragment SEQ ID NO:37063 from patent EP1033405-A2 - Arabidopsis thaliana	-1,15837	-0,54056	0,193226
An08g09500		similarity to kinesin light chain - Loligo pealei	-1,15806	-0,35906	-0,11779
An04g02080		questionable ORF	-1,13981	-0,04675	0,110133
An07g08960		similarity to hypothetical protein SPAC15A10.09c - Schizosaccharomyces pombe	-1,13787	-0,41752	0,117001
An14g05400		weak similarity to proteinase inhibitor PID -Solanum tuberosum	-1,1373	0,055327	0,556293
An15g07810	agsB	strong similarity to hypothetical cell wall alpha-glucan synthase ags1p - Schizosaccharomyces pombe	-1,13429	-1,60882	0,820233
An15g06810		strong similarity to cytochrome-b5 reductase Mcr1 - Saccharomyces cerevisiae	-1,10789	-0,52089	0,190846
An16g00670		similarity to hypothetical protein AAO51454.1 - Dictyostelium discoideum	-1,1049	-2,41718	-1,4801
An15g07800	agtC	strong similarity to precursor of alpha-amylase A - Aspergillus niger	-1,09426	-2,0984	1,05342
An01g14760		strong similarity to 6-hydroxy-D-nicotine oxidase 6-HDNO - Arthrobacter oxidans	-1,07989	-1,96049	-0,32764
An04g02970		similarity to dimethylaniline monooxygenase FMO - Sus scrofa	-1,07933	-1,63091	-0,15527
An10g01040		strong similarity to hypothetical IgE-binding protein - Aspergillus fumigatus	-1,04148	-1,87928	-1,69728
An12g07170		strong similarity to urea transport protein Dur3 - Saccharomyces cerevisiae	-1,03479	0,122894	0,05072
An01g05270		weak similarity to extracellular proteinase prtY - Lactobacillus helveticus	-2,58771	-3,23757	-3,1902

Table S 8 continued

An03g03390		strong similarity to hypothetical protein encoded by An09g01480 - Aspergillus niger	-2,39321	-4,33805	-0,9539
An03g03390		strong similarity to hypothetical protein encoded by An09g01480 - Aspergillus niger	-2,39321	-4,33805	-0,9539
An13g03450		weak similarity to integral membrane protein PTH11 from patent WO9913094-A2 - Magnaporthe grisea	-2,33796	-1,20173	-0,30424
An09g01920		similarity to 6-hydroxy-D-nicotine oxidase 6-HDNO - Arthrobacter oxidans	-2,32939	-3,03623	-1,10035
An09g03230		similarity to integral membrane protein PTH11 - Magnaporthe grisea	-2,07957	-1,28224	0,044349
An12g10440		strong similarity to hypothetical protein CAD70539.1 - Neurospora crassa	-2,05026	-1,76489	-0,21071
An13g01520			-1,99725	-2,33628	0,120552
An09g03070	agsE	strong similarity to alpha-glucan synthase mok1p - Schizosaccharomyces pombe	-1,72514	-1,2825	0,550198
An03g00840		strong similarity to EST an_3113 -Aspergillus niger	-1,70241	-1,13884	-0,27913
An09g00530		similarity to salicylate hydroxylase nahW -Pseudomonas stutzeri	-7,82357	-7,73183	-5,39858
An11g07330		similarity to 6-hydroxynicotinic acid mono-oxygenase 6-HNAMO from patent JP09121864-A -Pseudomonas fluorescens	-3,89277	-4,2555	#NAME?
An11g07040		strong similarity to EST an_2779 -Aspergillus niger	-3,66159	-7,88797	-2,33033
An13g03000		strong similarity to n-alkane-inducible cytochrome P450 protein ALK1 - Yarrowia lipolytica	-3,49254	-3,24912	-0,02877
An11g07300		similarity to fluconazole resistance protein FLU1 - Candida albicans [truncated ORF]	-3,28219	-5,24933	-3,13715
An13g03050		weak similarity to hypothetical protein encoded by An04g04070 - Aspergillus niger	-3,26309	-3,9947	0,795139
An04g09820		strong similarity to fructosyl amino acid oxidase faoA - Aspergillus terreus	-3,17989	-1,57827	-0,77753
An11g07730		similarity to mucin MUC4 - Homo sapiens	-3,04268	-3,99963	-2,40562
An05g01120		strong similarity to hypothetical cytochrome P450 monooxygenase TRI11 - Fusarium sporotrichioides	-2,91758	-2,86214	-2,15567

Table S 8 continued

An12g02070		similarity to ribonuclease T1 precursor rntA - Aspergillus oryzae	-2,85403	-4,89273	-2,51738
An02g11390		strong similarity to hypothetical protein encoded by DR0708 - Deinococcus radiodurans	-2,79919	-2,23058	-0,18043
An09g00590		similarity to salicylate hydroxylase nahG -Pseudomonas putida	-8,08228	-6,5964	-3,91319
An12g05020	hfbE	similarity to hydrophobin HFBI - Trichoderma reesei	0,322842	1,01227	0,787842
An08g00210		strong similarity to glycerol-3-phosphate dehydrogenase gdm1 - Mus musculus	0,917811	1,02134	0,184384
An11g08980		weak similarity to hypothetical protein CAD70538.1 - Neurospora crassa	0,877211	1,03217	0,851881
An03g00770		strong similarity to hypothetical allergic bronchopulmonary aspergillosis allergen rAsp f 4 from patent WO9828624-A1 - Aspergillus fumigatus	-0,16053	1,12349	-0,3145
An01g14370		strong similarity to uronate dehydrogenase from patent DE19604798-A1 - Saccharomyces cerevisiae	0,509367	1,14375	0,625004
An16g02230		similarity to beta transducin-like protein het-e1 - Podospora anserina	0,121045	1,14646	1,72257
An10g00380			0,457237	1,16696	1,48375
An18g00980		weak similarity to integral membrane protein PTH11 - Magnaporthe grisea	0,838658	1,21015	1,29877
An12g07500	pgaX	strong similarity to exopolygalacturonase pgaX - Aspergillus tubingensis	0,667133	1,21622	-0,68369
An12g07500	pgaX	strong similarity to exopolygalacturonase pgaX - Aspergillus tubingensis	0,667133	1,21622	-0,68369
An04g02410		strong similarity to cobalamin and cobamide biosynthesis protein COB W from patent WO9111518-A -Pseudomonas denitrificans	0,574862	1,34043	0,372098
An02g14090		questionable ORF	-0,06882	1,40548	0,015627
An08g09030	chiD	strong similarity to chitinase 1 cts1 -Coccidioides immitis	-0,41268	1,4908	-0,09548
An06g02130			-0,42261	-4,7591	#NAME?
An11g00200		strong similarity to beta-glucosidase bgln -Candida molischiana	0,248776	-3,81327	-4,62826

Table S 8 continued

An04g09490			-0,07102	-3,53302	-5,02803
An03g06310	pmeA		-0,37376	-3,42645	-0,86747
An04g08380		strong similarity to diacylglycerol acyl transferase MR1 from patent WO200001713-A2 - Mortierella ramanniana	-0,93188	-3,20579	-1,21015
An07g08640		strong similarity to mutanase mutA -Penicillium purporogenum	-0,52106	-3,0996	-2,29618
An07g01320	anafp	strong similarity to antifungal protein precursor paf - Penicillium chrysogenum	-0,47912	-3,0438	5,04632
An07g01320	anafp	strong similarity to antifungal protein precursor paf - Penicillium chrysogenum	-0,47912	-3,0438	5,04632
An10g00970		strong similarity to hypothetical protein encoded by An03g01670 - Aspergillus niger	-0,70993	-2,76182	-2,77065
An11g00190		weak similarity to high affinity glucose transporter HGT1 - Kluyveromyces lactis	-0,24587	-2,4589	-1,02598
An05g02350			-0,83174	-2,33608	1,26658
An15g07790		similarity to hypothetical protein encoded by An11g02730 - Aspergillus niger	-0,68956	-2,33195	0,528048
An02g00730		similarity to cutinase A gene CutA - Botrytis cinerea	-0,52945	-2,26751	-0,61246
An03g00830		weak similarity to intestinal mucin MUC2 -Homo sapiens	-0,97436	-2,13922	-0,29354
An08g03070		strong similarity to glycine decarboxylase subunit T Gcv1 - Saccharomyces cerevisiae	-0,98768	-2,11675	0,142936
An07g00950		similarity to aspartyl proteinase candidapepsin - Candida albicans	-0,65546	-2,0722	-0,44769
An15g03550		weak similarity to protopectinase from patent WO9806832-A1 - Bacillus subtilis	-0,98871	-1,9914	-3,37592
An13g02180		strong similarity to ferric reductase CFL1 -Candida albicans	0,32263	-1,96169	-1,15166
An15g07700	protD	strong similarity to aspergillopepsin II precursor (acid proteinase A) - Aspergillus niger	0,863763	-1,95733	-0,82204
An02g09690		strong similarity to lipase I precursor TFLI - Geotrichum fermentans	0,840813	-1,86955	-3,03174
An05g02340	mcoF	strong similarity to precursor of laccase -Neurospora crassa	-0,98244	-1,71999	0,397369

Table S 8 continued

An16g02810		weak similarity to nucleoporin Rat7 -Saccharomyces cerevisiae	-0,49981	-1,71556	-0,35041
An13g04080		strong similarity to cytochrome P450 monooxygenase P450II - Gibberella fujikuroi	-0,40013	-1,68136	-1,96898
An02g00150		strong similarity to cytochrome P450 pisatin demethylase PDAT9 - Nectria haematococca	-0,54418	-1,65644	-1,71094
An15g05000			-0,08337	-1,62193	-1,75088
An14g01820	phiA	strong similarity to hypothetical cell wall protein binB - Aspergillus nidulans	-0,25532	-1,6162	-0,16124
An12g10630		similarity to acid phosphatase aphA -Aspergillus ficuum	0,365628	-1,56142	-0,34126
An01g03090		strong similarity to 1,3-beta-glucanosyltransferase gel1 - Aspergillus fumigatus	-0,49315	-1,56084	-1,4105
An04g04280		similarity to hypothetical protein SPBC800.14c - Schizosaccharomyces pombe	-0,80053	-1,54981	-0,52148
An14g01130		strong similarity to rhamnogalacturonase B precursor rhgB - Aspergillus aculeatus	0,534344	-1,54858	-0,89522
An14g02760	eglA		-0,39224	-1,5484	0,070735
An09g00260	aglC		0,087261	-1,53986	-1,97408
An08g04390		strong similarity to glycine decarboxylase subunit H Fun40 - Saccharomyces cerevisiae	-0,54557	-1,53816	-0,01451
An01g01870		strong similarity to hypothetical Avicelase III aviIII - Aspergillus aculeatus	-0,20113	-1,50149	-2,87209
An01g12440		similarity to hypothetical protein BAA13766.1 - Schizosaccharomyces pombe	-0,45133	-1,50113	-0,73037
An01g10450		weak similarity to mucin-like protein Muc1 -Saccharomyces cerevisiae	0,429983	-1,50043	-2,28838
An05g00410		strong similarity to serine hydroxymethyl-transferase I Shm1 - Candida albicans	-0,63978	-1,48506	0,169465
An12g05710		strong similarity to L-fucose permease fucP -Escherichia coli	0,463591	-1,47118	-2,10787
An14g02980		weak similarity to mucin-like glycoprotein 900 GP900 - Cryptosporidium parvum	-0,38281	-1,44722	-1,25785

Table S 8 continued

An08g05230		strong similarity to hypothetical endoglucanase IV - Trichoderma reesei	-0,47215	-1,41415	-0,56639
An14g04370	pelA		-0,73672	-1,3787	-1,67759
An01g11660	cbhB		0,413075	-1,37322	-4,00103
An02g13650			-0,09079	-1,35627	-0,43699
An12g10200		weak similarity to ice nucleation gene inaX -Xanthomonas campestris	-0,8642	-1,35527	-0,3671
An14g04200	rhgB		-0,48588	-1,33336	-0,73602
An04g08550		strong similarity to endoglucanase IV EGIV -Trichoderma reesei	-0,53321	-1,32996	-0,91461
An01g04560		strong similarity to mixed-linked glucanase precursor MLG1 - Cochliobolus carbonum	0,236078	-1,29773	-1,0728
An01g14600		strong similarity to endo-1,4-beta-xylanase B xynB from patent WO9414965 - Aspergillus tubingensis	0,368919	-1,29091	-0,59292
An10g00680		strong similarity to H+-ATPase V0 domain 17 KD subunit Cup5 - Saccharomyces cerevisiae	-0,29322	-1,28715	0,344211
An07g09330	cbhA		-0,09997	-1,28697	-0,96086
An08g03060		strong similarity to hypothetical protein CC0533 - Caulobacter crescentus	-0,06286	-1,27807	-1,48803
An08g04640	protB	strong similarity to hypothetical lysosomal pepstatin insensitive protease CLN2 - Canis lupus	0,990667	-1,26499	-0,14395
An08g04490	protA		0,932143	-1,25886	-0,26615
An08g04490	protA		0,932143	-1,25886	-0,26615
An01g11670		strong similarity to endo-beta-1,4-glucanase A eglA - Aspergillus nidulans	0,419835	-1,25465	-4,74461
An18g01700		strong similarity to quinate transport protein qutD - Aspergillus nidulans	0,311576	-1,25197	-2,50442
An14g00860		strong similarity to triacylglycerol lipase Lip5 - Candida rugosa	-0,16547	-1,24474	-3,38321
An08g04630			-0,028	-1,24406	-0,69755
An16g05710		strong similarity to cytochrome P450 pisatin demethylase PDAT9 - Nectria haematococca	0,323839	-1,23474	-2,31886

Table S 8 continued

An01g00780	xynB		0,103013	-1,23374	-0,85854
An02g13300		similarity to hypothetical protein ID880 -Bradyrhizobium japonicum	0,8493	-1,23012	-2,04369
An02g11550		strong similarity to hypothetical protein ydcJ - Escherichia coli	0,317969	-1,22918	-1,85311
An02g01550		strong similarity to secreted serine protease 19 kDa CS antigen CS-Ag - Coccidioides immitis	-0,25463	-1,22618	0,073085
An02g11560		strong similarity to versicolorin B synthase vbs - Aspergillus parasiticus	0,395992	-1,2216	-0,00407
An05g01800			-0,4678	-1,21988	-0,13188
An02g13270		strong similarity to benzoate 4-monooxygenase cytochrome P450 53 bphA - Aspergillus niger	-0,67305	-1,20043	-1,23171
An01g01920		similarity to beta-N-acetylhexosaminidase -Vibrio furnissii	-0,18012	-1,19724	-1,16538
An09g04970		similarity to transcription cofactor Pirin -Homo sapiens	-0,13279	-1,18781	-1,06735
An18g03990		similarity to fluoroquinolone resistance factor NorA - Staphylococcus aureus	-0,55866	-1,18436	-1,20879
An16g07950			-0,89784	-1,16034	-0,24919
An12g10810		strong similarity to EST an_2678 -Aspergillus niger	0,007865	-1,14371	0,588282
An13g02060		strong similarity to cytochrome P450 monooxygenase TRI4 - Fusarium sporotrichioides	0,033583	-1,13948	-1,53648
An15g07740		strong similarity to leucine-specific regulatory protein Leu3 - Saccharomyces cerevisiae	-0,82013	-1,13928	-2,06912
An07g02380		weak similarity to T-2 toxin biosynthesis protein TRI7 - Fusarium sporotrichioides	0,085259	-1,1364	0,089977
An15g07550		strong similarity to neutral amino acid permease mtr - Neurospora crassa	-0,58572	-1,13026	0,346092
An14g02670		strong similarity to endoglucanase IV egl4 -Trichoderma reesei	-0,42545	-1,11919	-0,68283
An16g02910		strong similarity to hypothetical protein CC0533 - Caulobacter crescentus	-0,6763	-1,08859	-2,16992
An05g02390		similarity to 6-hydroxy-D-nicotine oxidase 6-HDNO - Arthrobacter oxidans	0,63071	-1,086	-1,1956

Table S 8 continued

An14g02660		strong similarity to hypothetical necrosis and ethylene inducing protein BH0395 - Bacillus halodurans	0,641417	-1,05948	-0,96506
An12g10330		weak similarity to hypothetical protein encoded by An02g14500 - Aspergillus niger [truncated ORF]	-0,43076	-1,05627	-0,20848
An12g09780		weak similarity to alkyl salicylate esterase salE - Acinetobacter sp.	0,726523	-1,04531	-0,89106
An08g09710		similarity to 2,2-dihydroxy-3,3-dimethoxy-5,5-dicarboxybiphenyl meta-cleavage compound hydrolase ligY -Sphingomonas paucimobilis	0,661101	-1,01621	-1,65687
An01g13590		strong similarity to saccharopine reductase LYS3 - Magnaporthe grisea	-0,01488	-1,00298	-0,40079
An15g02300	abfB		0,965591	-0,69417	-3,11717
An05g01730			0,763536	-0,36496	-2,56147
An08g08370		similarity to alpha-1,2-mannosidase aman2 -Bacillus sp.	0,056535	-0,77894	-2,09912
An14g01800		strong similarity to alpha-galactosidase -Cyamopsis tetragonoloba	-0,30361	-0,98109	-2,07733
An01g00210		strong similarity to hypothetical protein AAO27753.1 - Fusarium sporotrichioides	0,841582	-0,35913	-2,05649
An18g03570	bglA		0,660053	0,126312	-1,689
An12g09560		strong similarity to cytochrome P450 monooxygenase avnA - Aspergillus parasiticus	0,891436	-0,47361	-1,62786
An14g04280		strong similarity to quinate transport protein qutD - Aspergillus nidulans	0,834477	0,561484	-1,52709
An08g01720		strong similarity to quinate transport protein qutD - Aspergillus nidulans	0,799434	-0,32294	-1,42301
An15g01500		strong similarity to fructose symporter Fsy1 - Saccharomyces pastorianus	0,843495	-0,61831	-1,39895
An01g12550	msdS	strong similarity to mannosyl-oligosaccharide 1,2-alpha-mannosidase msdS - Aspergillus saitoi	0,781697	-0,58745	-1,36788
An14g05800	aguA		0,874381	0,075251	-1,32868
An18g02740		similarity to cytochrome P450 3A7 - Homo sapiens	-0,89242	-0,80907	-1,26323

Table S 8 continued

An11g00120		similarity to glucose permease Rgt2 -Saccharomyces cerevisiae	-0,14645	-0,85823	-1,24233
An02g08230		strong similarity to high affinity glucose transporter HGT1 - Kluyveromyces lactis	0,502515	-0,62028	-1,23606
An14g00520		similarity to root-specific homeotic protein HRS1 - Helianthus annuus	0,507456	-0,99165	-1,23456
An08g09430		similarity to notchless Nle - Drosophila melanogaster	0,829138	0,037746	-1,18087
An14g01110		strong similarity to alkane-inducible cytochrome P450 gene ALK1 - Yarrowia lipolytica	0,070086	-0,62556	-1,14773
An09g03300	axlA	strong similarity to alpha-xylosidase XylS -Sulfolobus solfatari-cus	0,803947	0,834257	-1,06568
An11g03700	hxt1	strong similarity to hexose transporter HXT1 - Uromyces fabae	0,408884	-0,6801	-1,05657
An14g03850		strong similarity to cytochrome P450 monooxygenase TRI4 - Fusarium sporotrichioides	-0,2844	-0,60649	-1,04605
An15g06860		similarity to hypothetical protein encoded by An06g02540 - Aspergillus niger	0,783208	0,634012	-1,00947
An07g06300		strong similarity to member of the hexose transporter family of the major facilitator superfamily Hxt16 - Saccharomyces cerevisiae	0,843523	0,672745	1,02453
An02g11620			-0,80273	0,628176	1,09411
An16g04280		weak similarity to precursor of salivary glue protein sgs-3 - Dro-sophila yakuba	-0,1527	0,747879	1,57297
An07g04850		strong similarity to hypothetical protein AAM96660.1 - Sphingo-bium chlorophenolicum	0,332419	0,882047	1,6562
An01g08630		similarity to protein involved in mitomycin C resistance McrA - Streptomyces lavendulae	0,9427	-0,05587	1,69967
An02g09010		weak similarity to intestinal mucin MUC2 -Homo sapiens	-0,24315	0,848944	2,18062

Table S 9. Differentially expressed XlnR-regulated genes (van Peij et al., 1998b, van Peij et al., 1998a, Gielkens et al., 1999, de Vries and Visser, 2001, Hasper et al., 2000, Hasper et al., 2004) in the central zone 1, the intermediate zone 3, and the outer zone 5 of 7-day-old maltose-grown colonies of N402 and Δ*fluG*. The ^{2}log ratio of expression values of N402 vs Δ*fluG* is indicated. A number ≥1 (red) and ≤-1 (green) represent a ≥2 fold decrease and increase in Δ*fluG* colonies, respectively. Pink red and olive green shading indicate a >1 fold and significant down- and up-regulation in Δ*fluG* colonies.

Gene id	Name	Description	log2_fold_change		
			N402 zone 1 / Δ*fluG* zone 1	N402 zone 3 / Δ*fluG* zone 3	N402 zone 5 / Δ*fluG* zone 5
An01g00780	xynB		0,103013	-1,23374	-0,85854
An03g00940	xynA		-0,29898	-0,80642	0,894221
An01g09960	xlnD		0,27645	0,185712	-1,75537
An12g05010	axeA		1,35626	-0,61555	-2,23092
An03g00960	axhA		0,07826	-0,52736	0,557168
An01g00330	abfA		0,619718	0,659881	-0,37331
An15g02300	abfB		0,965591	-0,69417	-3,11717
An14g05800	aguA		0,874381	0,075251	-1,32868
An02g11150	aglB		0,711788	0,544418	-0,09495
An01g12150	lacA		1,83027	-0,24463	-2,35327
An09g00120	faeA		1,68131	-2,58169	-0,31692
An14g02760	eglA		-0,39224	-1,5484	0,070735
An07g08950	eglC		1,31633	-0,33999	-2,04195
An16g06800	eglB	strong similarity to endoglucanase eglB -Aspergillus niger	0,136117	-0,23759	-0,32498
An07g09330	cbhA		-0,09997	-1,28697	-0,96086
An01g11660	cbhB		0,413075	-1,37322	-4,00103
An15g05810	xlnR		0,044666	-0,46179	-0,89828

Table S 10. Differentially expressed genes encoding carbohydrases (Pel et al., 2007) in the central zone 1, the intermediate zone 3, and the outer zone 5 of 7-day-old maltose-grown colonies of N402 and Δ*fluG*. The ^{2}log ratio of expression values of N402 vs Δ*fluG* is indicated. A number ≥1 (red) and ≤-1 (green) represent a ≥2 fold decrease and increase in Δ*fluG* colonies, respectively. Pink red and olive green shading indicate a >1 fold and significant down- and up-regulation in Δ*fluG* colonies.

Gene id	Name	Description	log 2 fold change		
			N402 zone 1 / ΔfluG zone 1	N402 zone 3 / ΔfluG zone 3	N402 zone 5 / ΔfluG zone 5
An01g01340		similarity to unsaturated glucuronyl hydrolase UGL - Bacillus sp.	1,02329	0,342232	-1,04556
An04g03170		strong similarity to beta-glucosidase bglB -Candida wickerhamii	1,03831	0,227806	-0,531895
An02g00610		similarity to beta-galactosidase bgaM -Bacillus megaterium	1,05545	0,17568	-0,581721
An01g14670	pgaE		1,06873	0,143097	-1,40498
An09g00270			1,07795	-0,798254	-1,53063
An13g03710	agdD	strong similarity to alpha-glucosidase aglU -Bacillus sp.	1,12053	1,00779	-0,101938
An01g06120	gdbA	strong similarity to 4-alpha-glucanotransferase / amylo-1,6-glucosidase Gdb1 -Saccharomyces cerevisiae	1,1256	1,00539	0,122363
An03g01050		similarity to endo-beta-1,4-glucanase -Bacillus polymyxa	1,16957	-0,180368	-1,18703
An07g08950	eglC	0	1,31633	-0,339992	-2,04195
An11g02100		strong similarity to furostanol glycoside 26-O-beta-glucosidase CSF26G1 - Costus speciosus	1,32785	0,224845	-2,12927
An18g04810	rgxC	strong similarity to exo-polygalacturonase PGX from patent WO9414966-A - Aspergillus tubingensis	1,35287	0,519242	-1,60756
An12g05010	axeA		1,35626	-0,615552	-2,23092
An01g10930	agdB	strong similarity to enzyme with sugar transferase activity from patent JP11009276-A - Acremonium sp.	1,4731	-0,0125536	-1,01005
An09g02160			1,60586	-0,0936179	-1,63007
An03g02080	rgxB	strong similarity to exopolygalacturonase pgaX - Aspergillus tubingensis	1,65282	0,109435	-2,41187
An15g05370	pgaII		1,67319	-1,48041	-0,745916

Table S 10 continued

An15g04550		strong similarity to xylanase A xynA from patent WO200068396-A2 - Aspergillus niger	1,73039	0,977136	2,31095
An01g12150	lacA		1,83027	-0,244629	-2,35327
An05g02440	pgaC		1,87869	-0,14043	-1,73371
An09g01190	abnA		1,89196	-1,61343	-4,34834
An04g09690		strong similarity to pectin methylesterase pme1 - Aspergillus aculeatus	1,94315	-1,42846	-1,63738
An12g08280	inuE		1,97412	-0,431062	-2,44168
An03g06550	glaA		1,98288	0,210809	-0,740003
An04g06920	agdA		2,17737	0,389808	-0,681626
An02g03260	agsD	strong similarity to hypothetical cell wall alpha-glucan synthase ags1p - Schizosaccharomyces pombe	2,2054	-0,992225	-0,0978089
An16g00540		similarity to large secreted protein -Streptomyces coelicolor [truncated ORF]	2,30179	1,17815	-2,03002
An04g09700		strong similarity to endo-xylogalacturonan hydrolase xghA - Aspergillus tubingensis	2,41411	-1,50939	-0,520339
An12g03070	glaB	strong similarity to hypothetical protein SPAC4H3.03c - Schizosaccharomyces pombe	2,43551	1,75094	0,429164
An11g03340	aamA		2,49646	-0,532945	-1,42909
An09g03070	agsE	strong similarity to alpha-glucan synthase mok1p - Schizosaccharomyces pombe	-1,72514	-1,2825	0,550198
An01g11520	pgaI		-1,60026	-1,79939	-0,0927152
An15g04900		strong similarity to endoglucanase IV egl4 -Trichoderma reesei	-1,44313	-1,81293	-0,11189
An15g07810	agsB	strong similarity to hypothetical cell wall alpha-glucan synthase ags1p - Schizosaccharomyces pombe	-1,13429	-1,60882	0,820233
An15g07800	agtC	strong similarity to precursor of alpha-amylase A - Aspergillus niger	-1,09426	-2,0984	1,05342
An11g00200		strong similarity to beta-glucosidase bgln -Candida molischiana	0,248776	-3,81327	-4,62826
An03g06310	pmeA		-0,373761	-3,42645	-0,867471

Table S 10 continued

An15g03550		weak similarity to protopectinase from patent WO9806832-A1 - Bacillus subtilis	-0,98871	-1,9914	-3,37592
An14g01130		strong similarity to rhamnogalacturonase B precursor rhgB - Aspergillus aculeatus	0,534344	-1,54858	-0,895222
An14g02760	eglA		-0,392241	-1,5484	0,0707353
An09g00260	aglC		0,0872608	-1,53986	-1,97408
An01g01870		strong similarity to hypothetical Avicelase III aviIII - Aspergillus aculeatus	-0,201128	-1,50149	-2,87209
An08g05230		strong similarity to hypothetical endoglucanase IV - Trichoderma reesei	-0,472149	-1,41415	-0,566394
An14g04370	pelA		-0,736722	-1,3787	-1,67759
An01g11660	cbhB		0,413075	-1,37322	-4,00103
An14g04200	rhgB		-0,485875	-1,33336	-0,736019
An04g08550		strong similarity to endoglucanase IV EGIV -Trichoderma reesei	-0,533205	-1,32996	-0,914607
An01g14600		strong similarity to endo-1,4-beta-xylanase B xynB from patent WO9414965 - Aspergillus tubingensis	0,368919	-1,29091	-0,592924
An07g09330	cbhA		-0,0999668	-1,28697	-0,960855
An01g11670		strong similarity to endo-beta-1,4-glucanase A eglA - Aspergillus nidulans	0,419835	-1,25465	-4,74461
An01g00780	xynB		0,103013	-1,23374	-0,85854
An14g02670		strong similarity to endoglucanase IV egl4 -Trichoderma reesei	-0,425447	-1,11919	-0,682826
An14g01800		strong similarity to alpha-galactosidase -Cyamopsis tetragonoloba	-0,303611	-0,981089	-2,07733
An12g07500	pgaX	strong similarity to exopolygalacturonase pgaX - Aspergillus tubingensis	0,667133	1,21622	-0,683694
An17g00520		strong similarity to beta-glucosidase precursor BGLUC - Kluyveromyces marxianus	0,552953	1,7187	-0,207229
An18g04100	exgA	strong similarity to 43 kDa secreted glycoprotein precursor gp43 - Paracoccidioides brasiliensis	0,310338	-0,255353	1,19065
An15g02300	abfB		0,965591	-0,694169	-3,11717

Table S 10 continued

An08g01900		strong similarity to xylan 1,4-beta-xylosidase - Butyrivibrio fibrisolvens	0,702329	0,0982146	-2,47725
An03g06740	pgxB	strong similarity to exo-alpha 1,4-polygalacturonase PGX1 - Cochliobolus carbonum	0,694498	0,14473	-2,29061
An02g00140		strong similarity to xylan 1,4-beta-xylosidase xynB - Bacillus subtilis	-0,474601	-0,875782	-1,94404
An14g05820		strong similarity to beta-galactosidase lacA - Aspergillus niger	0,106617	-0,575454	-1,84419
An01g09960	xlnD		0,27645	0,185712	-1,75537
An18g03570	bglA		0,660053	0,126312	-1,689
An17g00300	xarB	strong similarity to bifunctional xylosidase-arabinosidase xarB - Thermoanaerobacter ethanolicus [putative frameshift]	-0,111647	-0,498251	-1,6257
An01g04880	axlB	strong similarity to alpha-glucosidase II -Bacillus thermoamyloliquefaciens	0,484766	-0,37126	-1,46154
An14g05800	aguA		0,874381	0,0752507	-1,32868
An04g09360		strong similarity to hypothetical protein CC0812 - Caulobacter crescentus	0,760069	-0,0595972	-1,24115
An08g01710	abfC	strong similarity to alpha-L-arabinofuranosidase abfA - Bacillus stearothermophilus	0,762329	0,282416	-1,20403
An09g03300	axlA	strong similarity to alpha-xylosidase XylS -Sulfolobus solfataricus	0,803947	0,834257	-1,06568
An03g03740	bgl4	strong similarity to beta-glucosidase bgl4 -Humicola grisea	0,543805	-0,319059	-1,04635

Table S 11. Differentially expressed transcription factor genes (Pel et al., 2007) in the central zone 1, the intermediate zone 3, and the outer zone 5 of 7-day-old maltose-grown colonies of N402 and Δ*fluG*. The ^{2}log ratio of expression values of N402 vs Δ*fluG* is indicated. A number ≥1 (red) and ≤-1 (green) represent a ≥2 fold decrease and increase in Δ*fluG* colonies, respectively. Pink red and olive green shading indicate a >1 fold and significant down- and up-regulation in Δ*fluG* colonies.

Gene_id	Name	Description	log 2 fold change		
			N402 zone 1 / ΔfluG zone 1	N402 zone 3 / ΔfluG zone 3	N402 zone 5 / ΔfluG zone 5
An01g09410		similarity to Kruppel-like transcription factor biklf - Danio rerio	-2.17732	-1.51304	0.035522
An01g14350		similarity to transcription factor Upc2 -Saccharomyces cerevisiae	-1.92126	-1.56521	-0.68651
An04g00480		similarity to hypothetical protein CAE85614.1 - Neurospora crassa	-1.2017	-1.34522	0.761344
An01g07830		similarity to transcription factor ste11p -Schizosaccharomyces pombe	-1.54625	0.618967	1.2453
An14g05670		similarity to AK-toxin regulating protein AktR-1 - Alternaria alternata	-1.32396	-0.747807	0.135518
An13g03030		similarity to hypothetical protein CAB91400.2 - Neurospora crassa [putative sequencing error]	-1.00539	-0.476331	-0.06238
An08g06850		similarity to hypothetical C2H2 zinc-finger protein SPBC1105.14 - Schizosaccharomyces pombe	-0.80466	-1.20817	-1.04245
An09g00430		strong similarity to transcription activator prnA - Aspergillus nidulans	-0.28096	-1.76875	-1.16704
An03g05850		weak similarity to hypothetical transcription factor Arg81 - Saccharomyces cerevisiae	-0.02528	-1.15215	-2.0091
An12g10660		similarity to nitrate assimilation regulatory protein nirA - Aspergillus nidulans	-0.77215	-0.834718	-1.73264
An03g02140		similarity to regulator protein Uga3 -Saccharomyces cerevisiae	0.003147	-0.850629	-1.8977
An11g03780		strong similarity to hypothetical transcription regulator SPBC530.05 - Schizosaccharomyces pombe	0.027759	-0.790736	-1.33717
An14g00520		similarity to root-specific homeotic protein HRS1 - Helianthus annuus	0.507456	-0.991645	-1.23456

Table S 11 continued

An13g02140		similarity to MAL-activator 23-C Mal23-c -Saccharomyces cerevisiae	-0.33525	-0.403334	-1.42497
An04g08600	araR	strong similarity to transcription activator xlnR - Aspergillus niger	-0.05447	-0.300049	-1.34227
An03g01480		strong similarity to hypothetical C2H2 zinc finger protein - Schizosaccharomyces pombe	0.081198	-0.292831	-1.32229
An07g01380		strong similarity to hypothetical transcriptional activator CMR1 - Colletotrichum lagenarium	0.202823	-0.207374	-1.15947
An01g01330		similarity to acetate regulatory DNA binding protein facB - Aspergillus nidulans	0.258394	-0.101625	-1.223
An16g00040		similarity to zinc-finger protein CZF1 -Candida albicans	0.421503	-0.20611	-1.50401
An08g04740		similarity to protein PRIB - Lentinus edodes	0.652039	-0.207395	-1.11795
An09g01390		similarity to transcriptional activator Mut3 - Pichia angusta	0.866179	0.0314038	-1.04655
An17g00650		similarity to cercosporin resistance protein Crg1 - Cercospora nicotianae	-0.98782	-1.89759	-0.89933
An09g01870		similarity to hypothetical binuclear zinc transcription factor PRF - Nectria haematococca	-0.85905	-1.46968	-2.48601
An08g01460		similarity to hypothetical transcriptions regulator CAB91400.2 - Neurospora crassa	-0.40782	-1.11789	-0.17609
An01g07140		similarity to transcription factor ntf1p -Schizosaccharomyces pombe	-0.32496	-1.81312	-0.40713
An05g01040		similarity to hypothetical protein CAD60719.1 - Podospora anserina	-0.31387	-2.32397	0.522749
An07g00670		similarity to nitrogen assimilation regulatory protein nit-4 - Neurospora crassa	-0.03675	-1.236	-0.40563
An16g00380		similarity to thiamine-repressible protein thi1p - Schizosaccharomyces pombe	0.217092	-1.34988	-0.14876
An15g00120		similarity to Wilms tumor susceptibility protein WT1 - Homo sapiens	0.685814	0.839217	1.32681
An02g02600		strong similarity to hypothetical transcriptional regulator CON7 - Magnaporthe grisea	0.777533	0.69759	1.18346

Table S 11 continued

An03g02000		strong similarity to nitrate assimilation regulatory protein nirA - Aspergillus nidulans	0.90971	0.836248	0.01077
An01g10540		strong similarity to developmental regulatory protein brlA - Aspergillus nidulans	1.11456	1.35146	1.1185
An12g00830		strong similarity to nitrogen assimilation regulatory protein nit-4 - Neurospora crassa	1.26397	0.901738	-0.90182
An03g01760		strong similarity to transcription factor ntf1p - Schizosaccharomyces pombe	1.41892	0.832691	-0.65472
An12g02880		weak similarity to zinc binuclear cluster protein sequence #124 from patent WO200224865-A2 -Unclassified organism	1.53498	1.16617	3.8303
An12g00840		strong similarity to transcription factor ntf1p - Schizosaccharomyces pombe	1.63801	1.0554	-0.82796
An15g06960		weak similarity to hypothetical regulator protein CAB16735.1 - Schizosaccharomyces pombe	1.65488	0.906385	-0.3953
An16g04420		strong similarity to meiotic sister-chromatid recombination protein Msc1 - Saccharomyces cerevisiae	2.57514	2.43798	0.120154
An08g01860		strong similarity to ROK1-suppressor SUR1 -Candida albicans	-0.01068	0.9659	-0.18963
An14g06250		weak similarity to transcription factor atf21p - Schizosaccharomyces pombe	0.15941	0.777875	0.510931
An12g06420	riaB	similarity to gag-like protein protein from transposon TART-B1 - Drosophila melanogaster [truncated ORF]	0.201973	0.912792	0.224811
An01g13080		similarity to thiamin repressible genes regulatory protein ntf1p - Schizosaccharomyces pombe	0.3455	0.847925	0.874055
An16g06530		similarity to transcription activator CMR1 -Colletotrichum lagenarium	0.498819	0.872279	0.086149
An12g01840		similarity to hypothetical protein related to meiosis-specific protein NDT80 - Neurospora crassa	0.537458	0.73432	0.575625
An12g06190		weak similarity to transcription activator acu-15 - Neurospora crassa	0.604491	0.745714	0.686233
An02g05420		strong similarity to hypothetical zinc-finger protein flbC - Aspergillus nidulans	1.01728	0.515692	0.407467

Table S 11 continued

An02g08210	strong similarity to hypothetical protein EAA61130.1 - Aspergillus nidulans	1.1196	0.601264	-0.10209
An15g04590	similarity to acetate regulatory DNA binding protein facB - Aspergillus nidulans	1.13638	0.621782	0.680857
An04g06950	similarity to homeobox transcription factor hth - Drosophila melanogaster	1.16892	0.428508	0.082928
An14g02780	similarity to positive regulator of purine utilisation uaY - Aspergillus nidulans	1.19158	-0.657884	-0.16428
An15g05310	strong similarity to RNA polymerase II transcription factor Upc2 - Saccharomyces cerevisiae	1.23541	0.256665	1.21281
An09g05200	similarity to hypothetical transcription regulator SPAC18G6.01c - Schizosaccharomyces pombe	1.44116	-0.350566	0.34881
An01g02050	similarity to gene expression regulator At221 from patent WO200257456-A2 - Unclassified organism	-0.48592	-0.0015251	1.2791
An08g07710	strong similarity to hypothetical C6 hypothetical protein CAD37146.1 - Aspergillus fumigatus	-0.21645	0.786833	1.05752
An01g08710	similarity to protein cnjB - Tetrahymena thermophila	0.632289	-0.0674908	1.88218

REFERENCES

ANDERSEN, M. R., SALAZAR, M. P., SCHAAP, P. J., VAN DE VONDERVOORT, P. J., CULLEY, D., THYKAER, J., FRISVAD, J. C., NIELSEN, K. F., ALBANG, R., ALBERMANN, K., BERKA, R. M., BRAUS, G. H., BRAUS-STROMEYER, S. A., CORROCHANO, L. M., DAI, Z., VAN DIJCK, P. W., HOFMANN, G., LASURE, L. L., MAGNUSON, J. K., MENKE, H., MEIJER, M., MEIJER, S. L., NIELSEN, J. B., NIELSEN, M. L., VAN OOYEN, A. J., PEL, H. J., POULSEN, L., SAMSON, R. A., STAM, H., TSANG, A., VAN DEN BRINK, J. M., ATKINS, A., AERTS, A., SHAPIRO, H., PANGILINAN, J., SALAMOV, A., LOU, Y., LINDQUIST, E., LUCAS, S., GRIMWOOD, J., GRIGORIEV, I. V., KUBICEK, C. P., MARTINEZ, D., VAN PEIJ, N. N., ROUBOS, J. A., NIELSEN, J. & BAKER, S. E. 2011. Comparative genomics of citric-acid-producing *Aspergillus niger* ATCC 1015 versus enzyme-producing CBS 513.88. *Genome Res,* 21**,** 885-897.

BOS, C. J., DEBETS, A. J., SWART, K., HUYBERS, A., KOBUS, G. & SLAKHORST, S. M. 1988. Genetic analysis and the construction of master strains for assignment of genes to six linkage groups in *Aspergillus niger*. *Curr Genet,* 14**,** 437-443.

BREAKSPEAR, A. & MOMANY, M. 2007. *Aspergillus nidulans* conidiation genes *dewA, fluG*, and *stuA* are differentially regulated in early vegetative growth. *Eukaryot Cell,* 6**,** 1697-1700.

CONESA, A., PUNT, P. J., VAN LUIJK, N. & VAN DEN HONDEL, C. A. 2001. The secretion pathway in filamentous fungi: a biotechnological view. *Fungal Genet and Biol,* 33**,** 155-171.

DE BEKKER, C., VAN VELUW, G. J., VINCK, A., WIEBENGA, L. A. & WÖSTEN, H. A. 2011. Heterogeneity of *Aspergillus niger* microcolonies in liquid shaken cultures. *Appl Environm Microbiol,* 77**,** 1263-1267.

DE VRIES, R. P. & VISSER, J. 2001. *Aspergillus* enzymes involved in degradation of plant cell wall polysaccharides. *Microbiol Mol Biol Rev,* 65**,** 497-522, table of contents.

DOBIN, A., DAVIS, C. A., SCHLESINGER, F., DRENKOW, J., ZALESKI, C., JHA, S., BATUT, P., CHAISSON, M. & GINGERAS, T. R. 2012. STAR: ultrafast universal RNA-seq aligner. *Bioinformatics,* 29**,** 15-21.

FINKELSTEIN, D. B., RAMBOSEK, J., CRAWFORD, M. S., SOLIDAY, C. L., MCADA, P. C., LEACH, J., HERSHBERGER, C. L., QUEENER, S. W. & HEGEMAN, G. 1989. *Protein secretion in Aspergillus niger,* Washington, DC, American Society for Microbiology.

FULLER, K. K., RINGELBERG, C. S., LOROS, J. J. & DUNLAP, J. C. 2013. The fungal pathogen *Aspergillus fumigatus* regulates growth, metabolism, and stress resistance in response to light. *MBio,* 4.

GIELKENS, M. M., DEKKERS, E., VISSER, J. & DE GRAAFF, L. H. 1999. Two cellobiohydrolase-encoding genes from *Aspergillus niger* require D-xylose and the xylanolytic transcriptional activator XlnR for their expression. *Appl Environ Microbiol,* 65**,** 4340-4345.

HASPER, A. A., TRINDADE, L. M., VAN DER VEEN, D., VAN OOYEN, A. J. & DE GRAAFF, L. H. 2004. Functional analysis of the transcriptional activator XlnR from *Aspergillus niger*. *Microbiology,* 150**,** 1367-1375.

HASPER, A. A., VISSER, J. & DE GRAAFF, L. H. 2000. The *Aspergillus niger* transcriptional activator XlnR, which is involved in the degradation of the polysaccharides xylan and cellulose, also regulates D-xylose reductase gene expression. *Mol Microbiol,* 36**,** 193-200.

HATAKEYAMA, R., NAKAHAMA, T., HIGUCHI, Y. & KITAMOTO, K. 2007. Light represses conidiation in koji mold *Aspergillus oryzae*. *Biosci Biotechnol Biochem,* 71**,** 1844-1849.

HOUBRAKEN, J., DE VRIES, R. P. & SAMSON, R. A. 2014. Modern taxonomy of biotechnologically important Aspergillus and penicillium species. *Adv Appl Microbiol,* 86**,** 199-249.

KRIJGSHELD, P., ALTELAAR, A. F., POST, H., RINGROSE, J. H., MULLER, W. H., HECK, A. J. & WÖSTEN, H. A. 2012. Spatially resolving the secretome within the mycelium of the cell factory *Aspergillus niger*. *J Proteome Res,* 11**,** 2807-2818.

KRIJGSHELD, P., BLEICHRODT, R., VAN VELUW, G. J., WANG, F., MULLER, W. H., DIJKSTERHUIS, J. & WÖSTEN, H. A. 2013a. Development in *Aspergillus*. *Stud Mycol,* 74**,** 1-29.

KRIJGSHELD, P., NITSCHE, B. M., POST, H., LEVIN, A. M., MULLER, W. H., HECK, A. J., RAM, A. F., ALTELAAR, A. F. & WÖSTEN, H. A. 2013b. Deletion of *flbA* Results in Increased Secretome Complexity and Reduced Secretion Heterogeneity in Colonies of *Aspergillus niger*. *J Proteome Res,* 12**,** 1809-1819.

KRIJGSHELD, P. & WÖSTEN, H. A. 2013. Transcriptome analysis of zones of colonies of the Δflba strain of *Aspergillus niger Fungal Genom Bio,* 3**,** 109.

LEE, B. N. & ADAMS, T. H. 1994. The *Aspergillus nidulans fluG* gene is required for production of an extracellular developmental signal and is related to prokaryotic glutamine synthetase I. *Genes Dev,* 8**,** 641-651.

LEE, B. N. & ADAMS, T. H. 1996. *fluG* and *flb*A function interdependently to initiate conidiophore development in *Aspergillus nidulans* through *brlA* beta activation. *EMBO J,* 15**,** 299-309.

LEVIN, A. M., DE VRIES, R. P., CONESA, A., DE BEKKER, C., TALON, M., MENKE, H. H., VAN PEIJ, N. N. & WÖSTEN, H. A. 2007a. Spatial differentiation in the vegetative mycelium of *Aspergillus niger*. *Eukaryot Cell,* 6**,** 2311-2322.
LEVIN, A. M., DE VRIES, R. P. & WÖSTEN, H. A. 2007b. Localization of protein secretion in fungal colonies using a novel culturing technique; the ring-plate system. *J Microbiol Methods,* 69**,** 399-401.
LOHSE, M., BOLGER, A. M., NAGEL, A., FERNIE, A. R., LUNN, J. E., STITT, M. & USADEL, B. 2012. RobiNA: a user-friendly, integrated software solution for RNA-Seq-based transcriptomics. *Nucleic Acids Res,* 40**,** W622-627.
MAH, J. H. & YU, J. H. 2006. Upstream and downstream regulation of asexual development in *Aspergillus fumigatus*. *Eukaryot Cell,* 5**,** 1585-1595.
NITSCHE, B. M., CRABTREE, J., CERQUEIRA, G. C., MEYER, V., RAM, A. F. & WORTMAN, J. R. 2011. New resources for functional analysis of omics data for the genus *Aspergillus*. *BMC Genomics,* 12**,** 486.
OGAWA, M., TOKUOKA, M., JIN, F. J., TAKAHASHI, T. & KOYAMA, Y. 2010. Genetic analysis of conidiation regulatory pathways in koji-mold *Aspergillus oryzae*. *Fungal Genet Biol,* 47**,** 10-18.
OTTO, T. D., DILLON, G. P., DEGRAVE, W. S. & BERRIMAN, M. 2011. RATT: Rapid Annotation Transfer Tool. *Nucleic Acids Res,* 39**,** e57.
PEL, H. J., DE WINDE, J. H., ARCHER, D. B., DYER, P. S., HOFMANN, G., SCHAAP, P. J., TURNER, G., DE VRIES, R. P., ALBANG, R., ALBERMANN, K., ANDERSEN, M. R., BENDTSEN, J. D., BENEN, J. A., VAN DEN BERG, M., BREESTRAAT, S., CADDICK, M. X., CONTRERAS, R., CORNELL, M., COUTINHO, P. M., DANCHIN, E. G., DEBETS, A. J., DEKKER, P., VAN DIJCK, P. W., VAN DIJK, A., DIJKHUIZEN, L., DRIESSEN, A. J., D'ENFERT, C., GEYSENS, S., GOOSEN, C., GROOT, G. S., DE GROOT, P. W., GUILLEMETTE, T., HENRISSAT, B., HERWEIJER, M., VAN DEN HOMBERGH, J. P., VAN DEN HONDEL, C. A., VAN DER HEIJDEN, R. T., VAN DER KAAIJ, R. M., KLIS, F. M., KOOLS, H. J., KUBICEK, C. P., VAN KUYK, P. A., LAUBER, J., LU, X., VAN DER MAAREL, M. J., MEULENBERG, R., MENKE, H., MORTIMER, M. A., NIELSEN, J., OLIVER, S. G., OLSTHOORN, M., PAL, K., VAN PEIJ, N. N., RAM, A. F., RINAS, U., ROUBOS, J. A., SAGT, C. M., SCHMOLL, M., SUN, J., USSERY, D., VARGA, J., VERVECKEN, W., VAN DE VONDERVOORT, P. J., WEDLER, H., WÖSTEN, H. A., ZENG, A. P., VAN OOYEN, A. J., VISSER, J. & STAM, H. 2007. Genome sequencing and analysis of the versatile cell factory *Aspergillus niger* CBS 513.88. *Nature Biotechnol,* 25**,** 221-231.
PUNT, P. J., VAN BIEZEN, N., CONESA, A., ALBERS, A., MANGNUS, J. & VAN DEN HONDEL, C. 2002. Filamentous fungi as cell factories for heterologous protein production. *Trends Biotechnol,* 20**,** 200-206.
PURSCHWITZ, J., MULLER, S., KASTNER, C., SCHOSER, M., HAAS, H., ESPESO, E. A., ATOUI, A., CALVO, A. M. & FISCHER, R. 2008. Functional and physical interaction of blue- and red-light sensors in *Aspergillus nidulans*. *Curr Biol,* 18**,** 255-259.
SCHUSTER, E., DUNN-COLEMAN, N., FRISVAD, J. C. & VAN DIJCK, P. W. 2002. On the safety of *Aspergillus niger*--a review. *Appl Microbiol Biotechnol,* 59**,** 426-435.
SEO, J. A., GUAN, Y. & YU, J. H. 2006. FluG-dependent asexual development in *Aspergillus nidulans* occurs via derepression. *Genetics,* 172**,** 1535-1544.
TRAPNELL, C., HENDRICKSON, D. G., SAUVAGEAU, M., GOFF, L., RINN, J. L. & PACHTER, L. 2013. Differential analysis of gene regulation at transcript resolution with RNA-seq. *Nat Biotechnol,* 31**,** 46-53.
VAN DIJCK, P. W., SELTEN, G. C. & HEMPENIUS, R. A. 2003. On the safety of a new generation of DSM *Aspergillus niger* enzyme production strains. *Regul Toxicol Pharmacol,* 38**,** 27-35.
VAN PEIJ, N. N., GIELKENS, M. M., DE VRIES, R. P., VISSER, J. & DE GRAAFF, L. H. 1998a. The transcriptional activator XlnR regulates both xylanolytic and endoglucanase gene expression in *Aspergillus niger*. *Appl Environ Microbiol,* 64**,** 3615-3619.
VAN PEIJ, N. N., VISSER, J. & DE GRAAFF, L. H. 1998b. Isolation and analysis of *xln*R, encoding a transcriptional activator co-ordinating xylanolytic expression in *Aspergillus niger*. *Mol Microbiol,* 27**,** 131-142.
VISHNIAC, W. & SANTER, M. 1957. The thiobacilli. *Bacteriol Rev,* 21**,** 195-213.
WÖSTEN, H. A., MOUKHA, S. M., SIETSMA, J. H. & WESSELS, J. G. 1991. Localization of growth and secretion of proteins in *Aspergillus niger*. *J Gen Microbiol,* 137**,** 2017-2023.

Chapter 4

Inactivation of *veA* affects vegetative growth and morphology of conidiophores in *Aspergillus niger*

Fengfeng Wang, Jan Dijksterhuis, Timon Wyatt, Han A. B. Wösten, Robert-Jan Bleichrodt

Submited for publication

ABSTRACT

The velvet gene *veA* regulates asexual and sexual development as well as secondary metabolism in *Aspergilli*. Here, the function of *veA* of *Aspergillus niger* was studied. Conidia of the Δ*veA* strain germinated faster when compared to those of the wild-type. In contrast, radial growth of colonies of the deletion strain was reduced when compared to the wild-type and was accompanied by a 2-fold reduction in biomass and a wavy phenotype of hyphae. Formation of conidiophores in the colony center of the Δ*veA* strain was reduced when compared to the wild-type. The morphology of the conidiophores of the Δ*veA* strain of *A. niger* was similar to that of *Aspergillus sydowii.* Vesicle diameter, and the length and width of the stalk of the conidiophore were reduced nearly 2-fold in the Δ*veA* strain when compared to the wild-type, while the diameter of the conidiophore was even reduced 3-fold. This implies that the spore chain length is also shorter than in the wild-type. The Δ*veA* strain formed 8 (in the dark) to 17 (in the light) times less conidia per surface area of the colony when compared to the wild-type. Like in the wild-type, no effect of light was observed on asexual development of the Δ*veA* strain of *A. niger*. Together, this is the first report on the role of VeA in the morphology of a reproductive structure. The architecture of the conidiophore and the reduced spore chain length explain, at least to a large part, the reduced numbers of spores formed by the Δ*veA* strain.

INTRODUCTION

Aspergilli colonize organic substrates in nature. Colony formation starts with the germination of a sexual or asexual spore. All *Aspergillus* species reproduce asexually by forming conidia. However, sexual reproduction is only known in about one-third of the species (Geiser, 2009). For instance, *Aspergillus nidulans* is known to reproduce sexually, but this has not yet been reported for *Aspergillus niger.* Analysis of the genome sequence of *A. niger* and those of other aspergilli, however, suggests that most, if not all, aspergilli should be able to reproduce sexually (Dyer and Paoletti, 2005). In the case of *A. nidulans,* asexual development mainly takes place in the light, whereas

sexual development dominates in the dark (Krijgsheld et al., 2013a, Bayram et al., 2010, Purschwitz et al., 2006). Light-regulated development involves light sensors and a light-mediated signaling pathway.

The velvet family of regulatory proteins is specific for the fungal kingdom and is highly conserved in ascomycetes and basidiomycetes (Bayram and Braus, 2011). The best studied member of this group is VeA of *A. nidulans.* A Δ*veA* strain of this fungus does not produce sexual fruiting bodies (i.e. cleistothecia) (Kim et al., 2002) but produces conidia both in the light and in the dark (Sarikaya Bayram et al., 2010). On the other hand, over-expression of *veA* reduces asexual development and increases production of cleistothecia. Thus, VeA is a positive regulator of sexual development and a suppressor of asexual development (Kim et al., 2002). Expression of *veA* is observed throughout the life cycle of *A. nidulans* but RNA levels are higher during sexual development. VeA contains the typical velvet domain, a nuclear localization signal (NLS), a nuclear export signal, and a PEST domain that would function in degradation of the protein (Kim et al., 2002, Stinnett et al., 2007, Bayram and Braus, 2011). VeA is predominantly localized in the cytoplasm in white or blue light, while it migrates to the nucleus in the dark or upon exposure to red light. Migration of VeA to the nucleus depends on the interaction between its NLS and the α-importin KapA (Stinnett et al., 2007). Apart from KapA, VeA interacts with the regulator of secondary metabolism LaeA (Bok and Keller, 2004) and the VeA-like protein VelB (Bayram et al., 2008a, Bok and Keller, 2004). The VeA/VelB/laeA complex mediates light regulated sexual and asexual development and links it to secondary metabolism (Bayram et al., 2008a).

The role of VeA varies in the ascomycetes. For instance, *veA* of *A. parasiticus* (Calvo et al., 2004) stimulates vegetative growth and production of conidia and sclerotia. Moreover, it is involved in formation of the secondary metabolite aflatoxin. VeA of *A. fumigatus* also stimulates asexual reproduction (Krappmann et al., 2005), while its counterpart in *Fusarium verticilloides* affects the microconidia macroconidia ratio, impacts cell wall formation, and is essential for mycotoxin production (Li et al., 2006, Myung et al., 2009). Here, the role of VeA of *A. niger* was assessed. It is shown

that this protein promotes vegetative growth and is involved in spatial position and morphology of conidiophores. As a result, Δ*veA* strains produce about ten times less spores per surface area.

MATERIAL AND METHODS

Strains and growth conditions

A. niger strains used in this study (Table 1) were grown at 30 °C in the dark or under constant white light (Osram Lumilux L36w/840, Osram, Munich, Germany) of 1200 lux. *A. niger* was grown on minimal medium (MM, pH 6, consisting of 6 g l^{-1} NaNO3, 1.5 g l^{-1} KH_2PO_4, 0.5 g l^{-1} KCL, 0.5 g l^{-1} $MgSO_4 \cdot 7H_2O$, 200 µl trace element solution l^{-1} (Vishniac and Santer, 1957), 1.5 % agar, and 25 mM xylose. Colonies were grown as sandwiched cultures in a water saturated box (Wösten et al., 1991). To this end, the fungus was grown in between two perforated polycarbonate (PC) membranes (diameter of 76 mm; pore size 0.1 µm; Osmonics, GE Water Technologies, Trevose, PA) in a 0.2 mm thin layer of 1.25 % agarose. Sandwiched cultures were inoculated in the centre of the PC membrane with 2 µl of spore suspension (1000 spores in total in saline Tween [0.8% NaCl, 0.005% Tween-80]). The top membrane was positioned on the agarose layer after 24 h of incubation.

Table 1. *A. niger* strains used in this study.

Name	Genotype	Reference
N402	*cspA1*	(Bos et al., 1988)
MA70.15	*cspA1, ΔkusA, pyrG*$^{-}$	(Meyer et al., 2007)
RB#210.1	*cspA1, ΔkusA, pyrG*$^{+}$	This study
VeA#6	*cspA1, ΔkusA, pyrG*$^{+}$*, ΔveA*	This study
VF#1	*cspA1, ΔkusA, pyrG*$^{+}$, Hyg^{+}, *ΔveA, ΔfluG*	This study
VR#1	*cspA1, ΔkusA, pyrG*$^{+}$, Hyg^{+}, *veA::TagRFP-T*	This study
VC#9	*cspA1, ΔkusA, pyrG*$^{+}$, Hyg^{+}, *veA+*	This study

Table 1 continued

VRG#1	*cspA1, ΔkusA, pyrG*$^+$, Hyg$^+$, Phleo$^+$, *veA::TagRFP-T, H2B::GFP*	This study

Construction of the *veA* deletion vector

Up- and downstream flanking regions and the coding sequence of *veA* (ANI_1_738074) were amplified from chromosomal DNA of *A. niger* N402 using accuTaq polymerase (Sigma-Aldrich, St. Louis, USA) and primer pair 1 (Table 2). The amplified product was introduced in pGEM®-T easy (Promega, Madison, USA). The XbaI fragment including the *veA* coding sequence was replaced in the resulting plasmid by the XbaI fragment of pXDRFP4 (Yang et al., 2004) that contains the *pyrG* selection cassette. This resulted in the *veA* deletion construct pVeAKO that contains 604 bp upstream and 509 bp downstream flanking sequence of *veA.*

Construction of the *veA* complementation vector

The coding sequence of *veA* and 1037 bp upstream and 573 bp downstream flanking sequences were amplified from chromosomal DNA of *A. niger* N402 using primer pair 2 (Table 2) and Phusion® High-Fidelity DNA polymerase (Finnzymes; www.finnzymes.com). As a result, a NotI and PciI site had been introduced at the 5' and 3' ends of the amplified fragment, respectively. These sites were used to introduce the PCR product into pGPDGFP (Lagopodi et al., 2002) that had been cut with the same enzymes. This resulted in the *veA* complementation construct pVC.

VeA TagRFP-T fusion constructs

TagRFP-T was amplified by PCR using Phusion® High-Fidelity DNA polymerase (Finnzymes; www.finnzymes.com), primer pair 3 (Table 2), and plasmid TagRFP-158T-C1 (Merzlyak et al., 2007) as template. The amplified fragment was inserted in the SmaI site of pUC19, cut from the resulting plasmid pRB068 with NcoI and HindIII, and introduced in pGPDGFP (Lagopodi et al., 2002) that had been digested with the same enzymes. This resulted in vector pRB069. In the next step, the promoter and ORF of *veA* were amplified by PCR using primer pair 4, *A. niger* N402 chromosomal DNA as

template, and Phusion® High-Fidelity DNA polymerase (Finnzymes; www.finnzymes.com). NotI and PciI sites had been introduced at the 5' and 3' ends of the amplified fragment, respectively. The fragment was cut with these enzymes and introduced in between the NotI and NcoI sites of vector PRB069 in front of TagRFP-T and the *trpC* terminator. The resulting vector pVeARFP thus contains *veA* under control of its own promoter fused at its C-terminus with TagRFP-T.

Construction of the nuclear GFP expression plasmid

The *mpdA* promoter (ANI_1_802024) was amplified from chromosomal DNA of *A. niger* N402 using prime pair 5 (Table 2) and Phusion® High-Fidelity DNA polymerase. The PCR product was digested with NotI and NcoI and ligated with the 4 kb NotI/NcoI fragment of pCB034 (de Bekker et al., 2011) harboring the H2B-GFP fusion sequence. This plasmid was named pRB009.

Table 2. primers used in this study.

Primer	Description	Sequence
1a	veA ko Fw	GTGGTCCACGGTAGGTATAG
1b	veA ko Rv	TGGAGCATTGGACACCAGAG
2a	veA compl-FW-NotI	GCTGGCGGCCGCAAAGTAGGTAAGTAGTCTGTAGAATC
2b	veA compl-REV-PciI	GCGGACATGTGGCAAACAATGCTATCGTCTG
3a	TagRFP-T-FW	GTTCCATGGGTGCTGGTGCTGGTGCTGGTGCTGGTGCTATGGTGTCTAAGGGCG
3b	TagRFP-T-REV	AAGCTTTCAATTAAGTTTGTGCCCCAG
4a	veA-RFP-FW	TATAGCGGCCGCGACGGTGTATGACGAATGAC
4b	veA-RFP-REV	GGCGACATGTAGATGGCCGGAGATATTTTGG
5a	PmpdA1500-FW	GCGGCCGCGCGGGAGGCATCACCAGTTTATTG
5b	mpdA(promotor)-REV	CCATGGGATGTAGTGGAAGTCTGATAGTAGAAGGGAGATAGAGTGTAATTG
6a	veA negtive marker Fw	AGGCTGACCATGTTTGACTG
6b	veA negtive marker Rv	GTGGCTGCGGCAAATTATTC
7a	veA KO B positive fw	GCCTGTCTCCATCCAGATTG
7b	veA KO B positive rv	TTACCTCGGTCGCAGCTTCG
8a	Chr1-2 GAP Fw	GTACAGCCACGTTTCTGATG
8b	Chr1-2 GAP Bw	GTATCCTGCGGCTAGAATTG

Table 2 continued

9a	fluG positive A fw	AAGGTACCACGTACGGACTG
9b	fluG positive A rv	ATACCGAGCTCCCAAATCTG
10a	ORFphleo-FW-NcoI	GTAGCCATGGATGCCCATCACCAACATG
10b	ORFphleo-REV-HindIII	GTAGAAGCTTTCAGTCCTGCTCCTCGG

Transformation

Transformation of *A. niger* was performed as described (de Bekker et al., 2009). Protoplasts of *A. niger* MA70.15 were generated using 40 mg lysing enzyme (L-1412, Sigma-Aldrich, Zwijndrecht, Netherlands), 2 mg chitinase (C6137, Sigma-Aldrich, Zwijndrecht, Netherlands), and 2 mg β-glucuronidase (G0751, Sigma-Aldrich, Zwijndrecht, Netherlands) per gram wet weight of mycelium. Transformants of MA70.15 in which pVeAKO was introduced were selected on MMS agar (MM containing per liter 325 g sucrose and 12 g agar). Inactivation of *veA* was confirmed by PCR analysis with primer pairs 6 and 7 (Table 2). Transformants of the Δ*veA* strain in which vector *BNOfluG* (Chapter 3) was introduced were selected on MMS agar supplemented with 200 µg ml^{-1} hygromycine and 50 µg ml^{-1} caffeine. Inactivation of *fluG* was confirmed by PCR analysis using primer pair 8 and 9 (Table 2). Transformants of the Δ*veA* strain resulting from a co-transformation of plasmid pVC and pAN7-1 harboring the hygromycin resistance cassette (Punt et al., 1987) were also selected on MMS medium with 200 µg ml^{-1} hygromycine and 50 µg ml^{-1} caffeine. Complementation was confirmed by PCR analysis using primer pair 6 (Table 2). A similar selection was used for transformants of the Δ*veA* strain resulting from the co-transformation of the reporter construct pveARFP and pAN7-1. Introduction of the reporter construct was confirmed by PCR using primer pair 6 (Table 2). Transformants expressing pVeARFP were re-transformed with pRB009 and pRB206 (Bleichrodt, 2012) and screened on MMS medium with 100 µg ml^{-1} phleomycin. The former plasmid encompasses the histone 2B-GFP fusion, while the latter plasmid contains the phleomycin resistance cassette. To construct pRB206, the ORF of the phleomycin resistance gene was amplified from pGEMphleoB-hom2 (Ohm et al., 2010) using primer pair 10. It was cut with NcoI and HindIII and ligated

in pGPDGFP (Lagopodi et al., 2002) that had been cut with the same enzymes. The resulting vector pRB206 contains the phleomycin resistance gene under control of the *gpdA* promoter of *A. nidulans* and the *trpC* terminator.

Light microscopy

Cultures were grown in glass bottom dishes (MatTek, www.glass-bottom-dishes.com, P35G-1.5-20-C, Ashland, USA) under water saturated conditions. To this end, glass bottom dishes were filled with 200 µl MM containing 1 % agarose and 25 mM xylose (pre-warmed at 60 °C). A round cover slip (diameter 18 mm) was placed on top of the medium and 0.5 µl of spore suspension (500 spores μl^{-1}) was placed next to the cover slip after the medium had solidified. The agar medium was overlaid with 2 ml liquid MM with 25 mM xylose. Hyphae had formed after 3 days in the agar medium. Germination, growth and development were monitored with a MULTIZOOM AZ100 microscope (Nikon Corporation Instruments, Tokyo, Japan).

Fluorescence microscopy

Pieces from 7-day-old sandwiched colonies (10 x 10 mm) were excised and placed up-side-down on an object glass after the upper PC membrane was removed. RFP and GFP fluorescence were monitored on a Zeiss LSM 700 laser scanning confocal microscope (Carl Zeiss Micro-Imaging, Oberkochen, Germany). GFP was excited with the 488 nm laser line and fluorescence was detected at 490-555 nm band pass (BP). RFP was excited with a 555 nm laser line and monitored using a 560 nm long pass. Images were captured as z-series of optical sections (~1 µm for hyphae and ~2 µm for conidiophore). Data sets were displayed as maximum intensity projections (1024 x 1024 pixels). Images were processed using ZEN 2010 software.

RFP images were captured using a Plan-Apochromat 63x/1.40 *Oil DIC M27* objective with a pixel time of 1.58 µs, the laser at 3 mW, and a pinhole of 70 µm. In case of co-localization of GFP and RFP expressing strains grown in the light, images were captured with the same objective and pixel time but the 488 nm laser was set at

0.6 mW and the 555 nm laser at 1.7 mW. The pinhole was set at 44 µm and 48 µm, respectively. In case of co-localization of GFP and RFP expressing strains grown in the dark, images were captured with a Plan-Neofluor 40x/1.30 Oil DIC objective. The pixel time was set at 0.79 µs, the 488 nm laser at 1.3 mW, the 555 nm laser at 1 mW, and the pinholes at 33 µm and 36 µm, respectively.

Scanning electron microscopy

Sandwiched colonies were grown for 7 days in the absence of an agarose layer. Samples (8 x 5 mm) were cut from the periphery and the center of the colony and prepared as described (Krijgsheld et al., 2013b). Samples were viewed using a Field Emission Scanning Election Microscope (FEI, Eindhoven, The Netherlands) at an acceleration voltage of 5 kV and a working distance about 5 mm.

Quantification of sporulation

The upper PC membrane was removed from 6-day-old sandwiched colonies grown in the dark or in the light. Growth in the dark or in the light was prolonged for 24 h, after which spores were harvested and counted using a haemoctyometer. The spore concentration was related to the surface area of the colony. To obtain a similar colony diameter as the Δ*veA* strain, the upper PC membrane of wild-type sandwiched colonies were removed after 3 days instead of 6 days of growth.

Biomass analysis

Sandwiched colonies were grown for 7 days in the absence of an agarose layer. Biomass of the colonies was determined after freeze-drying. To obtain a similar colony diameter as the Δ*veA* strain, the upper PC membrane of wild-type sandwiched colonies were removed after 4 days instead of 7 days of growth.

Sugar analysis

Samples were frozen in liquid nitrogen, freeze dried, and homogenized with the Qia-

gen Tissuelyser (2 min at 30 strokes s^{-1}) in a stainless steel grinding jar (*Qiagen, Valencia, USA*) cooled with liquid nitrogen. 1 ml milli Q water was added and grinding was continued for an additional 2 min at 30 strokes s^{-1}. Samples were thawed, transferred to a 2 ml Eppendorf tube and centrifuged at 4 °C for 30 min at 10000 *g*. The supernatant was heated for 30 min at 95 °C and centrifuged for 30 min at 10000 *g*. The supernatant was filtered using a 0.2 µm Acrodisc Cr 13 mm Syringe filter (Pall Life Science, Mijdrecht, The Netherlands). Quantitative analysis of saccharides and polyols was carried out by high-performance liquid chromatography (HPLC) equipped with a Sugar-Pak I cation-exchange column (Waters, Etten-Leur, The Netherlands). The column and detector were kept at 50 °C with a column heater (Waters) and internal heater, respectively. Samples were injected using the 717plus autosampler (Waters) and separated with 0.1 mM Ca EDTA at 0.5 ml min^{-1}. The carbohydrates were detected with an IR detector (2414 refractive index detector, Waters). Peak integrations and calculation were performed with Empower software delivered by Waters. The retention time of the peaks were compared with those of 0.01–0.50 % w/v trehalose, mannitol, glucose, glycerol, erythritol and arabitol.

Statistical analysis

Statistical analysis was performed with IBM Statistics 20 (SPSS statistics; IBM New York, USA).

RESULTS

Gene An08g05100 (ANI_1_738074) was annotated as the *veA* homologue of *A. niger* (Pel et al., 2007). It encodes a protein of 555 amino acids that shares 58 % identity and 69 % similarity with the 573 amino acid long VeA protein of *A. nidulans.* Like VeA of *A. nidulans,* the predicted VeA protein of *A. niger* contains three short PEST sequences (amino acid sequences rich in proline, glutamic acid, serine, and threonine; (Rogers et al., 1986), a nuclear export signal (Figure 1A) and is predicted to have a nuclear localization according to PSORT II (Horton and Nakai, 1997)

Inactivation of *veA* of *A. niger*

The *veA* deletion vector pVeAKO was introduced in *A. niger* strain MA70.15. Transformants were screened by PCR resulting in 4 Δ*veA* strains. In contrast to the parental strain, the coding sequence of *veA* could not be amplified in these strains. In contrast, fragments were obtained with primer pairs annealing in the *pyrG* cassette and upstream of the 5' flanking sequence and in the *pyrG* cassette and downstream of the 3' flanking sequence. These fragments could not be amplified from the genomic DNA of the parental strain (Supplemental Figure 1). All strains showed the same phenotype. Strain Δ*veA*6 was selected for further analysis (see below). This strain was complemented by introduction of pVC that contains an intact copy of *veA*. Deletion of *fluG* in the Δ*veA* strain of *A. flavus* further reduces conidiation when compared to the parental strain (Chang et al., 2013). Therefore, *fluG* was inactivated in the Δ*veA*6 (VeA#6) strain, resulting in strain Δ*veA*Δ*fluG* (VF#1) (Supplemental Figure 2).

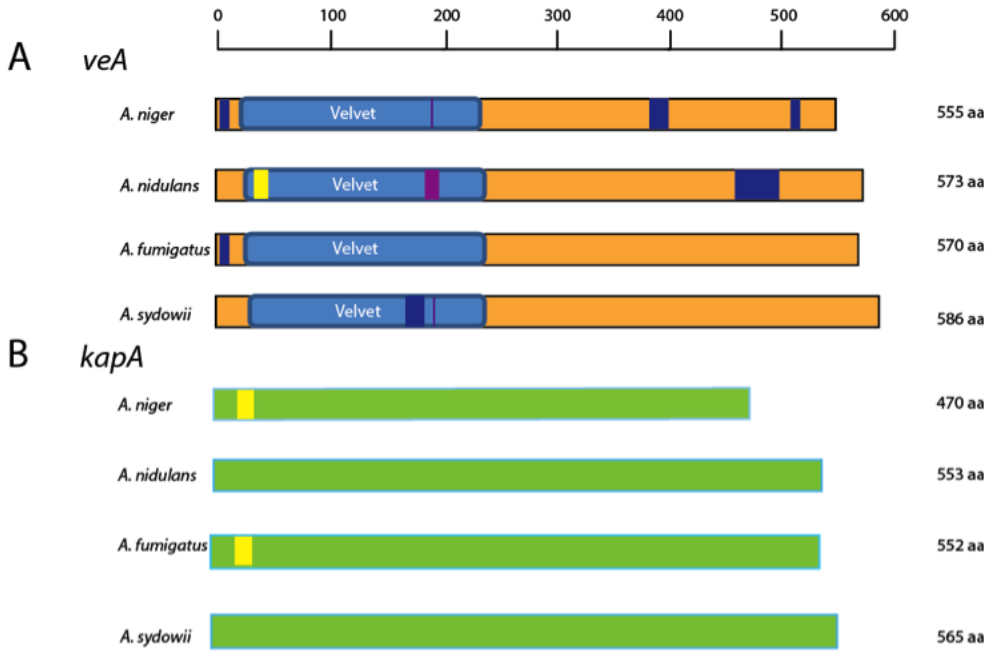

Figure1. Domains of VeA (A) and KapA (B) of *A. nidulans, A. niger, A. fumigatus* and *A. sydowii*. NLS (yellow box), NES (purple box), and PEST (blue box) represent nuclear localization signal, nuclear export signal, and PEST sequences, respectively.

Functional analysis of VeA of *A. niger*

Conidia of the Δ*veA* and Δ*veA*Δ*fluG* strains germinated faster when compared to the control strain RB#210.1 and the complemented Δ*veA* strain VC9 when grown on xylose (Data not shown) or in the absence of carbon source (Figure 2). In contrast, the Δ*veA* strain showed reduced radial growth on MM when compared to the control strain RB#210.1 (Figure 3) and the complemented Δ*veA* strain VC9 (data not shown). Inactivation of *fluG* in strain MA70.15 or the Δ*veA* strain did not impact radial growth. In all cases radial growth was not affected by light (data not shown). Reduced radial growth of the Δ*veA* strain and the Δ*veA*Δ*fluG* strain was accompanied by wavy-like growth of hyphae (Figure 4). Moreover, the biomass of 7-day-old Δ*veA* colonies was approximately 2-fold lower when compared to the wild-type and the complemented Δ*veA* strain (Figure 4D).

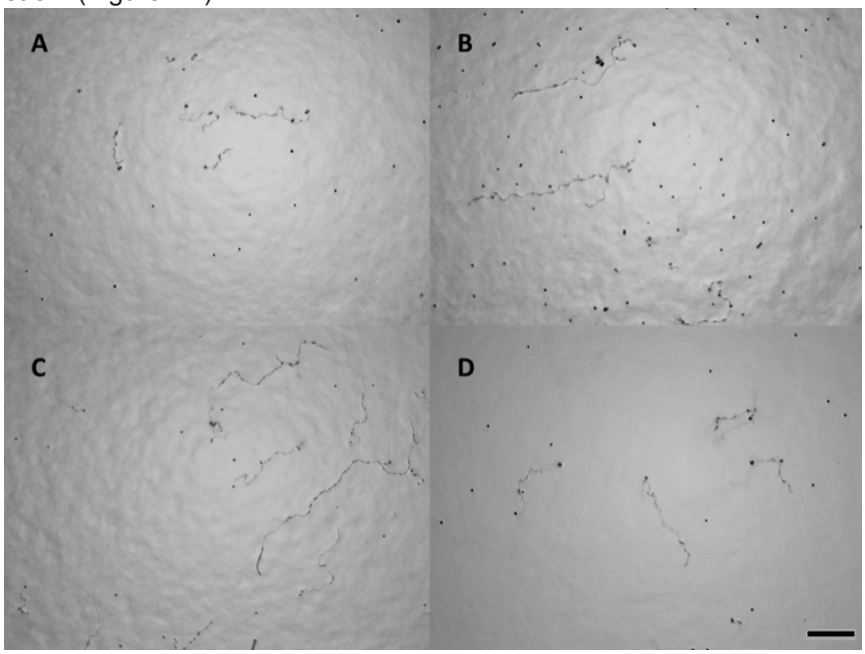

Figure 2. Germination of conidia of RB#210.1 (A), Δ*veA* (B), **Δ***veA*Δ*fluG* (C), and the **Δ***veA* complemented strain (D) after 24 h incubation on water agar. Bar represents 100 µm.

Seven-day-old sandwiched colonies of the Δ*veA* strain had mainly formed conidiophores in the sub-peripheral zone of the mycelium when the upper PC membrane had been removed at day 6 (Figure 3). The conidiophore density in the center

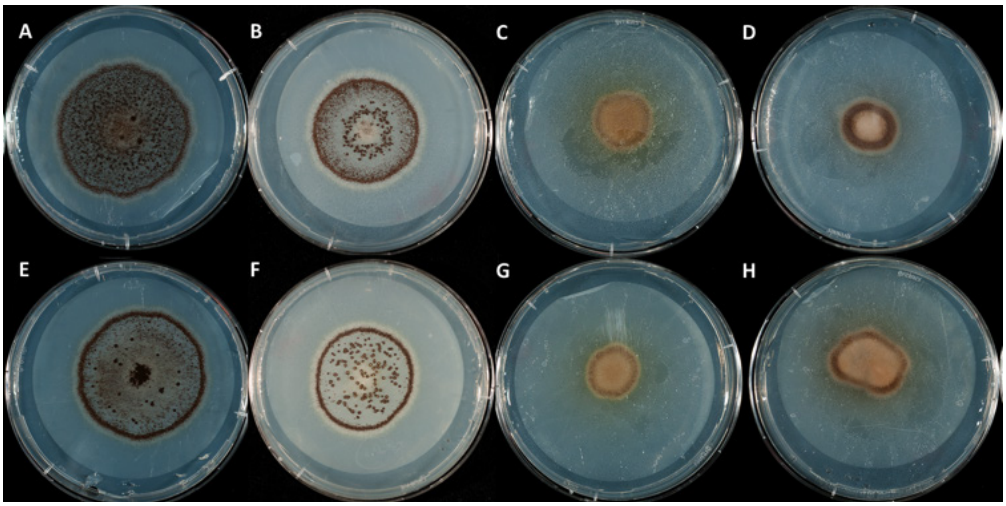

Figure 3. Radial growth and sporulation profile of 7-day-old xylose grown sandwiched colonies of the control strain RB#210.1 (A, E), the **Δ***fluG* strain (B, F), the **Δ***veA* strain (C, G) and the **Δ***veA***Δ***fluG* strain (D, H) from which the upper PC membrane was removed at day 6. Colonies were grown continuously in the light (A-D) or in the dark (E-H).

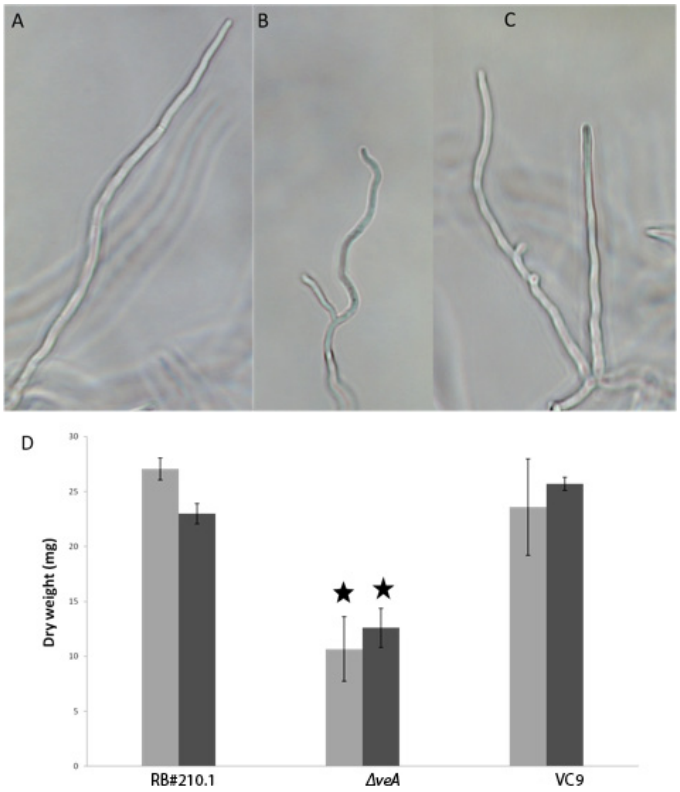

Figure 4. Morphology of hyphae of the control strain RB#210.1 (A), ΔveA (B), and the ΔveA complemented strain (C) and biomass (D) of 7 day-old xylose grown sandwiched colonies of these strains grown in the light (light gray shading) or in the dark (dark gray shading). *indicates significant difference to RB#210.1 and VC9 (anova $p<0.05$).

of Δ*veA* colonies was much less when compared to the control and the complemented strain. These colonies had formed conidiophores both in the center and at the periphery. Inactivation of *fluG* in the wild-type or Δ*veA* strain did not impact spatial distribution of conidiophores (data not shown). Conidiophore formation was also assessed in 4-day-old wild-type colonies to exclude that the spatial difference in conidiophore formation in the Δ*veA* strains is due to their reduced diameter. These control colonies with a similar diameter as 7-day-old Δ*veA* colonies also showed the two sporulation zones in the center and the periphery of the colony (data not shown).

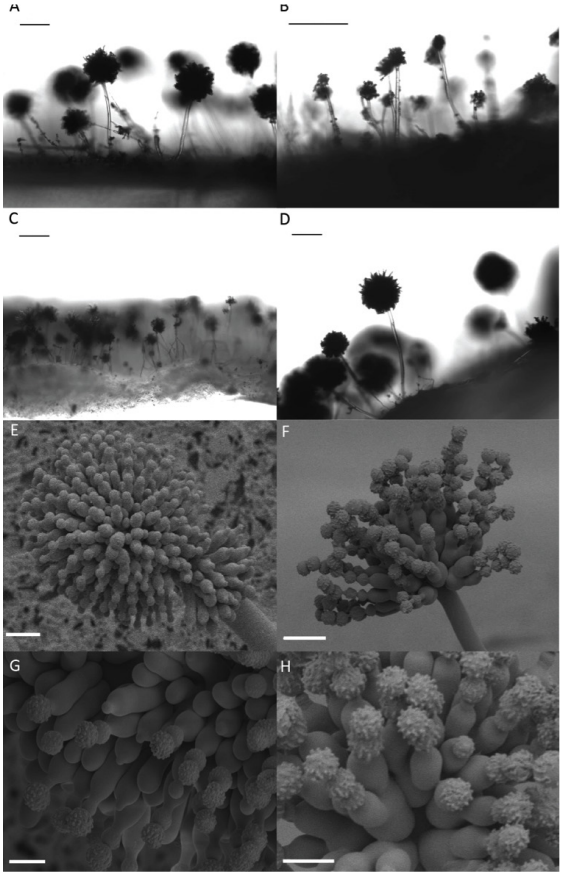

Figure 5. Light (A-D) and scanning electron (E-H) microscopy of the control strain RB#210.1 (A, E, and G), Δ*veA* (B, F, and H), Δ*veA*Δ*fluG* (C), and Δ*veA* complemented strain (D). Bar represents 100 µm (A-D), 10 µm (E, F) and 5 µm (G, H).

Light microscopy showed that Δ*veA* and Δ*veA*Δ*fluG* formed smaller conidiophores when compared to the wild type and the complemented VC9 strain (Figure 5; Table 3). The height of the stalks of Δ*veA* and Δ*veA*Δ*fluG* were 119 and 123 µm, while that of VC9 and the control strain was 199 and 224 µm (Table 3). The width of the stalk and the vesicle was also reduced when compared to the control strain and VC9. The stalk width of Δ*veA* and Δ*veA*Δ*fluG* was 6 and 5 µm, while that of the control and the complemented Δ*veA* strain VC9 was 11 and 10 µm, respectively. Vesicle diameter of Δ*veA* strain is 2-fold reduced when compared to the wild-type and the complemented strain. Di-

ameter of the conidiophore of Δ*veA* and Δ*veA*Δ*fluG* was even 3-fold reduced. These were 56 and 45 µm, respectively, while that of VC9 and the control strain was 150 and 151 µm (Table 3). This implies that the spore chain length has also been reduced in Δ*veA* and Δ*veA*Δ*fluG.*

Table 3. Length and width (µm) of stalks and diameter (µm) of vesicles and conidiophore of the control strain RB#210.1, Δ*veA,* Δ*veA*Δ*fluG* (ΔVF), and the complemented Δ*veA* strain VC9. Standard deviations are given.

	RB#210.1	***ΔveA***	**ΔVF**	**VC9**
Stalk length	225 ± 39	123 ± 39	119 ± 22	199 ± 61
Stalk width	11 ± 2	6 ± 1	5 ± 2	10 ± 1
Vesicle diameter	17 ± 5	8 ± 2	-	16 ± 4
Conidiophore diameter	150 ± 34	56 ± 13	45 ± 10	151 ± 27

The Δ*veA* strain had formed more than 8 (in the dark) and 17 (in the light) times less conidia per surface area, respectively, (Figure 6) when compared to the wild type and the complemented VC9 strain. This result was obtained when colonies were taken that had a similar size (i.e. differing in age) or that had a similar age (i.e. differing in colony diameter). Light and dark conditions had no effect on spore numbers both in the control strains and in Δ*veA* and Δ*veA*Δ*fluG*.

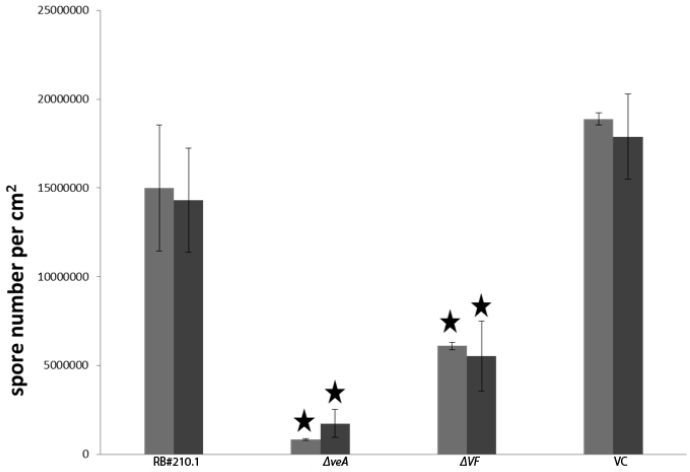

Figure 6. Number of conidia per surface area produced in the light (light shading) and in the dark (dark shading) in the control strain RB#210.1, Δ*veA*, Δ*veA*Δ*fluG* (ΔVF), and the complemented Δ*veA* strain VC9. Sandwiched colonies of control and VC9 strains were grown for 3 days on xylose medium, while the Δ*veA* and Δ*veA*Δ*fluG* strains were grown for 6 days before the upper PC membrane was removed to allow for conidia formation during a 24 h period. In this time interval all colonies had a diameter of about 20 mm. *indicates significant difference in spore density when compared to wild-type (anova $p<0.05$).

VeA localization

Construct pVeARFP that encompasses the gene encoding the VeA-TagRFP-T fusion was introduced in the Δ*veA* strain. Transformants were obtained that showed a wild-type phenotype, confirming that the fusion protein can replace wild-type VeA. VeA-TagRFP-T was detected both in light- (Figure 7AB) and dark- (data not shown) grown cultures in the vegetative mycelium and in conidiophores. The fusion protein was mainly present in nuclei in the dark, while it mainly resided in the cytosol when cultures were grown in the light (Figure 7C-F). The nuclear location of VeA-RFP was confirmed by introducing the gene encoding nuclear targeted H2B-GFP in the VeA-RFP strain. Fluorescence of RFP and GFP overlapped.

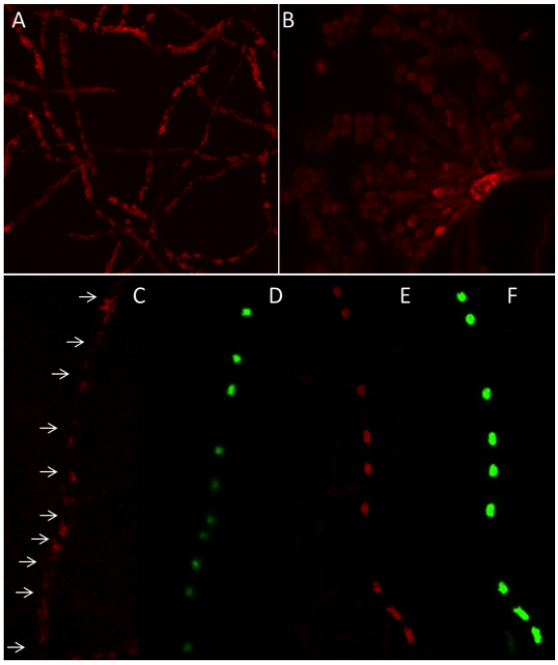

Figure 7. Confocal fluorescence microscopy shows the presence of VeA-RFP both in the vegetative mycelium (A) and in conidiophores (B) of cultures that had been grown in the light. Localization of VeA in light (1200 lux) (C, D) and dark (E, F) by localizing fluorescence of VeA-RFP (C, E) and the nuclear targeted H2B-GFP fusion protein (D, F). Arrows indicate positions of nuclei.

Inactivation of VeA influences compatible solute accumulation

The presence of compatible solutes in vegetative mycelium, mycelium with conidiophores and conidia, and conidia of the control strain and Δ*veA* was evaluated by means of HPLC analysis. No differences between the strains were observed for glucose, glycerol and arabitol. In contrast, both vegetative mycelium and conidia of Δ*veA* contained less trehalose when compared to wild type and the complemented strain (Table 4, 5). When compared to wild type, trehalose concentration had decreased about 4- and more than 10-fold, in mycelium and mycelium with conidia, respectively (Table 4). Trehalose was even completely absent in conidia of Δ*veA*

strain (Table 5). Erythritol was 2- to 3-fold lower in mycelium and mycelium with conidia of strain Δ*veA* when compared to wild type (Table 4). No difference in concentration of this polyol was observed in conidia (Table 5). In contrast, mannitol levels had been reduced 2-fold in conidia of Δ*veA*, while no difference was found in mycelium and mycelium with conidia. Notably, the total concentration of different compatible solutes didn't show significant differences between wild type, Δ*veA,* and VC9 in mycelium and conidia (Table 4).

Table 4. Accumulation (µmol solute / mg dry weight) of polyols, glucose and trehalose in vegetative mycelium and vegetative mycelium with conidia forming conidiophores of control strain RB#210.1, Δ*veA*, and the complemented Δ*veA* strain VC9. * indicates significant difference in sugar or polyol concentration when compared to wild-type (anova p<0.05). Standard deviations are given.

	RB#210.1 myc	**RB#210.1 myc+con**	**Δ*veA* myc**	**Δ*veA* myc+con**	**VC9 myc**	**VC9 myc+con**
Trehalose	0,171±0,041	0,059±0,016	*0,014±0,002	*0,016±0,000	0,129±0,031	0,084±0,006
Glucose	0,001±0,001	0,000	0,000	0,000	0,005±0,006	0,000
Erythritol	0,023±0,005	0,021±0,014	*0,073±0,003	*0,092±0,007	0,093±0,019	0,023±0,006
Glycerol	0,000	0,011±0,012	0,000	0,000	0,000	0,026±0,021
Mannitol	0,332±0,027	0,471±0,159	0,341±0,015	0,453±0,031	0,416±0,099	0,411±0,037
Arabitol	0,000	0,000	0,000	0,000	0,000	0,000
Total	0,526±0,073	0,562±0,201	0,428±0,017	0,561±0,038	0,642±0,142	0,543±0,027

Table 5. Accumulation (pmol per spore) of polyols, glucose and trehalose in conidia.of RB#210.1, Δ*veA*, and the complemented Δ*veA* strain (VC9). *indicates significant difference in sugar or polyol concentration when compared to wild-type and VC9 (anova p<0.05). ND indicates not detected. Standard deviations are given.

	RB#210.1 conidia	***ΔveA* conidia**	**VC9 conidia**
Trehalose	0,0002±0,0000	*ND	0,0002±0,0002
Glucose	0	0	0,0001±0,0001
Erythritol	0	0	0
Glycerol	0,0038±0,0005	0,0069±0,0035	0,0049±0,0047
Mannitol	0,0162±0,0002	*0,0090±0,0037	0,0165±0,0158
Arabitol	0	0	0
Total	0,0202±0,0008	0,0159±0,0072	0,0217±0,0207

DISCUSSION

VeA is conserved in *Aspergillus* and other fungi such as *F. verticillioides* and *Neurospora crassa* (Bayram et al., 2008b, Li et al., 2006). The function of this velvet protein varies between fungi (Bayram et al., 2008b). We here assessed the role of VeA in *A. niger.* It is shown that VeA of this fungus represses germination, stimulates growth and is involved in spatial positioning and morphology of conidiophores. The latter explains why a Δ*veA* strain produces less spores. Our data indicate that the role of VeA in *A. niger* is similar to *A. parasitus* and *A. fumigatus*. It is therefore tempting to speculate that this protein also determines conidiophore positioning and morphology in these aspergilli. The Δ*veA*Δ*fluG* strain showed a similar phenotype as the Δ*veA* strain in *A. niger*. We thus conclude that *fluG* is not involved in sporulation (Chapter 3) not even in the absence of *veA.*

The *veA* gene of *A. niger* encodes a velvet protein that contains three short PEST sequences, a nuclear export signal, and is predicted to have a nuclear localization. These predictions are in line with the finding that VeA of A*. niger* is predominantly present in the cytoplasm in the light and migrates to the nucleus in the dark. Nuclear migration of VeA of *A. nidulans* depends on the interaction between its NLS and the α importin KapA (Stinnett et al., 2007). A homoloque of KapA is present in the genome of *A. niger* (Figure 1B) suggesting that VeA of *A.niger* also co-migrates with KapA to the nucleus. Gene *veA* of *A. sydowii* also seems to encode a functional VeA protein with the domains found in *A. niger* and *A. nidulans*. Therefore, the phenotype of the *A. sydowii* conidiophore, which resembles that of the Δ*veA* strain of *A. niger* cannot be attributed to an (partly) inactive Vea protein.

The Δ*veA* strain was affected in growth. A similar role of VeA in biomass formation has been shown in *A. parasiticus* (Calvo et al., 2004). Reduced biomass formation in *A. niger* was accompanied by vegetative hyphae that were growing wavy in an irregular way. Zig-zag or meandering hyphal growth has been observed in strains that lack microtubule-associated kinesin motor proteins or the *teaA* or *teaR* cell end markers that localize actin nucleation to sterol-rich apical membranes (Konzack et al.,

2005). These data suggest that VeA of *A. niger* somehow functions in polar growth.

The *A. niger* control strains and the Δ*veA* strain did not show light dependent conidia formation as was shown in *A. nidulans* and *A. parasiticus* (Calvo et al., 2004, Bayram et al., 2010). Conidia and sclerotia formation seem also be independent of light in *Aspergillus carbonarius* (Crespo-Sempere et al., 2013) and *A. flavus* (Duran et al., 2007), respectively. We did observe an effect on spatial positioning of conidiophores in the Δ*veA* colony. Sandwiched Δ*veA* colonies mainly formed conidiophores at the sub-peripheral zone of the mycelium when conidiogenesis was induced by removing the upper PC membrane. In contrast, the control and the complemented strain formed conidiophores both in the center and at the sub-periphery. It is tempting to speculate that the conidiophores in the center result from carbon deprivation, while the conidiophores at the periphery result from a developmental program that is independent of the nutrient status (Krijgsheld et al., 2013a). This would imply that the *veA* strain has a role in the initiation of the conidiogenesis pathway resulting from nutrient deprivation. Whether this is also the case in other aspergilli is not known.

The Δ*veA* conidiophore stalks are shorter and they have a reduced stalk and vesicle diameter. It may be that this phenotype is due to reduced synthesis of trehalose and / or erythritol. However, total compatible solute levels were similar in the control strain and Δ*veA.* This implies that these strains have a similar turgor pressure that operates in hyphal extension. Trehalose was absent in conidia of Δ*veA* and it was strongly reduced (4-12 fold) in mycelium and mycelium with conidiophores and conidia. *A. niger* has three trehalose-6-phosphate synthase genes, *tpsA-C*, and three trehalose phosphate phosphatase genes*, tppA-C* (Svanstrom et al., 2014). In contrast to the other three deletion strains, Δ*tpsA*, Δ*tppA* and Δ*tppB* strains showed lower trehalose levels. The only mutant with a pronounced morphological difference was Δ*tppA*. This strain produced 600 times less conidia per surface area and vesicle swelling of the conidiophore was virtually absent. Yet, there seems not to be an effect on the stalk. These data also point to a role of trehalose in conidiophore formation.

The Δ*veA* strain produces 17- (in the light) and 8- (in the dark) fold less spores when compared to the control strain. This difference can be largely explained by the morphology of the conidiophores. A 2-fold reduction of the vesicle diameter will reduce its surface area 4-fold, thus restricting metulae and phialides to develop. The diameter of the conidiophore was even reduced 3-fold in the Δ*veA* strain, indicating that the length of the spore chains is reduced another 2-fold. Notably, the conidiophore morphology of Δ*veA* is similar to *A. sydowii.* It seems that *veA* of *A. sydowii* is functional (Figure 1). We therefore propose that the vesicle morphology of *A. sydowii* is due to a mutation in a gene up- or downstream of *veA.* Future studies should reveal the conidiophore morphology of the Δ*veA* strains of other aspergilli and whether this explains the reduced conidiospore numbers in the mutant strains. Although less in number, conidiospores were as viable as those of the wild-type. In fact, they germinated faster when compared to the control strains.

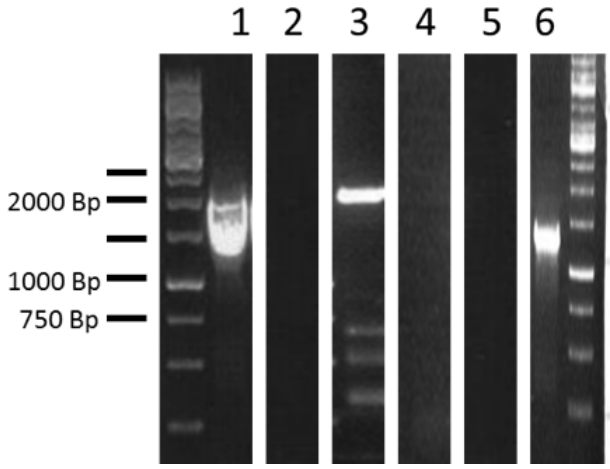

Supplemental Figure 1. PCR with genomic DNA of strains in which vector pVeAKO has been introduced using primers that anneal to the *pyrA* cassette and downstream of the 3′ flank of *veA* (lanes 1, 3, and 5) and that anneal to the 5′ and 3′ end of the coding sequence of *veA* (lanes 2, 4, 6). Strains Δ*veA* (lanes 1, 2), Δ*veA*Δ*fluG* (lanes 3, 4) and RB#210.1 control strain (lanes 5, 6).

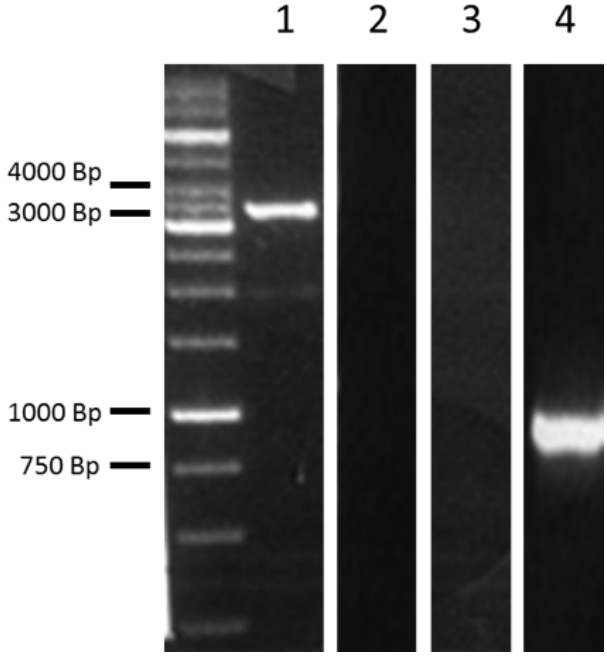

Supplemental Figure 2. PCR with genomic DNA of the control strain RB#210.1 (lanes 3 and 4) and Δ*veA* in which vector the *fluG* deletion construct has been introduced (lanes 1 and 2) using primers that anneal within the hygromicin cassette and the 5′ genomic region of the upstream flank (lanes 1 and 3) and that anneal within the coding sequence of *fluG* (lanes 2 and 4). From this it is concluded that the transformant (Δ*veA*Δ*fluG*) has a deletion in the *fluG* gene.

REFERENCES

BAYRAM, O. & BRAUS, G. H. 2011. Coordination of secondary metabolism and development in fungi: the velvet family of regulatory proteins. *FEMS Microbiol Rev,* 36**,** 1-24.

BAYRAM, O., BRAUS, G. H., FISCHER, R. & RODRIGUEZ-ROMERO, J. 2010. Spotlight on *Aspergillus nidulans* photosensory systems. *Fungal Genet Biol,* 47**,** 900-908.

BAYRAM, O., KRAPPMANN, S., NI, M., BOK, J. W., HELMSTAEDT, K., VALERIUS, O., BRAUS-STROMEYER, S., KWON, N. J., KELLER, N. P., YU, J. H. & BRAUS, G. H. 2008a. VelB/VeA/LaeA complex coordinates light signal with fungal development and secondary metabolism. *Science,* 320**,** 1504-1506.

BAYRAM, O., KRAPPMANN, S., SEILER, S., VOGT, N. & BRAUS, G. H. 2008b. *Neurospora crassa* ve-1 affects asexual conidiation. *Fungal Genet Biol,* 45**,** 127-138.

BLEICHRODT, R. 2012. Intercompartmental streaming in *Aspergillus*. *PhD Thesis, University of Utrecht.*

BOK, J. W. & KELLER, N. P. 2004. LaeA, a regulator of secondary metabolism in *Aspergillus spp*. *Eukaryot Cell,* 3**,** 527-535.

BOS, C. J., DEBETS, A. J., SWART, K., HUYBERS, A., KOBUS, G. & SLAKHORST, S. M. 1988. Genetic analysis and the construction of master strains for assignment of genes to six linkage groups in *Aspergillus niger*. *Curr Genet,* 14**,** 437-443.

CALVO, A. M., BOK, J., BROOKS, W. & KELLER, N. P. 2004. *veA* is required for toxin and sclerotial production in *Aspergillus parasiticus*. *Appl Environ Microbiol,* 70**,** 4733-4739.

CHANG, P. K., SCHARFENSTEIN, L. L., LI, P. & EHRLICH, K. C. 2013. *Aspergillus flavus* VelB acts distinctly from VeA in conidiation and may coordinate with FluG to modulate sclerotial production. *Fungal Genet Biol,* 58-59**,** 71-79.

DE BEKKER, C., WIEBENGA, A., AGUILAR, G. & WÖSTEN, H. A. 2009. An enzyme cocktail for efficient protoplast formation in *Aspergillus niger*. *J Microbiol Methods,* 76**,** 305-306.

DURAN, R. M., CARY, J. W. & CALVO, A. M. 2007. Production of cyclopiazonic acid, aflatrem, and aflatoxin by *Aspergillus flavus* is regulated by *veA*, a gene necessary for sclerotial formation. *Appl Microbiol Biotechnol,* 73**,** 1158-1168.

DYER, P. S. & PAOLETTI, M. 2005. Reproduction in *Aspergillus fumigatus*: sexuality in a supposedly asexual species? *Med Mycol,* 43 Suppl 1**,** S7-14.

GEISER, D. M. 2009. Sexual structures in *Aspergillus*: morphology, importance and genomics. *Med Mycol,* 47 Suppl 1**,** S21-26.

HORTON, P. & NAKAI, K. 1997. Better prediction of protein cellular localization sites with the k nearest neighbors classifier. *Proc Int Conf Intell Syst Mol Biol,* 5**,** 147-152.

KIM, H., HAN, K., KIM, K., HAN, D., JAHNG, K. & CHAE, K. 2002. The *veA* gene activates sexual development in *Aspergillus nidulans*. *Fungal Genet Biol,* 37**,** 72-80.

KONZACK, S., RISCHITOR, P. E., ENKE, C. & FISCHER, R. 2005. The role of the kinesin motor KipA in microtubule organization and polarized growth of *Aspergillus nidulans*. *Mol Biol Cell,* 16**,** 497-506.

KRAPPMANN, S., BAYRAM, O. & BRAUS, G. H. 2005. Deletion and allelic exchange of the *Aspergillus fumigatus veA* locus via a novel recyclable marker module. *Eukaryot Cell,* 4**,** 1298-1307.

KRIJGSHELD, P., BLEICHRODT, R., VAN VELUW, G. J., WANG, F., MULLER, W. H., DIJKSTERHUIS, J. & WÖSTEN, H. A. 2013a. Development in *Aspergillus*. *Stud Mycol,* 74**,** 1-29.

KRIJGSHELD, P., NITSCHE, B. M., POST, H., LEVIN, A. M., MULLER, W. H., HECK, A. J., RAM, A. F., ALTELAAR, A. F. & WÖSTEN, H. A. 2013b. Deletion of *flbA* Results in Increased Secretome Complexity and Reduced Secretion Heterogeneity in Colonies of *Aspergillus niger*. *J Proteome Res,* 12**,** 1809-1819.

LAGOPODI, A. L., RAM, A. F., LAMERS, G. E., PUNT, P. J., VAN DEN HONDEL, C. A., LUGTENBERG, B. J. & BLOEMBERG, G. V. 2002. Novel aspects of tomato root colonization and infection by *Fusarium oxysporum* f. sp. radicis-lycopersici revealed by confocal laser scanning microscopic analysis using the green fluorescent protein as a marker. *Mol Plant Microbe Interact,* 15**,** 172-179.

LI, S., MYUNG, K., GUSE, D., DONKIN, B., PROCTOR, R. H., GRAYBURN, W. S. & CALVO, A. M. 2006. FvVE1 regulates filamentous growth, the ratio of microconidia to macroconidia and cell wall formation in *Fusarium verticillioides*. *Mol Microbiol,* 62**,** 1418-1432.

MERZLYAK, E. M., GOEDHART, J., SHCHERBO, D., BULINA, M. E., SHCHEGLOV, A. S., FRADKOV, A. F., GAINTZEVA, A., LUKYANOV, K. A., LUKYANOV, S., GADELLA, T. W. & CHUDAKOV, D. M. 2007. Bright monomeric red fluorescent protein with an extended fluorescence lifetime. *Nat Methods,* 4**,** 555-557.

MEYER, V., ARENTSHORST, M., EL-GHEZAL, A., DREWS, A. C., KOOISTRA, R., VAN DEN HONDEL, C. A. & RAM, A. F. 2007. Highly efficient gene targeting in the *Aspergillus niger kusA* mutant. *J Biotechnol,* 128**,** 770-775.

MYUNG, K., LI, S., BUTCHKO, R. A., BUSMAN, M., PROCTOR, R. H., ABBAS, H. K. & CALVO, A. M. 2009. FvVE1 regulates biosynthesis of the mycotoxins fumonisins and fusa-

rins in *Fusarium verticillioides*. *J Agric Food Chem,* 57**,** 5089-5094.
OHM, R. A., DE JONG, J. F., BERENDS, E., WANG, F., WÖSTEN, H. A. & LUGONES, L. G. 2010. An efficient gene deletion procedure for the mushroom-forming basidiomycete *Schizophyllum commune*. *World J Microbiol Biotechnol,* 26**,** 1919-1923.
PEL, H. J., DE WINDE, J. H., ARCHER, D. B., DYER, P. S., HOFMANN, G., SCHAAP, P. J., TURNER, G., DE VRIES, R. P., ALBANG, R., ALBERMANN, K., ANDERSEN, M. R., BENDTSEN, J. D., BENEN, J. A., VAN DEN BERG, M., BREESTRAAT, S., CADDICK, M. X., CONTRERAS, R., CORNELL, M., COUTINHO, P. M., DANCHIN, E. G., DEBETS, A. J., DEKKER, P., VAN DIJCK, P. W., VAN DIJK, A., DIJKHUIZEN, L., DRIESSEN, A. J., D'ENFERT, C., GEYSENS, S., GOOSEN, C., GROOT, G. S., DE GROOT, P. W., GUILLEMETTE, T., HENRISSAT, B., HERWEIJER, M., VAN DEN HOMBERGH, J. P., VAN DEN HONDEL, C. A., VAN DER HEIJDEN, R. T., VAN DER KAAIJ, R. M., KLIS, F. M., KOOLS, H. J., KUBICEK, C. P., VAN KUYK, P. A., LAUBER, J., LU, X., VAN DER MAAREL, M. J., MEULENBERG, R., MENKE, H., MORTIMER, M. A., NIELSEN, J., OLIVER, S. G., OLSTHOORN, M., PAL, K., VAN PEIJ, N. N., RAM, A. F., RINAS, U., ROUBOS, J. A., SAGT, C. M., SCHMOLL, M., SUN, J., USSERY, D., VARGA, J., VERVECKEN, W., VAN DE VONDERVOORT, P. J., WEDLER, H., WÖSTEN, H. A., ZENG, A. P., VAN OOYEN, A. J., VISSER, J. & STAM, H. 2007. Genome sequencing and analysis of the versatile cell factory *Aspergillus niger* CBS 513.88. *Nature Biotechnol,* 25**,** 221-231.
PUNT, P. J., OLIVER, R. P., DINGEMANSE, M. A., POUWELS, P. H. & VAN DEN HONDEL, C. A. 1987. Transformation of *Aspergillus* based on the hygromycin B resistance marker from *Escherichia coli*. *Gene,* 56**,** 117-124.
PURSCHWITZ, J., MULLER, S., KASTNER, C. & FISCHER, R. 2006. Seeing the rainbow: light sensing in fungi. *Curr Opin Microbiol,* 9**,** 566-571.
ROGERS, S., WELLS, R. & RECHSTEINER, M. 1986. Amino acid sequences common to rapidly degraded proteins: the PEST hypothesis. *Science,* 234**,** 364-368.
SARIKAYA BAYRAM, O., BAYRAM, O., VALERIUS, O., PARK, H. S., IRNIGER, S., GERKE, J., NI, M., HAN, K. H., YU, J. H. & BRAUS, G. H. 2010. LaeA control of velvet family regulatory proteins for light-dependent development and fungal cell-type specificity. *PLoS Genet,* 6**,** e1001226.
STINNETT, S. M., ESPESO, E. A., COBENO, L., ARAUJO-BAZAN, L. & CALVO, A. M. 2007. *Aspergillus nidulans* VeA subcellular localization is dependent on the importin alpha carrier and on light. *Mol Microbiol,* 63**,** 242-255.
SVANSTROM, A., VAN LEEUWEN, M. R., DIJKSTERHUIS, J. & MELIN, P. 2014. Trehalose synthesis in Aspergillus niger: characterization of six homologous genes, all with conserved orthologs in related species. *BMC Microbiol,* 14**,** 90.
VISHNIAC, W. & SANTER, M. 1957. The thiobacilli. *Bacteriol Rev,* 21**,** 195-213.
WÖSTEN, H. A., MOUKHA, S. M., SIETSMA, J. H. & WESSELS, J. G. 1991. Localization of growth and secretion of proteins in *Aspergillus niger*. *J Gen Microbiol,* 137**,** 2017-2023.
YANG, L., UKIL, L., OSMANI, A., NAHM, F., DAVIES, J., DE SOUZA, C. P., DOU, X., PEREZ-BALAGUER, A. & OSMANI, S. A. 2004. Rapid production of gene replacement constructs and generation of a green fluorescent protein-tagged centromeric marker in *Aspergillus nidulans*. *Eukaryot Cell,* 3**,** 1359-1362.

Chapter 5

Light affects protein release into the culture medium of *Aspergillus niger*

Fengfeng Wang, Han A. B. Wösten and Robert-Jan Bleichrodt

ABSTRACT

Light plays an important role in the life cycle of *Aspergillus nidulans.* This fungus forms mainly asexual conidia in the light, whereas it preferentially forms sexual ascospores in the dark. Here, the role of light on asexual development and secretion was studied in *Aspergillus niger.* Cultures grown under white or blue light formed condiophores more equally distributed over the colony surface when compared to dark-grown cultures or cultures grown under red or green light. Yet, spore numbers per surface area of the colony were not affected by light. ^{14}C-labelling showed that light-grown wild-type and Δ*fluG* cultures secrete proteins mainly at the periphery, while protein secretion is more evenly distributed over the colony surface in the case of dark grown cultures. This light response was absent in the case of the Δ*veA* strain. This strain mainly secreted proteins in the colony center both in the light and the dark. This zone produced conidiophores, although most of these reproductive structures were produced in the sub-peripheral zone. Together, these data support the sporulation inhibited protein secretion theory and show that spatial position of conidiophores and protein release in the culture medium is light and VeA dependent.

INTRODUCTION

Light plays a key role in the lifecycle of many fungi. For instance, it regulates the circadian rhythm and induces the formation of reproductive structures (Purschwitz et al., 2006). The molecular mechanisms controlling the physiological responses of fungi to light is complex and far from understood. Photobiology has been studied most extensively in *Neurospora crassa* and *Aspergillus nidulans*. In the latter case, the effect of light has been studied in relation to sexual and asexual development (Bayram et al., 2010). This ascomycete forms asexual spores, known as conidia, mainly in the light, whereas it preferentially forms sexual ascospores in the dark. The phytochrome FphA is a red light receptor that represses sexual development but stimulates asexual reproduction (Blumenstein et al., 2005). Conversely, the blue light receptor complex consisting of LreA and LreB represses asexual development but stimulates sexual

reproduction. At least, this is concluded from gene inactivation of *lreA* or *lreB* (Purschwitz et al., 2008). Yet, light regulated development is more complex evidenced by the finding that inactivation of *lreA*, *lreB*, and *fphA* results in a stronger decrease in formation of asexual spores than inactivation of *fphA* alone, whereas formation of sexual fruiting bodies in the triple knock-out is less affected than in the Δ*lreA* and the Δ*lreB* strains. This and the fact that full stimulation of asexual reproduction is attained with a combination of red and blue light implies that there is an interaction between the phytochrome and the blue light sensing complex. Indeed, LreA, LreB and FphA form a light sensing complex together with VeA. VeA is a positive regulator of sexual development in *A. nidulans*, while simultaneously suppressing asexual development (Kim et al., 2002). VeA is also part of a complex with VelB, LaeA, and VosA as core components (Bayram et al., 2010). Like the Δ*veA* strain, the Δ*velB* strain does not show light-dependent development. The Δ*velB* strain is unable to form fruiting bodies in the light and in the dark. However, the effect on asexual sporulation is not as strong as in the Δ*veA* strain (Bayram et al., 2008b). LaeA is a negative regulator of sexual development in *A. nidulans* and has a positive effect on asexual development (Sarikaya Bayram et al., 2010). The Δ*laeA* strain produces five times less conidia in the light when compared to the wild-type, while fruiting body formation is markedly increased under this condition. *A. nidulans* has another blue light sensor, CryA (Bayram et al., 2008a). This cryptochrome also functions as a negative regulator of sexual development probably by integrating near-UV and blue light, resulting in repression of VeA-mediated initiation of sexual development.

Aspergillus niger has homologues of all genes involved in photobiology of *A. nidulans* (Pel et al., 2007). Yet, the role of these proteins has not been studied. Moreover, the role of light on physiology and development has not been assessed systematically in *A. niger*. White light impacts hyphal morphology of *A. niger* when grown in the presence of high sucrose levels in the medium (Gradisnik-Grapulin and Legisa, 1997) and can affect intracellular metabolism (Abraham and Chaudhur, 1976). Blue light stimulates both formation of glucoamylase and conidiophores (Zhu and Wang,

2005, Zhu and Wang, 2006, Zhu et al., 2006). However, our group reported that sporulation inhibits secretion (Levin et al., 2007, Krijgsheld et al., 2013) and we have no evidence that light stimulates conidia formation (Chapter 4).

In this study, the light response of *A. niger* was studied both in the wild-type and in the Δ*fluG* and the Δ*veA* strain. Asexual development is not affected in the Δ*fluG* strain but it releases amylolytic enzymes throughout the colony rather than releasing it predominantly at the colony periphery (Chapter 2 and 3). The Δ*veA* strain is affected in vegetative growth and in positioning and morphology of the conidiophores (Chapter 4). Here it is shown that light impacts spatial positioning of conidiophores and zonal secretion of proteins into the culture medium. VeA has a role in these zonal effects.

MATERIAL AND METHODS

Growth conditions and strains

Strains of *A. niger* (Table 1) were grown at 30 °C under constant white light (Osram Lumilux L36w/840, Osram, Munich, Germany) of 1200 lux or under 400 lux blue (400–500 nm), green (500–560 nm), or red (600–740 nm) light by using filters of deep blue, dark yellow green, and primary red, respectively (Rosco, London, United Kingdom). *A. niger* was grown on minimal medium (MM, pH 6, containing 6g l^{-1} NaNO3, 1.5 g l^{-1} KH_2PO_4, 0.5 g l^{-1} KCL, 0.5 g l^{-1} $MgSO_4 \cdot 7H_2O$, 200 µl trace element solution l^{-1} (Vishniac and Santer, 1957)) with 1.5 % agar and 25 mM xylose as carbon source. Cultures were grown as sandwiched colonies in a water saturated box (Wösten et al., 1991). To this end, *A. niger* was grown in between two perforated polycarbonate (PC) membranes (diameter 76 mm; pore size 0.1 µm; Osmonics, GE Water Technologies, Trevose, PA) in a 0.2 mm thin layer of 1.25 % agarose. Sandwiched colonies were inoculated in the centre of the PC membrane overlaying the agar medium with 1.5 µl spore suspension (500 spores $µl^{-1}$ in saline Tween [0.8% NaCl, 0.005% Tween-80]). The top membrane was positioned on the agarose layer after 24 h of incubation.

Table 1. *A. niger* strains used in this study.

Name	Genotype	Reference
N402	*cspA1*	(Bos et al., 1988)
FG#13	*cspA1, ΔfluG, hygro*$^{+}$	Chapter 3
VeA#6	*cspA1, ΔkusA, pyrG*$^{+}$*, ΔveA*	Chapter 4

Light response of *A. niger*

The upper PC membrane was removed from 6 day-old sandwiched colonies that had been grown in the dark, or under white, blue, red or green light. Growth was prolonged for 24 h using the same light regime. Spores were harvested using saline Tween and counted with a heamocytometer. Statistical analysis was performed with IBM Statistics 20 (SPSS statistics; IBM New York, USA).

Detection of protein secretion

Six-day-old sandwiched colonies were transferred for 24 h to a ring plate (Levin et al., 2007). The five concentric wells in this plate had been filled with liquid MM containing xylose. Alternatively, 7-day-old colonies were transferred to ring plates. These colonies were labelled with 185 kBq of a mixture of ^{14}C-labeled amino acids (specific activity, 189 gBq milliatom^{-1}; Amersham Biosciences, Amersham, United Kingdom) for 4 h. Proteins in the culture medium of ring plates were separated on 15% SDS poly-acrylamide gels and fixed with 45% methanol and 10% acetic acid. After this, gels were stained with 0.1 % Coomassie Brilliant Blue G250 (Sigma-Aldrich, Steinheim, Germany) in 25 % methanol and 10 % acetic acid (Merck, Darmstadt, Germany) or incubated with Amplify (Amersham Biosciences, United Kingdom). In the latter case, gels were dried and exposed to Kodak Biomax XAR film at -20 °C (Kodak Industrie, France).

RESULTS

The upper PC membrane of 6-day-old sandwiched cultures that had been grown in the dark or in the light was removed, allowing conidiophores to grow into the air and

to produce spores (Figure 1). After 24 h, conidiophores had formed more equally distributed over the colony surface of light-grown cultures of wild-type, Δ*fluG* and Δ*veA* when compared to dark-grown cultures. The wild-type and Δ*fluG* strains formed conidiophores in the sub-peripheral zone and in intermediate and central zones in the light. Conidiophore density was lowest in the colony center. In the dark, conidiophore density was higher in the sub-peripheral zone and lower in the intermediate and central zones. The Δ*veA* strain formed conidiophores in the sub-peripheral zone and in the colony center in the light. In the dark, conidiophore density also was higher in the sub-peripheral zone and lower in the colony center. Wild-type cultures grown continuously under blue light showed a conidiophore distribution most alike white light grown cultures, while culture grown under green light were more similar to dark-grown cultures (Figure 1 & 2). An intermediate phenotype was observed in the case of cultures that had been exposed to red light. Despite differences in spatial distribution of conidiophores, spore numbers of the wild-type were not affected by blue, red or green light (Table 2) and spore numbers of wild-type, Δ*fluG* and Δ*veA* was also not different in absence or presence of white light (Table 3).

Table 2. Spores per surface area of 7-day-old N402 sandwiched colonies grown in green, red, or blue light. The upper PC membrane was removed at day 6 allowing condia formation. Spore numbers were not different between the different conditions (p>0.05). Standard deviation is indicated.

light	**Spores (cm^{-2})**
green	$16\ 10^6 \pm 7\ 10^5$
red	$13\ 10^6 \pm 16\ 10^5$
blue	$14\ 10^6 \pm 12\ 10^5$

Table 3. Spores per surface area of 7-day-old N402, Δ*fluG,* and Δ*veA* sandwiched colonies grown in the dark or under white light. The upper PC membrane was removed at day 6 allowing condia formation. Spore numbers were not different between the different conditions (p>0.05). Standard deviation is indicated

	Spores (cm^{-2})
N402 light	$11\ 10^6 \pm 19\ 10^5$
N402 dark	$13\ 10^6 \pm 14\ 10^5$
Δ*fluG* Light	$17\ 10^6 \pm 39\ 10^5$
Δ*fluG* dark	$12\ 10^6 \pm 17\ 10^5$
Δ*veA*light	$24\ 10^5 \pm 21\ 10^5$
Δ*veA* dark	$12\ 10^5 \pm 5\ 10^5$

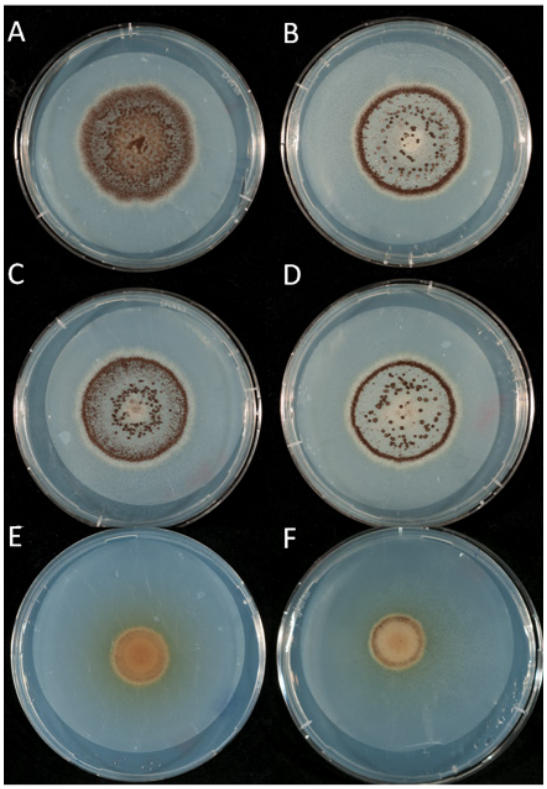

Figure 1. Conidiophore formation of 7-day-old sandwiched colonies of wild-type N402 (A, B), Δ*fluG* (C, D) and Δ*veA* (E, F) that had been grown in the light (A, C, E) or in the dark (B, D, F). The upper PC membrane was removed after 6 days of growth enabling conidiophores to form.

Protein profiles were analysed of 7-day-old light- and dark-grown colonies of N402, Δ*fluG* and Δ*veA* (Figure 3). Colonies had been transferred to the ring plate after 6 days of growth for CBB staining and at the 7th day for pulse labelling with ^{14}C-labelled amino acids. Pulse labelling shows all proteins that are immediately released into the culture medium after their secretion, while CBB staining reveals proteins that have been released in the last 24 h. These proteins may have been released directly or were trapped or linked to the cell wall prior to their release. The 7-day-old wild-type and Δ*fluG* colonies had just entered zone 5 of the ring plate, while the 7-day-old Δ*veA* colonies had entered zone 3. CBB staining did not show clear differences between the zones of the light- and dark-grown

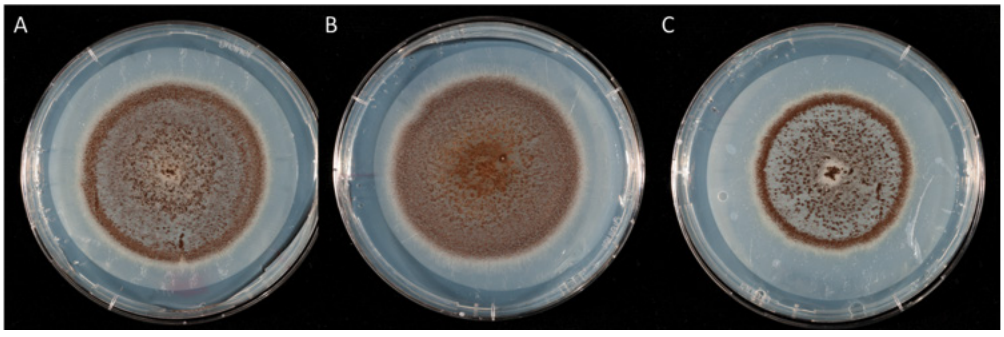

Figure 2. Conidiophore formation of 7-day-old sandwiched colonies of wild-type N402 that had been grown under red (A), blue (B) or green (C) light. The upper PC membrane was removed after 6 days of growth enabling conidiophores to be formed.

colonies of the wild-type and Δ*veA* (Figure 3). Proteins had been released in zones 1-4 (wild-type) and zone 1 (Δ*veA*). The Δ*fluG* colonies had released proteins in zones 1-5 both in the light and in the dark. Protein release was higher in zones 2 and 3 when cultured in the dark. ^{14}C-labelling showed a similar profile when compared to CBB staining in the case of Δ*veA* and Δ*fluG* colonies. In contrast, dark-grown wild-type colonies released more ^{14}C-labelled proteins in the central zones 1-3 when compared to the light-grown cultures, while protein release in the peripheral zones was similar.

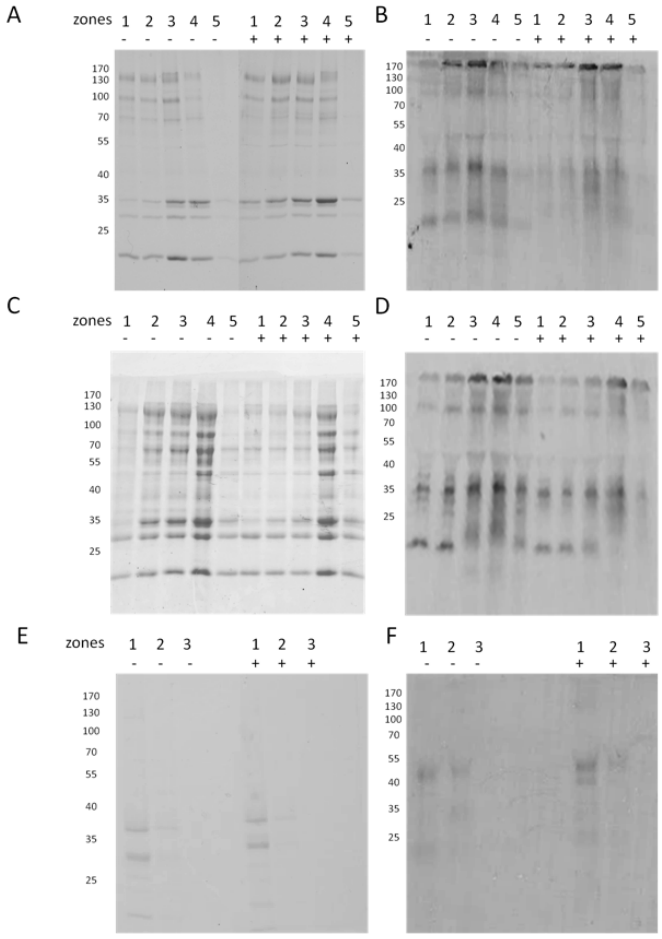

Figure 3. CBB stained (A, C, E) and ^{14}C-labelled (B, D, F) protein profiles of 7 day-old light- and dark-grown colonies of N402 (A, B), Δ*flu*G (C, D), and Δ*veA* (E, F) that had been transferred after 6 vdays to a ring plate (A, C, E) or during the last 4 h of culturing (B, D, F). Zone 1 and 5 (in case of N402 and Δ*flu*G) and zone 1 and 3 (in case of Δ*veA*) represent the most central and peripheral zone, respectively. + and - represent the presence and absence of white light during growth, respectively.

DISCUSSION

The effect of light has hardly been studied in *A. niger*. Blue light has been reported to stimulate formation of glucoamylase and conidiophores (Zhu and Wang, 2005, Zhu and Wang, 2006, Zhu et al., 2006). On the other hand, we did not observe differences in numbers of conidia in light- and dark-grown cultures (Chapter 4). Moreover, results from our lab indicate that sporulation inhibits secretion (Levin et al., 2007, Krijgsheld et al., 2013). Here, a more systematic study was performed to assess the effect of light on sporulation and secretion in *A. niger.* Conidiophore formation in the wild-type was most abundant in the sub-peripheral part of the colony irrespective of light conditions. Cultures grown under white or blue light also formed abundant conidiophores in intermediate and central parts of the colony. This was not the case for dark-grown cultures and cultures grown under green light. Cultures grown under red light showed an intermediate phenotype between light- and dark-grown cultures. Previously, it has been reported that conidiophore formation in *A. nidulans* can be initiated by stresses like carbon starvation or by a developmental program that does not depend on environmental conditions (Adams et al., 1998). It is tempting to speculate that the sandwiched mode of growth spatially separates these two pathways. Conidiophores that are formed in the sub-peripheral zone would result from the developmental program, whereas the conidiophores in more central zones would result from starvation. Assuming this, blue light, and to a lesser extent red light, would stimulate the starvation program but would repress the developmental program. The results indicate that the red and blue light receptors have an effect on asexual sporulation by determining spatial distribution of conidiophores. However, they do not impact total numbers of spores produced by the colony. This contrasts the situation in *A. nidulans* and *A. oryzae* (Hatakeyama et al., 2007). Conidiation is most strongly induced by a combination of red and blue light in *A. nidulans* (Mooney and Yager, 1990, Bayram et al., 2010), while it is repressed by white and red light in *A. oryzae* (Hatakeyama et al., 2007). This shows that the light response of aspergilli with respect to asexual development has

diverged. It would be interesting to assess the conidiophore positioning in colonies of other aspergilli in the presence and absence of light.

Previously, it was shown that sporulating zones of sandwiched colonies of *A. niger* do not release proteins in the culture medium, whereas all non-sporulating zones do secrete proteins (Levin, 2007, Levin et al., 2007, Krijgsheld et al., 2013). From this it was proposed that sporulation inhibits protein secretion. Indeed, the non-sporulating colonies of the Δ*flbA* strain secreted proteins throughout the mycelium (Krijgsheld et al., 2013). Here, ^{14}C-labelling showed that central zones of dark-grown wild-type colonies secreted more proteins than light-grown colonies. This agrees with sporulation inhibited secretion since light-grown colonies sporulate more profoundly in the colony center. Notably, no differences between dark- and light-grown colonies were observed when protein gels were stained with CBB. These data indicate that similar total amounts of proteins are released under these conditions but that initial release is faster in dark-grown colonies. This may be explained by the cell wall composition of light- and dark-grown colonies. Pores in the cell wall of dark-grown colonies may be more abundant or more wide, enabling faster release into the culture medium.

Based on CBB and ^{14}C-labelling, Δ*veA* colonies released most protein in the central zone of the colony. Light and dark-grown colonies released similar amounts of protein and protein profiles were also alike. Notably, the central zone of dark and light grown colonies did from conidiophores, albeit at lower density than the sub-peripheral zone. Together, these data imply that VeA not only impacts conidiophore positioning (Chapter 4) but also has a role in sporulation inhibited secretion. In addition, VeA is involved in the light response similar to *A. nidulans* (Kim et al., 2002).

REFERENCES

ABRAHAM, T. K. & CHAUDHUR, K. L. 1976. Light stimulated 'shunt-metabolism' succinate-alpha-ketoglutarate-isocitrate cycle and accumulation of citric acid in *Aspergillus niger*. *Experientia,* 32**,** 1506-1507.

ADAMS, T. H., WIESER, J. K. & YU, J. H. 1998. Asexual sporulation in Aspergillus nidulans. *Microbiol Mol Biol Rev,* 62**,** 35-54.

BAYRAM, O., BIESEMANN, C., KRAPPMANN, S., GALLAND, P. & BRAUS, G. H. 2008a. More than a repair enzyme: *Aspergillus nidulans* photolyase-like CryA is a regulator of sexual development. *Mol Biol Cell,* 19**,** 3254-3262.

BAYRAM, O., BRAUS, G. H., FISCHER, R. & RODRIGUEZ-ROMERO, J. 2010. Spotlight on *Aspergillus nidulans* photosensory systems. *Fungal Genet Biol,* 47**,** 900-908.

BAYRAM, O., KRAPPMANN, S., NI, M., BOK, J. W., HELMSTAEDT, K., VALERIUS, O., BRAUS-STROMEYER, S., KWON, N. J., KELLER, N. P., YU, J. H. & BRAUS, G. H. 2008b. VelB/VeA/LaeA complex coordinates light signal with fungal development and secondary metabolism. *Science,* 320**,** 1504-1506.

BLUMENSTEIN, A., VIENKEN, K., TASLER, R., PURSCHWITZ, J., VEITH, D., FRANKENBERG-DINKEL, N. & FISCHER, R. 2005. The *Aspergillus nidulans* phytochrome FphA represses sexual development in red light. *Curr Biol,* 15**,** 1833-1838.

BOS, C. J., DEBETS, A. J., SWART, K., HUYBERS, A., KOBUS, G. & SLAKHORST, S. M. 1988. Genetic analysis and the construction of master strains for assignment of genes to six linkage groups in *Aspergillus niger*. *Curr Genet,* 14**,** 437-443.

GRADISNIK-GRAPULIN, M. & LEGISA, M. 1997. A spontaneous change in the intracellular cyclic AMP level in *Aspergillus niger* is influenced by the sucrose concentration in the medium and by light. *Appl Environ Microbiol,* 63**,** 2844-2849.

HATAKEYAMA, R., NAKAHAMA, T., HIGUCHI, Y. & KITAMOTO, K. 2007. Light represses conidiation in koji mold *Aspergillus oryzae*. *Biosci Biotechnol Biochem,* 71**,** 1844-1849.

KIM, H., HAN, K., KIM, K., HAN, D., JAHNG, K. & CHAE, K. 2002. The *veA* gene activates sexual development in *Aspergillus nidulans*. *Fungal Genet Biol,* 37**,** 72-80.

KRIJGSHELD, P., NITSCHE, B. M., POST, H., LEVIN, A. M., MULLER, W. H., HECK, A. J., RAM, A. F., ALTELAAR, A. F. & WOSTEN, H. A. 2013. Deletion of *flbA* Results in Increased Secretome Complexity and Reduced Secretion Heterogeneity in Colonies of *Aspergillus niger*. *J Proteome Res,* 12**,** 1809-1819.

LEVIN, A. M. 2007. Differentiation in colonies of *Aspergillus niger*. *PhD Thesis, University of Utrecht.*

LEVIN, A. M., DE VRIES, R. P. & WÖSTEN, H. A. 2007. Localization of protein secretion in fungal colonies using a novel culturing technique; the ring-plate system. *J Microbiol Methods,* 69**,** 399-401.

MOONEY, J. L. & YAGER, L. N. 1990. Light is required for conidiation in *Aspergillus nidulans*. *Genes Dev,* 4**,** 1473-1482.

PEL, H. J., DE WINDE, J. H., ARCHER, D. B., DYER, P. S., HOFMANN, G., SCHAAP, P. J., TURNER, G., DE VRIES, R. P., ALBANG, R., ALBERMANN, K., ANDERSEN, M. R., BENDTSEN, J. D., BENEN, J. A., VAN DEN BERG, M., BREESTRAAT, S., CADDICK, M. X., CONTRERAS, R., CORNELL, M., COUTINHO, P. M., DANCHIN, E. G., DEBETS, A. J., DEKKER, P., VAN DIJCK, P. W., VAN DIJK, A., DIJKHUIZEN, L., DRIESSEN, A. J., D'ENFERT, C., GEYSENS, S., GOOSEN, C., GROOT, G. S., DE GROOT, P. W., GUILLEMETTE, T., HENRISSAT, B., HERWEIJER, M., VAN DEN HOMBERGH, J. P., VAN DEN HONDEL, C. A., VAN DER HEIJDEN, R. T., VAN DER KAAIJ, R. M., KLIS, F. M., KOOLS, H. J., KUBICEK, C. P., VAN KUYK, P. A., LAUBER, J., LU, X., VAN DER MAAREL, M. J., MEULENBERG, R., MENKE, H., MORTIMER, M. A., NIELSEN, J., OLIVER, S. G., OLSTHOORN, M., PAL, K., VAN PEIJ, N. N., RAM, A. F., RINAS, U., ROUBOS, J. A., SAGT, C. M., SCHMOLL, M., SUN, J., USSERY, D., VARGA, J., VERVECKEN, W., VAN DE VONDERVOORT, P. J., WEDLER, H., WÖSTEN, H. A., ZENG, A. P., VAN OOYEN, A. J., VISSER, J. & STAM, H. 2007. Genome sequencing and analysis of the versatile cell factory *Aspergillus niger* CBS 513.88. *Nature Biotechnol,* 25**,** 221-231.

PURSCHWITZ, J., MULLER, S., KASTNER, C. & FISCHER, R. 2006. Seeing the rainbow: light sensing in fungi. *Curr Opin Microbiol,* 9**,** 566-571.

PURSCHWITZ, J., MULLER, S., KASTNER, C., SCHOSER, M., HAAS, H., ESPESO, E. A., ATOUI, A., CALVO, A. M. & FISCHER, R. 2008. Functional and physical interaction of blue- and red-light sensors in *Aspergillus nidulans*. *Curr Biol,* 18**,** 255-259.

VISHNIAC, W. & SANTER, M. 1957. The thiobacilli. *Bacteriol Rev,* 21**,** 195-213.

WÖSTEN, H. A., MOUKHA, S. M., SIETSMA, J. H. & WESSELS, J. G. 1991. Localization of growth and secretion of proteins in *Aspergillus niger*. *J Gen Microbiol,* 137**,** 2017-2023.

ZHU, J. C. & WANG, X. J. 2005. Effect of blue light on conidiation development and glucoamylase enhancement in *Aspergillus niger*. *Wei Sheng Wu Xue Bao,* 45**,** 275-278.

ZHU, J. C. & WANG, X. J. 2006. Study on the asexual sporulation of *Aspergillus niger* under blue light induction and analysis of its subtractive library. *Sheng Wu Gong Cheng Xue Bao,* 22**,** 263-267.

ZHU, J. C., WANG, X. J., ZHANG, G., SU, J. & ZHU, M. 2006. Glucoamylase enhancement

regulated by blue light in *Aspergillus niger*. *Wei Sheng Wu Xue Bao,* 46**,** 734-739.

Chapter 6

Summary and general discussion

INTRODUCTION

Aspergillus niger is a common saprotrophic fungus. It is widely used as a cell factory because of its enormous capacity to produce organic acids (Schrickx et al., 1995) and secreted proteins (Conesa et al., 2001, Punt et al., 2002). This is exemplified by the fact that some strains secrete up to 30 gram of the starch degrading enzyme glucoamylase per liter (Finkelstein et al., 1989). The life cycle of *A. niger* starts with the germination of an asexual spore known as conidium. This results in the formation of hyphae that grow at their apices and that branch subapically. As a result, a network of interconnected hyphae is formed. This mycelium was also known as colony, initiates formation of asexual reproductive structures. These conidiophores form conidia that can start to form a new mycelium after being dispersed by wind or insects.

The compartments of hyphae are divided by septa. Peroxisome-like organelles called Woronin bodies can close the pores in these septa (Bleichrodt, 2012, Bleichrodt et al., 2012), explaining why heterogeneity is observed within and between zones of colonies of *A. niger* with respect to growth (Wösten et al., 1991), formation of aerial structures (Krijgsheld et al., 2013b), secretion (Levin et al., 2007b, Wösten et al., 1991) and RNA composition (de Bekker et al., 2011, Levin et al., 2007a, Vinck et al., 2005, Vinck et al., 2010, van Veluw et al., 2013). For instance, the zone of colonies that have the capacity for asexual reproduction do not secrete proteins (Krijgsheld et al., 2013b). This suggests that asexual reproduction inhibits secretion. Hardly anything is known about asexual reproduction in *A. niger* but it has been well studied in *Aspergillus nidulans.* Several genes have been identified in this model fungus that are involved in this developmental process. Inactivation of one of these genes *flbA* results in a mycelium without conidiophores (Lee and Adams, 1996), A similar phenotype was observed in *A. niger,* which was accompanied by protein secretion throughout the colony (Krijgsheld et al., 2013b). This confirmed the hypothesis of sporulation inhibited secretion. In contrast, inactivation of the central regulator of development *brlA* did abolish conidia formation but did not impact spatial release of proteins (Krijgsheld et al., 2013b). This can be explained by the fact that conidiophore development is

initiated in this strain but not completed.

The aim of this Thesis was to study mechanism involved in zonal secretion in colonies of *A. niger* with emphasis on sporulation inhibited secretion. These mechanisms may be targets to improve *A.* niger as a cell factory. I focused in particular on *A. niger* homologues of *fluG* and *veA* that are known sporulation genes in *A. nidulans.* Moreover, I studied the role of light because asexual reproduction is known to occur mainly in the light in *A. nidulans*, whereas sexual reproduction dominates in the dark (Krijgsheld et al., 2013a, Bayram et al., 2010, Purschwitz et al., 2006). This suggests that sporulation and, as a consequence of this, secretion are influenced by light in *A.* niger.

THE ROLE OF FLUG IN SPORULATION AND SECRETION.

Introduction of multiple copies of the amylolytic regulator *amyR* is an effective strategy to improve production of glucoamylase in *Aspergillus awamori* (Vinetskii Iu et al., 2010). Multi-copy insertion of *amyR* also improved glucoamylase expression (vanKuyk et al., 2011) and production in *A. niger* (Chapter 2). Zonal secretion was not affected in most transformants over-expressing *amyR*. Like the parental strain, glucoamylase was mainly secreted at the outer part of the colony. Interestingly, zonal expression of *glaA* and secretion of its encoded product was affected in the multicopy *amyR* transformant UU-A001.13. This transformant showed identical expression of *glaA* in all zones of the colony similar to that found at the periphery of wild-type colonies. This was accompanied by release of glucoamylase and starch degrading activity throughout the mycelium. Since most transformants did show spatial heterogeneity, loss of heterogeneity in UU-A001.13 could not be due to over-expression of *amyR*. Sequencing the genome of strain UU-A001.13 revealed three intregration sites of the introduced vectors (Chapter 2). Insertion in chromosome 1 had occurred in the 3' end of the coding sequence of *fluG*. This was accompanied by a deletion of coding sequence upstream of the insertion. Another insertion site was found in chromosome 4 in the untranslated region of a phosphate / phosphoenolpyruvate translocator gene.

Finally, integration in chromosome 6 had disrupted the 5' end of the open reading frame of the α-glucosidase gene *agdA*. This was accompanied by deletion of the coding sequence of the endogenous copy of *amyR* with its up-and downstream flanking regions. I decided to assess whether inactivation of *fluG* by vector integration resulted in the abolished secretion heterogeneity of glucoamylase. This would make sense since *fluG* of *A. nidulans* (Lee and Adams, 1996) and *A. oryzae* (Ogawa et al., 2010) function in asexual reproduction, possibly by involvement in formation of a signaling molecule. Absence of *fluG* would abolish asexual reproduction and thus would alleviate sporulation inhibited secretion. However, inactivation of *fluG* in a wild-type background did not affect sporulation (Chapter 3) as was found in *A. fumigatus* (Mah and Yu, 2006). Notably, *A. oryzae* and *A. niger* are most related of these four aspergilli, while *A. nidulans* is most unrelated (Houbraken et al., 2014). This indicates that the role of FluG in asexual development has been lost at least two times in divergence of the aspergilli. Deletion of *fluG* gene in *A. niger* did also not affect the number of spores produced per surface area of colony, germination of conidia, the spatial growth pattern, biomass formation, and spatial positioning and morphology of conidiophores (Chapter 3). However, Δ*fluG* colonies did show a different zonal starch degrading activity under the colony when compared to the wild-type. In fact, it was similar to that of UU-A001.13 (Chapter 2). Apparently, FluG affects spatial release of proteins in the colony. This was studied in more detail by determining zonal profiles of secreted proteins. Colonies of the Δ*fluG* strain secreted more proteins when grown on maltose (Chapter 3), while similar or decreased levels were observed when grown on xylose (Chapter 3). This indicates that FluG is not a general repressor of protein secretion. This was also indicated by expression studies. Out of 2554 genes encoding secreted proteins, 433 were differentially expressed. A total of 60 and 157 genes were ≥ 2-fold up- and down-regulated, respectively, in the center of the Δ*fluG* colony when compared to the central zone of the wild-type. This ratio was reversed in the intermediate and peripheral zones. 135 and 50 genes and 165 and 57 genes were up- and down-regulated in these zones, respectively. For instance, 6 out of 16 AmyR

regulated genes (including *glaA*) were ≥ 2-fold down-regulated in the center of Δ*fluG* colonies when compared to N402. This contrasts the increased amylolytic activity in the centre of Δ*fluG* colonies. This may be explained by post-transcriptional regulation. The discrepancy between gene expression and secretome composition has also been observed in the case of the Δ*flbA* strain of *A. niger*. It was shown that 70 proteins are secreted by the Δ*flbA* strain that are not found in the medium of the wild-type (Krijgsheld et al., 2013b). Only in the case of 22 proteins this could be explained by upregulation of their encoding genes (Krijgsheld and Wösten, 2013). This discrepancy was suggested to be due to (post)-transcriptional regulation or by induction of genes after transfer to fresh medium. Gene expression profiling was performed with colonies that had not been transferred, while secretome analysis was done after transfer to fresh medium. I used a similar approach; RNA profiling was done without transfer, while starch degrading activity included a transfer to fresh medium. The discrepancy between starch degrading activity and gene expression could also be explained by an increased retention time of secreted proteins in the cell wall. Proteins secreted at the periphery would thus be mainly released in the medium when this part of the colony has become a more central zone.

Expression studies also confirmed that FluG hardly, if at all affects asexual reproduction. Only 5 out of 72 genes identified in *A. nidulans* to be directly or indirectly involved in asexual reproduction were differentially expressed in the Δ*fluG* strain when compared to the wild-type strain. In the case of the Δ*flbA* strain of *A. niger* 13 sporulation genes were differentially expressed (Krijgsheld and Wösten, 2013). This number is probably too low since in this case expression in whole colonies rather than zones was assessed. By taking whole colonies, upregulation of a gene in a particular zone is leveled out by averaging with the other zones. Of the 5 genes affected in the Δ*fluG* strain, *brlA* and *flbC* are known to play a central role in asexual development of *A. nidulans*. Gene *brlA* of *A. niger* was downregulated throughout the mycelium, while *flbC* was downregulated in the colony center. The downregulation of the central regulator of asexual development in the Δ*fluG* strain was expected from expression

data of *A. nidulans* (Lee and Adams, 1996). However, in *A. niger* this did not result in a phenotypic change in asexual development although it is known that *brlA* is essential for sporulation in *A. niger* (Krijgsheld et al., 2013b). Apparently, the reduced *brlA* expression is still sufficient to induce sporulation. The impact of FluG on *flbC* expression was not expected a priori. Expression of this gene in the Δ*fluG* strain of *A. nidulans* was not assessed in the past.

The genome of *A. niger* contains 623 genes encoding transcription factors (Pel et al., 2007) Of these genes, 56 were differentially expressed with a fold change ≥ 2 in at least one zone of Δ*fluG* colony. The expression analysis and the changed zonal amylolytic activity do indicate that FluG has a role in *A. niger* although it is not clearly linked to asexual reproduction or growth. A role as a suppressor of secretion under particular environmental conditions may be the link of FluG to asexual development.

THE ROLE OF VEA AND LIGHT IN SPORULATION AND SECRETION.

The velvet family of regulatory proteins is highly conserved in ascomycetes and basidiomycetes and is unique for the fungal kingdom (Bayram and Braus, 2011). The best studied member of this group is VeA of *A. nidulans.* This protein is a positive regulator of sexual development and a suppressor of asexual development (Kim et al., 2002). VeA contains the typical velvet domain, a nuclear localization signal (NLS), a nuclear export signal and a PEST domain that would function in degradation of the protein (Kim et al., 2002, Stinnett et al., 2007, Bayram and Braus, 2011). The protein migrates from the cytoplasm to nuclei when exposed to dark or to red light. VeA has different functions in ascomycetes. It stimulates vegetative growth and production of conidia and sclerotia in *A. parasiticus* and is involved in formation of the secondary metabolite aflatoxin (Calvo et al., 2004). VeA of *A. fumigatus* also stimulates asexual reproduction (Krappmann et al., 2005), while its counterpart in *Fusarium verticilloides* affects the ratio between microconidia and macroconidia, impacts cell wall formation, and is essential for mycotoxin production (Li et al., 2006, Myung et al., 2009). The function of VeA of *A. niger* was assessed in Chapter 4. The predicted VeA protein of *A.*

niger contains the velvet domain, three PEST sequences, a NES and and is predicted to have a nuclear localization. These predictions are in line with the finding that VeA of A. *niger* is predominantly present in the cytoplasm in the light and migrates to the nucleus in the dark.

Inactivation of *veA* of *A. niger* affected asexual development (Chapter 4). The length and width of the stalk as well as the diameter of the vesicle of the conidiophore were reduced nearly 2-fold in the Δ*veA* strain when compared to the wild-type strain. The diameter of the conidiophore of Δ*veA* and Δ*veA*Δ*fluG* was even 3-fold reduced when compared to VC9 and the control. This implies that the length of spore chains that develop on the phialides are also reduced in Δ*veA* strain. Notably, the morphology of the Δ*veA* conidiophores was similar to that of a wild-type *Aspergillus sydowii*. We assumed that this phenotype was due to reduced turgor pressure as a result of a decrease in synthesis of compatible solutes. Indeed, synthesis of trehalose and / or erythritol was reduced in the Δ*veA* strain. For instance, trehalose was absent in conidia of Δ*veA* and it was 4-12 fold reduced in mycelium with or without conidiophores and conidia. However, total compatible solute levels were similar when compared to the control implying that turgor pressure is not affected. It may be that trehalose in another way affects conidiophore morphology. Inactivation of the trehalose phosphate phosphatase gene *tppA* showed lower trehalose levels, which was accompanied by virtual absence of conidiophore vesicle swelling (Svanstrom et al., 2014). Yet, there seems not to be an effect on the stalk, implying that the role of VeA in conidiophore morphology is more complex than simply an effect on trehalose levels.

A small vesicle diameter restricts metulae and phialides to develop. The vesicle diameter is 2-fold reduced when compared to wild-type. The surface area will thus be reduced 4-fold. As a consequence, the spore number per conidiophore would also be reduced 4-fold when spore chain lengths would be the same. The reduction of the conidiophore diameter implies that spore chains are also shorter. Vesicle surface area and spore chain length would result in a 9-fold decrease of spore numbers, which

is well in line with the observed 8 (in the dark) and 17 (in the light) fold reduction of spore numbers. The changed conidiophore positioning (see below) may have impacted conidiophore numbers and thus may also have contributed to the reduced spore numbers. Conidia of the Δ*veA* strain germinated faster than those of the wild-type (Chapter 4). In contrast, radial growth of colonies of the deletion strain was reduced when compared to the wild-type and was accompanied by a 2-fold reduction in biomass and a wavy phenotype of hyphae (Chapter 4). The latter suggests that VeA of *A. niger* somehow functions in polar growth. The ΔveAΔ*fluG* strain showed a similar phenotype as the ΔveA strain in *A. niger*. We thus conclude that *fluG* is not involved in sporulation (Chapter 3) not even in the absence of *veA.*

As mentioned above, asexual development in *A. nidulans* mainly takes place in the light whereas sexual development dominates in the dark (Krijgsheld et al., 2013a, Bayram et al., 2010, Purschwitz et al., 2006). The red light receptor FphA and the blue light receptors LreA, LreB, and CryA are involved in light regulated development. LreA, LreB and FphA form a light sensing complex together with VeA (Purschwitz et al., 2008). The effect of light on sporulation and secretion in *A. niger* was studied in Chapter 5. Colonies of *A. niger* were grown for 6 days between polycarbonate membranes after which the upper membrane was removed. Conidiophore formation in the wild-type was most abundant in the sub-peripheral part of the colony irrespective of light conditions. However, cultures grown under white or blue light also formed abundant conidiophores in intermediate and central parts of the colony. This was not the case for dark-grown cultures or cultures grown under green light, while cultures grown under red light showed an intermediate phenotype between light- and dark-grown cultures.

Previously, it has been reported that conidiophore formation in *A. nidulans* can be initiated by stresses like carbon starvation or by a developmental program that does not depend on environmental conditions (Adams et al., 1998). It is tempting to speculate that our way of culturing (i.e. inducing conidiophore formation at day 6 by removing the upper polycarbonate membrane) separates these two pathways.

Conidiophores that are formed in the sub-peripheral zone would result from the developmental program since carbon source was still available at the moment the polycarbonate membrane was removed. In contrast, conidiophores in more central zones would result from starvation. Assuming this, blue light, and to a lesser extent red light, would stimulate the starvation program but would repress the developmental program. However, they do not impact total numbers of spores produced by the colony. This contrasts the situation in *A. nidulans* and *A. oryzae* (Hatakeyama et al., 2007).Thus, the light response of aspergilli with respect to asexual development has diverged. It would be interesting to assess the conidiophore positioning in colonies of other aspergilli in the presence and absence of light. Sandwiched Δ*veA* colonies mainly formed conidiophores at the sub-peripheral zone of the mycelium when conidiogenesis was induced by removing the upper PC membrane. In contrast, the control and the complemented strain formed conidiophores both in the center and at the sub-periphery. This suggests that VeA, like the red and blue light receptors, is involved in the starvation pathway of asexual development. This would agree with the light response in *A. nidulans* where FphA, LreA, LreB and VeA form a light sensing complex (Purschwitz et al., 2008). Like in the wild-type, no effect of light was observed on the total number of conidia that were formed in the Δ*veA* strain of *A. niger*.

The fact that light affects conidiophore positioning (Chapter 5) and the phenomenon of sporulation inhbited secretion predict that zonal release of proteins is affected by light. ^{14}C-labelling showed that central zones of dark-grown wild-type colonies secreted more proteins than light-grown colonies (Chapter 5). This agrees with sporulation inhibited secretion since light-grown colonies sporulate more abundantly in the colony center. No differences between dark- and light-grown colonies were observed when protein profiles were compared after 24 h incubation on the ring plate followed by staining with CBB. These data indicate that similar total amounts of proteins are released in the dark and in the light but that initial release is faster in dark-grown colonies. This may be caused by differences in cell wall structure in light- and dark-grown colonies. Pores in the cell wall of dark-grown colonies may be more abundant

or more wide, enabling faster release into the culture medium.

Based on CBB and ^{14}C-labelling, Δ*veA* colonies released most protein in the central zone of the colony. Light and dark-grown colonies released similar amounts of protein and protein profiles were also alike. Notably, the central zone of dark and light grown colonies did from conidiophores, albeit at lower density than the sub-peripheral zone. Together, these data imply that VeA not only impacts conidiophore positioning (Chapter 4) but also impacts sporulation inhibited secretion.

REFERENCES

ADAMS, T. H., WIESER, J. K. & YU, J. H. 1998. ASEXUAL SPORULATION IN ASPERGILLUS NIDULANS. *MICROBIOL MOL BIOL REV,* 62**,** 35-54.

BAYRAM, O. & BRAUS, G. H. 2011. COORDINATION OF SECONDARY METABOLISM AND DEVELOPMENT IN FUNGI: THE VELVET FAMILY OF REGULATORY PROTEINS. *FEMS MICROBIOL REV,* 36**,** 1-24.

BAYRAM, O., BRAUS, G. H., FISCHER, R. & RODRIGUEZ-ROMERO, J. 2010. SPOTLIGHT ON *ASPERGILLUS NIDULANS* PHOTOSENSORY SYSTEMS. *FUNGAL GENET BIOL,* 47**,** 900-908.

BLEICHRODT, R. 2012. INTERCOMPARTMENTAL STREAMING IN *ASPERGILLUS*. *PHD THESIS, UNIVERSITY OF UTRECHT.*

BLEICHRODT, R. J., VAN VELUW, G. J., RECTER, B., MARUYAMA, J., KITAMOTO, K. & WÖSTEN, H. A. 2012. HYPHAL HETEROGENEITY IN *ASPERGILLUS ORYZAE* IS THE RESULT OF DYNAMIC CLOSURE OF SEPTA BY WORONIN BODIES. *MOL MICROBIOL,* 86**,** 1334-1344.

CALVO, A. M., BOK, J., BROOKS, W. & KELLER, N. P. 2004. *VEA* IS REQUIRED FOR TOXIN AND SCLEROTIAL PRODUCTION IN *ASPERGILLUS PARASITICUS*. *APPL ENVIRON MICROBIOL,* 70**,** 4733-4739.

CONESA, A., PUNT, P. J., VAN LUIJK, N. & VAN DEN HONDEL, C. A. 2001. THE SECRETION PATHWAY IN FILAMENTOUS FUNGI: A BIOTECHNOLOGICAL VIEW. *FUNGAL GENET AND BIOL,* 33**,** 155-171.

DE BEKKER, C., BRUNING, O., JONKER, M. J., BREIT, T. M. & WÖSTEN, H. A. 2011. SINGLE CELL TRANSCRIPTOMICS OF NEIGHBORING HYPHAE OF *ASPERGILLUS NIGER*. *GENOME BIOL,* 12**,** R71.

FINKELSTEIN, D. B., RAMBOSEK, J., CRAWFORD, M. S., SOLIDAY, C. L., MCADA, P. C., LEACH, J., HERSHBERGER, C. L., QUEENER, S. W. & HEGEMAN, G. 1989. *PROTEIN SECRETION IN ASPERGILLUS NIGER,* WASHINGTON, DC, AMERICAN SOCIETY FOR MICROBIOLOGY.

HATAKEYAMA, R., NAKAHAMA, T., HIGUCHI, Y. & KITAMOTO, K. 2007. LIGHT REPRESSES CONIDIATION IN KOJI MOLD *ASPERGILLUS ORYZAE*. *BIOSCI BIOTECHNOL BIOCHEM,* 71**,** 1844-1849.

HOUBRAKEN, J., DE VRIES, R. P. & SAMSON, R. A. 2014. MODERN TAXONOMY OF BIOTECHNOLOGICALLY IMPORTANT ASPERGILLUS AND PENICILLIUM SPECIES. *ADV APPL MICROBIOL,* 86**,** 199-249.

KIM, H., HAN, K., KIM, K., HAN, D., JAHNG, K. & CHAE, K. 2002. THE *VEA* GENE ACTIVATES SEXUAL DEVELOPMENT IN *ASPERGILLUS NIDULANS*. *FUNGAL GENET BIOL,* 37**,** 72-80.

KRAPPMANN, S., BAYRAM, O. & BRAUS, G. H. 2005. DELETION AND ALLELIC EXCHANGE OF THE *ASPERGILLUS FUMIGATUS VEA* LOCUS VIA A NOVEL RECYCLABLE MARKER MODULE. *EUKARYOT CELL,* 4**,** 1298-1307.

KRIJGSHELD, P., BLEICHRODT, R., VAN VELUW, G. J., WANG, F., MULLER, W. H., DIJKSTERHUIS, J. & WÖSTEN, H. A. 2013A. DEVELOPMENT IN *ASPERGILLUS*. *STUD MYCOL,* 74**,** 1-29.

KRIJGSHELD, P., NITSCHE, B. M., POST, H., LEVIN, A. M., MULLER, W. H., HECK, A. J., RAM, A. F., ALTELAAR, A. F. & WÖSTEN, H. A. 2013B. DELETION OF *FLBA* RESULTS IN INCREASED SECRETOME COMPLEXITY AND REDUCED SECRETION HETEROGENEITY IN COLONIES OF *ASPERGILLUS NIGER*. *J PROTEOME RES,* 12**,** 1809-1819.

KRIJGSHELD, P. & WÖSTEN, H. A. 2013. TRANSCRIPTOME ANALYSIS OF ZONES OF COLONIES OF THE ΔFLBA STRAIN OF *ASPERGILLUS NIGER FUNGAL GENOM BIO,* 3**,** 109.

LEE, B. N. & ADAMS, T. H. 1996. *FLUG* AND *FLBA* FUNCTION INTERDEPENDENTLY TO INITIATE CONIDIOPHORE DEVELOPMENT IN *ASPERGILLUS NIDULANS* THROUGH *BRLA* BETA ACTIVATION. *EMBO J,* 15**,** 299-309.

LEVIN, A. M., DE VRIES, R. P., CONESA, A., DE BEKKER, C., TALON, M., MENKE, H. H., VAN PEIJ, N. N. & WÖSTEN, H. A. 2007A. SPATIAL DIFFERENTIATION IN THE VEGETATIVE MYCELIUM OF *ASPERGILLUS NIGER*. *EUKARYOT CELL,* 6**,** 2311-2322.

LEVIN, A. M., DE VRIES, R. P. & WÖSTEN, H. A. 2007B. LOCALIZATION OF PROTEIN SECRETION IN FUNGAL COLONIES USING A NOVEL CULTURING TECHNIQUE; THE RINGPLATE SYSTEM. *J MICROBIOL METHODS,* 69**,** 399-401.

LI, S., MYUNG, K., GUSE, D., DONKIN, B., PROCTOR, R. H., GRAYBURN, W. S. & CALVO, A. M. 2006. FVVE1 REGULATES FILAMENTOUS GROWTH, THE RATIO OF MICROCONIDIA TO MACROCONIDIA AND CELL WALL FORMATION IN *FUSARIUM VERTICILLIOIDES*. *MOL MICROBIOL,* 62**,** 1418-1432.

MAH, J. H. & YU, J. H. 2006. UPSTREAM AND DOWNSTREAM REGULATION OF ASEXUAL DEVELOPMENT IN *ASPERGILLUS FUMIGATUS*. *EUKARYOT CELL,* 5**,** 1585-1595.

MOONEY, J. L. & YAGER, L. N. 1990. LIGHT IS REQUIRED FOR CONIDIATION IN *ASPERGILLUS NIDULANS*. *GENES DEV,* 4**,** 1473-1482.

MYUNG, K., LI, S., BUTCHKO, R. A., BUSMAN, M., PROCTOR, R. H., ABBAS, H. K. & CALVO, A. M. 2009. FVVE1 REGULATES BIOSYNTHESIS OF THE MYCOTOXINS FUMONISINS AND FUSARINS IN *FUSARIUM VERTICILLIOIDES*. *J AGRIC FOOD CHEM,* 57**,** 5089-5094.

OGAWA, M., TOKUOKA, M., JIN, F. J., TAKAHASHI, T. & KOYAMA, Y. 2010. GENETIC ANALYSIS OF CONIDIATION REGULATORY PATHWAYS IN KOJI-MOLD *ASPERGILLUS ORYZAE*. *FUNGAL GENET BIOL,* 47**,** 10-18.

PEL, H. J., DE WINDE, J. H., ARCHER, D. B., DYER, P. S., HOFMANN, G., SCHAAP, P. J., TURNER, G., DE VRIES, R. P., ALBANG, R., ALBERMANN, K., ANDERSEN, M. R., BENDTSEN, J. D., BENEN, J. A., VAN DEN BERG, M., BREESTRAAT, S., CADDICK, M. X., CONTRERAS, R., CORNELL, M., COUTINHO, P. M., DANCHIN, E. G., DEBETS, A. J., DEKKER, P., VAN DIJCK, P. W., VAN DIJK, A., DIJKHUIZEN, L., DRIESSEN, A. J., D'ENFERT, C., GEYSENS, S., GOOSEN, C., GROOT, G. S., DE GROOT, P. W., GUILLEMETTE, T., HENRISSAT, B., HERWEIJER, M., VAN DEN HOMBERGH, J. P., VAN DEN HONDEL, C. A., VAN DER HEIJDEN, R. T., VAN DER KAAIJ, R. M., KLIS, F. M., KOOLS, H. J., KUBICEK, C. P., VAN KUYK, P. A., LAUBER, J., LU, X., VAN DER MAAREL, M. J., MEULENBERG, R., MENKE, H., MORTIMER, M. A., NIELSEN, J., OLIVER, S. G., OLSTHOORN, M., PAL, K., VAN PEIJ, N. N., RAM, A. F., RINAS, U., ROUBOS, J. A., SAGT, C. M., SCHMOLL, M., SUN, J., USSERY, D., VARGA, J., VERVECKEN, W., VAN DE VONDERVOORT, P. J., WEDLER, H., WÖSTEN, H. A., ZENG, A. P., VAN OOYEN, A. J., VISSER, J. & STAM, H. 2007. GENOME SEQUENCING AND ANALYSIS OF THE VERSATILE CELL FACTORY *ASPERGILLUS NIGER* CBS 513.88. *NATURE BIOTECHNOL,* 25**,** 221-231.

PUNT, P. J., VAN BIEZEN, N., CONESA, A., ALBERS, A., MANGNUS, J. & VAN DEN HONDEL, C. 2002. FILAMENTOUS FUNGI AS CELL FACTORIES FOR HETEROLOGOUS PROTEIN PRODUCTION. *TRENDS BIOTECHNOL,* 20**,** 200-206.

PURSCHWITZ, J., MULLER, S., KASTNER, C. & FISCHER, R. 2006. SEEING THE RAINBOW: LIGHT SENSING IN FUNGI. *CURR OPIN MICROBIOL,* 9**,** 566-571.

PURSCHWITZ, J., MULLER, S., KASTNER, C., SCHOSER, M., HAAS, H., ESPESO, E. A., ATOUI, A., CALVO, A. M. & FISCHER, R. 2008. FUNCTIONAL AND PHYSICAL INTERACTION OF BLUE- AND RED-LIGHT SENSORS IN *ASPERGILLUS NIDULANS*. *CURR BIOL,* 18**,** 255-259.

SCHRICKX, J. M., RAEDTS, M. J., STOUTHAMER, A. H. & VAN VERSEVELD, H. W. 1995. ORGANIC ACID PRODUCTION BY *ASPERGILLUS NIGER* IN RECYCLING CULTURE ANALYZED BY CAPILLARY ELECTROPHORESIS. *ANAL BIOCHEM,* 231**,** 175-181.

STINNETT, S. M., ESPESO, E. A., COBENO, L., ARAUJO-BAZAN, L. & CALVO, A. M. 2007. *ASPERGILLUS NIDULANS* VEA SUBCELLULAR LOCALIZATION IS DEPENDENT ON THE IMPORTIN ALPHA CARRIER AND ON LIGHT. *MOL MICROBIOL,* 63**,** 242-255.

SVANSTROM, A., VAN LEEUWEN, M. R., DIJKSTERHUIS, J. & MELIN, P. 2014. TREHALOSE SYNTHESIS IN ASPERGILLUS NIGER: CHARACTERIZATION OF SIX HOMOLOGOUS GENES, ALL WITH CONSERVED ORTHOLOGS IN RELATED SPECIES. *BMC MICROBIOL,* 14**,** 90.

VAN VELUW, G. J., TEERTSTRA, W. R., DE BEKKER, C., VINCK, A., VAN BEEK, N., MULLER, W. H., ARENTSHORST, M., VAN DER MEI, H. C., RAM, A. F., DIJKSTERHUIS, J. & WÖSTEN, H. A. 2013. HETEROGENEITY IN LIQUID SHAKEN CULTURES OF *ASPERGILLUS NIGER* INOCULATED WITH MELANISED CONIDIA OR CONIDIA OF PIGMENTATION MUTANTS. *STUD MYCOL,* 74**,** 47-57.

VANKUYK, P. A., BENEN, J. A., WÖSTEN, H. A., VISSER, J. & DE VRIES, R. P. 2011. A BROADER ROLE FOR AMYR IN *ASPERGILLUS NIGER*: REGULATION OF THE UTILISATION OF D-GLUCOSE OR D-GALACTOSE CONTAINING OLIGO- AND POLYSACCHARIDES. *APPL MICROBIOL BIOTECHNOL,* 93**,** 285-293.

VINCK, A., DE BEKKER, C., OSSIN, A., OHM, R. A., DE VRIES, R. P. & WOSTEN, H. A. 2010. HETEROGENIC EXPRESSION OF GENES ENCODING SECRETED PROTEINS AT THE PERIPHERY OF ASPERGILLUS NIGER COLONIES. *ENVIRONMENTAL MICROBIOLOGY,* 13**,** 216-225.

VINCK, A., TERLOU, M., PESTMAN, W. R., MARTENS, E. P., RAM, A. F., VAN DEN HONDEL, C. A. & WÖSTEN, H. A. 2005. HYPHAL DIFFERENTIATION IN THE EXPLORING MYCELIUM OF *ASPERGILLUS NIGER*. *MOL MICROBIOL,* 58**,** 693-699.

VINETSKII IU, P., ROZHKOVA, A. M., SEREDA, A. S., TSURIKOVA, N. V., NURTAEVA, A. K., SEMENOVA, M. V., ZOROV, I. N. & SINITSYN, A. P. 2010. INCREASE IN GLUCOAMYLASE PRODUCTIVITY OF *ASPERGILLUS AWAMORI* STRAIN BY COMBINATION OF RADIATING MUTAGENESIS AND PLASMID TRANSFORMATION METHODS. *PRIKL BIOKHIM MIKROBIOL,* 46**,** 685-692.

WÖSTEN, H. A., MOUKHA, S. M., SIETSMA, J. H. & WESSELS, J. G. 1991. LOCALIZATION OF GROWTH AND SECRETION OF PROTEINS IN *ASPERGILLUS NIGER*. *J GEN MICROBIOL,* 137**,** 2017-2023.

Nederlandse Samenvatting

INTRODUCTION

Aspergillus niger is een veel voorkomende schimmel die leeft op dood organisch materiaal. Dit organisme wordt gebruikt door de industrie om enzymen en organische zuren (zoals citroenzuur) te produceren. De levenscyclus van *A. niger* begint met de kieming van een spore die conidium wordt genoemd. Hierdoor ontstaan schimmeldraden de zogenaamde hyfen. Deze draden zijn met elkaar verbonden en vormen samen een netwerk dat mycelium of kolonie wordt genoemd. Dit mycelium kan conidiophoren vormen waaruit zich conidia ontwikkelen die weer een nieuw mycelium kunnen vormen nadat zij door wind of insecten zijn verspreid.

Hyfen worden opgedeeld in compartimenten middels septa. De poren in deze septa worden afgesloten door organellen die Woronin bodies worden genoemd. Door deze afsluiting kunnen hyfen in het mycelium van elkaar verschillen qua celinhoud en activiteit. Zo is er een zone in het mycelium, net achter de buitenkant, dat de capaciteit heeft om conidioforen te vormen. Deze zone scheidt geen eiwitten uit die het substraat kunnen afbreken. Dit suggereert dat sporenvorming eiwituitscheiding onderdrukt. Slechts weinig is bekend over sporenvorming in *A. niger* maar het is goed onderzocht in *Aspergillus nidulans.* Zo zijn er genen geïdentificeerd die betrokken zijn bij dit proces. Inactivatie van één van deze genen, *flbA,* resulteert in een mycelium dat geen conidioforen kan maken. Een soortgelijk fenotype werd gevonden in *A. niger* en deze schimmelstam scheidde overal in het mycelium eiwitten uit. Dit was een bevestiging dat sporulatie eiwituitscheiding onderdrukt.

Het doel van dit proefschrift was mechanismen te onderzoeken die betrokken zijn bij sporulatie geremde eiwituitscheiding in *A. niger*. Begrip van deze mechanismen kan gebruikt worden om *A. niger* te verbeteren als productiesysteem. In dit proefschrift heb ik mij met name gericht op de genen *fluG* en *veA* die betrokken zijn bij sporenvorming in *A. nidulans.* Daarnaast bestudeerde ik de invloed van licht op eiwituitscheiding omdat bekend is dat licht sporulatie in *A. nidulans* beïnvloedt.

DE ROL VAN FLUG IN SPORULATIE EN EIWITUITSCHEDING

Meerdere kopieën van *amyR* werden in *A. niger* ingebracht (Hoofdstuk 2). Het eiwit dat wordt gecodeerd door dit gen reguleert de vorming van enzymen die zetmeel kunnen afbreken zoals glucoamylase GlaA. Het inbrengen van meerdere kopieën verbeterde de vorming van GlaA. Het merendeel van het eiwit werd net als in het wildtype nog steeds uitgescheiden aan de rand van de kolonie, wat correleerde met de plek waar het coderende gen het meest actief was. Er was echter één stam, UU-A001.13, die *glaA* door het hele mycelium tot expressie bracht en het coderende eiwit in het hele mycelium uitscheidde. Omdat de meeste stammen GlaA aan de buitenkant van de kolonie uitscheidde kon dit niet komen door de introductie van *amyR*. Daarom werd de genoomsequentie van UU-A001.13 bepaald. Het bleek dat het geïntroduceerde DNA onder andere in het *fluG* gen was terechtgekomen, waardoor dit gen was geïnactiveerd. Ik besloot om het *fluG* gen te inactiveren in het wildtype. De hypothese was dat hierdoor de schimmel geen conidioforen meer kon maken en daarom overal eiwit zou uitscheiden. Dit bleek niet het geval. Inactivatie van *fluG* (de Δ*fluG* stam) had geen effect op sporulatie, kieming van conidia, en groei (Hoofdstuk 3). Echter, inactivatie had wel effect op het vermogen van de stam om zetmeel af te breken. Dit vond plaats onder de gehele kolonie in tegenstelling tot het wildtype dat het slechts aan de buitenkant deed. Dit was dus overeenkomstig UU-A001.13 (Hoofdstuk 2). Daarnaast scheidde de Δ*fluG* stam meer eiwit uit dan het wildtype wanneer het gegroeid was op zetmeel, maar niet wanneer het gegroeid was op xylose (Hoofdstuk 3). Blijkbaar is FluG geen algemene remmer van eiwituitscheiding. Dit bleek ook uit expressiestudies in het wildtype en de de Δ*fluG* stam. Van de 2554 genen die uitgescheiden eiwitten coderen waren er respectievelijk 60 en 157 genen die meer dan 2 keer hoger en lager tot expressie kwamen in het centrum van de Δ*fluG* kolonie in vergelijking tot het centrum van het wildtype. In het midden en aan de buitenkant van de kolonie kwamen er juist meer genen voor uitgescheiden eiwtten hoger tot expressie (respectievelijk 135 en 50 genen en 165 en 57 genen; Hoofdstuk 3). Het was onverwacht dat *glaA* juist lager in het centrum tot expressie kwam van de Δ*fluG* stam, wat in tegenspraak lijkt met de verbeterde zetmeel afbraak in deze zone. Mogelijk komt dit doordat de

celwand van de Δ*fluG* stam meer doorlaatbaar is waardoor eiwitten makkelijker naar buiten komen (Hoofdstuk 3 en 5). Samengevat zou FluG een link kunnen zijn tussen sporenvorming en remming van eiwituitscheiding.

DE ROL VAN VEA EN LICHT IN SPORENVORMING EN EIWITUITSCHEIDING

VeA van *A. niger* bevat een typisch velvet domein, een signaalsequentie waarmee het de kern uitgaat (NES), drie PEST domeinen die betrokken zijn bij de afbraak van het eiwit, en wordt voorspeld een lokalisatie in de kern te hebben (Hoofdstuk 4). Dit klopt met de vinding dat het eiwit in het donker migreert van het cytoplasma naar de kern. Inactivatie van *veA* in *A. niger* (Δ*veA* stam) had invloed op conidiofoorvorming. De lengte en breedte van de stam van de conidiofoor alsmede de kop van deze structuur waren twee keer kleiner dan in het wildtype. De diameter van de gehele conidiofoor met sporen was zelfs drie keer kleiner. Dit impliceert dat de sporenketens ook kleiner zijn dan in het wild-type. De verkorte sporenketens en de verkleinde conidiofoorkop verklaren waarom de Δ*veA* stam tot wel 17 keer minder sporen vormt. Het is interessant dat de conidiofoor van de Δ*veA* stam lijkt op die van het wildtype van *Aspergillus sydowii*. We dachten dat het fenotype verklaard kon worden doordat de Δ*veA* stam minder druk kon genereren in de hyfen, waardoor lengte en breedte van de conidiofoor vermindert. Echter, het totale gehalte aan moleculen die turgordruk kunnen genereren was gelijk in wildtype en de Δ*veA* stam. Het gehalte aan trehalose en erythritol was wel verminderd in de Δ*veA* stam. Eerdere studies duiden ook op een rol van trehalose in de morfogenese van de conidiofoor.

Conidia van de Δ*veA* stam kiemden sneller dan die van het wildtype (Hoofdstuk 4). Echter, radiale groei van de Δ*veA* kolonie was verminderd, wat gepaard ging met een tweevoudige reductie van de biomassa en hyfen die kronkelig van vorm waren. Dit laatste suggereert dat VeA betrokken is bij polaire groei van hyfen.

Het effect van licht op sporenvorming en eiwituitscheiding werd onderzocht in hoofdstuk 5. Kolonies werden tussen membranen gegroeid, waarvan de bovenste

werd verwijderd na zes dagen. Vorming van conidioforen vond in het wildtype met name plaats direct achter de buitenkant van de kolonie. Kolonies die waren gegroeid in wit of blauw licht vormden deze voortplantingsstructuren ook in het midden en centrum van de kolonie. Dit was veel minder in kolonies die gegroeid waren in het donker of in groen licht, terwijl kolonies gegroeid in rood licht een fenotype vertoonden tussen donker en wit licht gegroeide kolonies. Deze resultaten tonen aan dat rood en blauw licht de ruimtelijke verdeling van conidioforen op het mycelium oppervlak beïnvloeden. Kolonies van de Δ*veA* stam vormden de meeste conidiophoren direct achter de buitenkant van de kolonie. Vorming van deze voortplantingsstructuren was veel minder in het midden en het centrum van de kolonie vergeleken met het wild-type. Dit toont aan dat VeA net als licht betrokken is bij de ruimtelijke conidiofoor verdeling. Echter, net als in het wild-type was er geen effect op het totaal aan sporen in donker- en licht-gegroeide kolonies.

Het feit dat licht de ruimtelijke conidiofoor verdeling beïnvloedt en het fenomeen van sporulatie geremde eiwituitscheiding voorspelt dat licht een effect heeft op eiwituitscheiding in de kolonie. ^{14}C-labeling toonde inderdaad aan dat het centrum van donker-gegroeide kolonies meer eiwit uitscheidde dan licht-gegroeide kolonies (Hoofdstuk 5). Dit bevestigt dat sporulatie de eiwituitscheiding beïnvloedt omdat sporulatie meer voorkomt in het centrum in licht-gegroeide kolonies. De Δ*veA* kolonies bleken hun eiwitten met name in het centrum uit te scheiden, daar waar in beperkte mate sporulatie voorkomt, terwijl eiwituitscheiding in niet sporulerende zones veel lager was. Hieruit wordt geconcludeerd dat VeA niet alleen conidiofoor distributie beïnvloedt maar ook een rol heeft in sporulatie geremde eiwituitscheiding.

Curriculum vitae

Fengfeng Wang was born October 25, 1979 in Beijing, P.R. China. He followed his bachelor program at Beijing Agricultural College and graduated in 2003. He started the master major in the Department of Plant Sciences at Wageningen University, The Netherlands, September 2005. The internships of this master were performed at Plant Research International (supervisor Dr CG van der Linden) and at the Laboratory of Phytopathology of Wageningen University (supervisor Dr H Meijer). Fengfeng Wang obtained his MSc diploma September 2008. From July 2008 to March 2009, he worked as a guest researcher in the Molecular Microbiology group of the Biology Department of Utrecht University under supervision of Dr LG Lugones and Prof Dr HAB Wösten. He started his PhD project in the same research group July 2009. His project was financed by the Netherlands Genomics Initiative Kluyver Center for Genomics of Industrial Fermentation. The results of this project are described in this Thesis.

List of publications

Wang F (2014). Inhibition of secretion by asexual reproduction in *Aspergillus niger*. PhD Thesis, Utrecht University.

Wang F, Krijgsheld P, de Bekker C, Hulsman M, Nitsche BM, Ram AFJ, Reinders M, de Vries RP, Muller WH, Dijksterhuis J & Wösten HAB (2014) FluG affects zonal expression of genes and is involved in spatial expression of AmyR regulates genes in *Aspergillus niger* (to be submitted).

Wang, F., Dijksterhuis, J., Wyatt, T., Wösten H. A. B., Bleichrodt, R. (2014) Inactivation of *veA* affects vegetative growth and morphology of conidiophores in *Aspergillus niger* (to be submitted).

Krijgsheld P, Bleichrodt R, van Veluw GJ, **Wang F**, Muller WH, Dijksterhuis J & Wösten HAB (2013) Development in *Aspergillus*. Stud Mycol, 74, 1-29.

Ohm RA, de Jong JF, Berends E, **Wang F**, Wösten HAB & Lugones LG (2010) An efficient gene deletion procedure for the mushroom-forming basidiomycete *Schizophyllum commune*. World J Microbiol Biotechnol, 26, 1919-1923.

van Peer AF, **Wang F**, van Driel KG, de Jong JF, van Donselaar EG, Muller WH, Boekhout T, Lugones LG & Wösten HAB (2009) The septal pore cap is an organelle that functions in vegetative growth and mushroom formation of the wood-rot fungus *Schizophyllum commune*. Environ Microbiol, 12, 833-844.

Acknowledgements

When I arrived The Netherlands in the summer of 2005, I didn't expect that I would stay here for so long. During these years, I was very pleasure to meet many people and collaborated with them. I would like to take the opportunity in this section to express deep gratitude to all of them.

First of all, I would like to give great thanks to Prof Han A. B. Wösten. Dear Han, I thank you lot for providing me the opportunity to join your group in 2008 and start my PhD study in 2009. I especially thank you for your great supervision and fruitful discussion. With your help, I improve my research level needed to reach final goal, PhD degree.

Second my thanks go to Dr Wieke R. Teertstra and Dr Luis G. Lugones. Dear Wieke, thank you for your continuous support on my lab work especially on the *A. niger* experiment and help me find out the way I really appreciate your generous help and contribution to my thesis, and working together with you. Dear Luis, I am so lucky to have your excellent supervision during my internship. Your rich knowledge and original on idea on fungal genetics field impressed me a lot, thank your suggestion and help on my project.

To continue, I would like to thank all of colleagues from Microbiology department. The workmates of W406, Dear Isabelle, Birgit, and Arman, Woking together with you is really enjoyable. Thank you for your daily conversation and help. I really miss the days in W406. Dear Jesus, thank you for many valuable suggestions on my work. Good luck with your future work. Dear Karin, thank you for your help and sharing your research experience with me. Wish you all the best in your project and enjoy fungal genetics research. I am grateful to Filippo for offering me helpful tips on lab work and "cigarette" discussion. I would like to thank Helene for offer me lots of help and suggestions during my job hunting and thesis print. I also want to thank Florian for your tips on Western analysis and good luck on your new career. I thanks all the other (old) members of microbiology department, Ad, Arend, Aurin, Brand, Carlo, Charissa,

Charlotte, Elsa, Frank, Hans, Iva, Jan D., Jan G., Jan de J., Jan T, Jordi, Lennard, Maloes, Margot, Michiel, Natalia, Ourdia, Pim, Ria K., Ria T., Robin, Roeland, Ronald de V., Savani, Stefanie, Sylvia, Timon, Vincent, Virginie for all the happy hours of working together, lab trip, etc. Then, I would like to thank Frits and Ronald L. for excellent microscope training and photograph assistance, as reflected in my thesis.

Besides works, you always need friends, here I would like to thank all of my friends for their friendship and help in both science and personal life. Special thanks to Rianne, Zhao Zhang, Jun Guo, Lisong Ma and Fang Xu. Dear Rianne, nine years friendship is stronger than everything. I thank you for your help and support past few years. Zhao Zhang, Jun Guo, Lisong Ma and Fang Xu, I really appreciated your suggestions and encouragement for my career development. Without your suggestions, I can't obtain the opportunity to start my PhD journey. I also would like to thank my other old friends who are till in or have left the Netherlands, Lei Cui, Xu Cheng, Xiao Cui, Xi Chen, Carel F., Xiao Gao, Xingning Hao, Chenlei Hua, Yao Liu, Yuchen Long, Teck Yew Low, Kevin Lu, Songyan Lu, Yu lu, Haisheng Nie, Ke Peng, Weicong QI, Yin Qin, Yinghua Xiao, Qiushi Wang, Yiding Wang, Lisha Zhang, Ran Zhang, Chunhui Zhou and Feng Zhu for your friendship and help.

Finally, I express my deepest gratitude to my parents for their endless love, understanding, strong support, and encouragement, my cousin brother for been there whenever I needed and for taking care of my parent when I was away from home.
最后我要由衷的感谢我父母无私的爱，鼓励，理解和支持，感谢表哥, 姨父和姨姨在我远行的日子里对我父母的照料。

Fengfeng Wang
Beijing, P. R. China
September 2014